CLONING, EXPRESSION, PURIFICATION AND PRODUCT CHARACTERIZATION OF A NOVEL CHITINASE FROM *Bacillus aryabhattai*

Thesis

Submitted in partial fulfilment of the requirement for the degree of

DOCTOR OF PHILOSOPHY

By

S. ARUN KUMAR (197108CH002)

DEPARTMENT OF CHEMICAL ENGINEERING

NATIONAL INSTITUTE OF TECHNOLOGY KARNATAKA,

SURATHKAL, MANGALORE – 575025

August 2024

DECLARATION

I am declaring with my complete knowledge that the Research Thesis entitled **"Cloning, Expression, Purification and Product Characterization of Novel Chitinase from *Bacillus aryabhattai*,"** which is being submitted to the **National Institute of Technology Karnataka, Surathkal,** in partial fulfilment of the requirements for the award of the Degree of **Doctor of Philosophy** in the Department of Chemical Engineering is a *bonafide report of the research work carried out by me*. The material in this Research Thesis has not been submitted to any University or Institution for the award of any degree.

S. Arun

Place: NITK, Surathkal
Date: 01-07-2024

Name: S. ARUN KUMAR
Reg No: 197108CH002

CERTIFICATE

This is to certify that the Research Thesis entitled "**Cloning, Expression, Purification and Product Characterization of Novel Chitinase from *Bacillus aryabhattai*,**" submitted by Mr. S. ARUN KUMAR (Register Number: 197108CH002) as the record of the research work carried out by him, is accepted as the research thesis submission in partial fulfilment of the requirements for the award of degree of Doctor of Philosophy.

Research Guide
Dr. Keyur Raval
Professor
Department of Chemical Engineering
NITK, Surathkal

Chairman - DRPC
Professor. I. Regupathi
Head of the Department
Department of Chemical Engineering
NITK, Surathkal

Head of the Department
विभागाध्यक्ष
Department of Chemical Engineering
रासायनिक अभियांत्रिकी विभाग
National Institute of Technology Karnataka - Surathkal
राष्ट्रीय प्रौद्योगिकी संस्थान कर्नाटक, सुरत्कल
PO Srinivasnagar, Mangalore - 575025 Karnataka
पी.ओ. श्रीनिवासनगर, मंगलौर – ५७५०२५ कर्नाटक

ACKNOWLEDGEMENT

Pursuing the path of a doctorate has been a core part of my journey. This research thesis has been successfully compiled with the support and motivation of many people. Through this platform, I wish to thank each one who made this research journey an outstanding experience by providing their precious support.

First and foremost, I want to thank my research guide, Dr. Keyur Raval, for his encouraging guidance and gracious support during this journey. He relentlessly guided me to stay motivated to achieve my goal. His opinions and comments have always given me the right direction to proceed with this in-depth research.

I am sincerely thankful to the RPAC committee member Dr. Hari Prasad Dasari for his valuable comments, which have enabled me to practice several ideas for this thesis and Dr. Arun Kumar Thalla for his valuable direction at different stages of my research, which were inspirational and helped me to work intelligibly. I am highly grateful to Dr. Ritu Raval, MAHE, for her constant guidance and friendly support during this research journey.

I am thankful to the Department of Science & Technology (DST), Government of India and the Ministry of Human Resource Development (MHRD), Government of India, for the funding received towards my work.

My respectful gratitude to the Director, NITK and the present Head of the Department of Chemical Engineering, NITK, Dr. I. Regupathi, and the former heads of the department, Dr. P.E Jagadeeshbabu and Dr. Prasanna B D, for providing me with all the facilities to pursue my research work.

I am grateful to the Department of Chemical Engineering and Central Research Facility (CRF), NITK, for providing an efficient research ambience and supporting my research. I sincerely thank the Faculty members and non-teaching staff of the Department of Chemical Engineering for their well- timed assistance in official documentation works and their help handling different equipment types.

I am gratifying all my former and current research colleagues for providing a fun-filled work environment during my stay at NITK. I specifically thank my Lab senior, Mrs. Priyanka Bhat, who has been a constant mentor for the past few years, and I am thankful to My lab mates and M. Tech students who worked in my lab for their support during this research work.

My highest gratitude to my family for being with me and providing immense support and encouragement throughout this journey. I thank my parents, Mr. Subramani Mrs. Mahalakshmi, and my sister Ms. S. Sindu Mathi. I am incredibly thankful to my wife, Mrs. Nivetha Laksmi, for her outstanding support and motivation to finish my work successfully. I also thank other members and my wife's family and friends for their constant support, love, and motivation in this life journey.

Finally, I would like to thank God for all the grace bestowed upon me.

S. ARUN KUMAR

ABSTRACT

Chitin, an abundant polysaccharide in the world, is a primary byproduct of the seafood industry. Efficiently converting chitin into valuable products is crucial. Chitinase transforms chitin into chitin oligomers, which holds significant industrial potential. However, chitin's crystalline and insoluble nature makes the conversion process challenging. This study isolated a novel marine bacterium, *Bacillus aryabhattai,* from the Arabian Sea. Bacterial growth in different crystalline chitin substrates like chitin powder, flakes, and colloidal chitin confirmed the chitinase presence in bacterium could act upon insoluble crystalline chitin and produce chitin oligomers. The domain architecture analysis of the chitinase confirmed the presence of two N-terminal LysM domains, which helps chitinase act on crystalline chitin. Statistical optimization of media and process parameters revealed glycerol, yeast extract, magnesium chloride, and manganese sulphate as significant media components and 1% colloidal chitin. The optimum process parameters such as pH 7, temperature 40℃, inoculum size 12.5% (v/v), and inoculum age 20 hours enhanced the specific chitinase activity to ±115.2 U· mg^{-1}, ±63.02 U· mg^{-1} and ±146.1 U· mg^{-1} against chitin powder, flakes and colloidal chitin respectively, which is five to six times higher than basal level activity. Also, TLC and LC-MS analysis confirmed that chitin oligomers (monomer to hexamer) were produced from insoluble chitin powder and flakes by spent media of *Bacillus aryabhattai*. A recombinant chitinase from the marine bacteria *Bacillus aryabhattai* (*Ba*ChiA) was developed in the future. The chitinase gene was cloned into the pET 23a plasmid and transformed into *E. coli* Rosetta pLysS. Chitinase characterization against colloidal chitin revealed optimum parameters such as Tris buffer at pH 8, temperature 55℃, with 400 mM sodium chloride. Enzyme kinetics studies for colloidal chitin substrates revealed V_{max} of 112.3 μmole· min^{-1} and K_m of 2.5 mg· mL^{-1}. The specific chitinase activity against chitin powder and flakes reached 875 U· mg^{-1} and 625 U· mg^{-1}, respectively. The chitinase showed antifungal activity against *Candida albicans*, *Fusarium solani*, and *Penicillium chrysogenum* growth with the zone of inhibition of 14 mm and 25 mm diameter for wildtype and recombinant *Ba*ChiA, respectively. Thin Layer Chromatography (TLC) and LC-MS confirmed the production of chitin trimer,

tetramer, pentamer, and hexamer from chitin powder and flakes using recombinant chitinase.

TABLE OF CONTENTS:

LIST OF FIGURES

LIST OF TABLES

LIST OF ABBREVIATIONS

GlcNaC	-	N acetyl Glucosamine
CTOS	-	Chitin Oligosaccharides
NAG	-	N-acetyl glucosamine
LPS	-	Lipopolysalicylic acid
PBD	-	Plackert Berman Design
RSM	-	Response Surface Methodology
KH_2PO_4	-	Potassium dihydrogen phosphate
K_2HPO_4	-	Dipotassium hydrogen phosphate
NaCl	-	Sodium Chloride
$MgSO_4$ / $MgCl_2$	-	Magnesium sulphate/chloride
$MnSO_4$ / $MnCl_2$	-	Manganese sulphate/chloride
NaOH	-	Sodium Hydroxide
$FeSO_4$	-	Ferrous sulphate
$CuSO_4$	-	Copper Sulphate
HCl	-	Hydrogen chloride
Na_2HPO_4	-	Disodium hydrogen phosphate
NaH_2PO_4	-	Sodium dihydrogen phosphate
NH_4Cl	-	Ammonium Chloride
KCl	-	Potassium Chloride
LC-MS	-	Liquid Chromatography – Mass Spectrometry
TLC	-	Thin Layer Chromatography
CBP	-	Carbohydrate binding protein
IPTG	-	Isopropyl β-D-1-thiogalactopyranoside
SCP	-	Single Cell Protein
PKD	-	Polycystic Kidney Disease
Ni – NTA	-	Nickle nitrilotriacetic acid
UV – VIS	-	Ultra vilot – Visible
OD	-	Optical Density

UPLC	-	Ultra performance Liquid Chromatography
$CaSO_4$ / $CaCl_2$	-	Calcium Chloride / Calcium Sulphate
$CoCl_2$	-	Cobalt Chloride
$NiCl_2$	-	Nickel Chloride
PCR	-	Polymerase Chain reaction
PMSF	-	Phenylmethylsulfonyl fluoride
SDS PAGE	-	Sodium dodecyl sulfate polyacrylamide gel Electrophoresis
APS	-	Ammonium persulfate
TEMED	-	N,N,N′,N′ -Tetramethylethylenediamine
TB	-	Terrific Broth
DNSA	-	3. 5 Dintrosalicylic acid
BSA	-	Bovine serum albumin
DD / DP / DA	-	Degree of Deacetylation / Polymerisation / acetylation
MW	-	Molecular weight
kHz	-	Kilo hertz
kDa	-	Kilo Daltons
mL/ mg	-	Milli litre / Milli gram
µL/ µg	-	Micro litre / Micro gram
L / g	-	Litre / gram
%	-	Percentage
w/v	-	weight/volume
v/v	-	Volume /volume
rpm	-	Rotation per minute
mM / µM	-	millimolar / micromolar
m/z	-	mass/ charge

CHAPTER 1

INTRODUCTION

Globally, seafood is one of the majorly consumed non-vegetarian foods. In 2022-23, the global consumption of processed seafood reached nearly 16.9 million tons, with projections indicating an expected increase to 20.3 million tons by 2028. China, Norway, Vietnam, the USA, and India lead the global seafood export market. These countries collectively contribute significantly to the global seafood export, with frozen shrimp emerging as the most substantial export commodity. The rate of seafood consumption globally is shown in **Figure 1.1**.

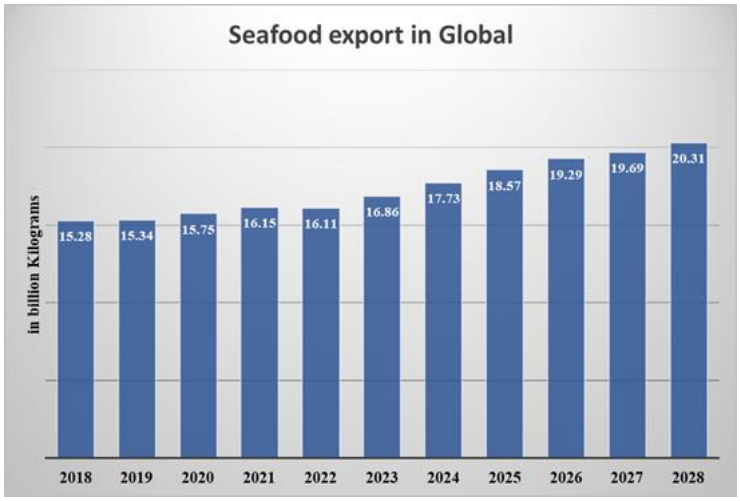

Figure 1.1 Expected global seafood consumption in 2028 based on data from 2018 to 2024.

India is the fifth largest seafood exporter, such as shrimp, lobster, fish, crab, etc. In 2022-23, India exported 1.75 million tons of seafood, 11.08% more than in 2021-22.

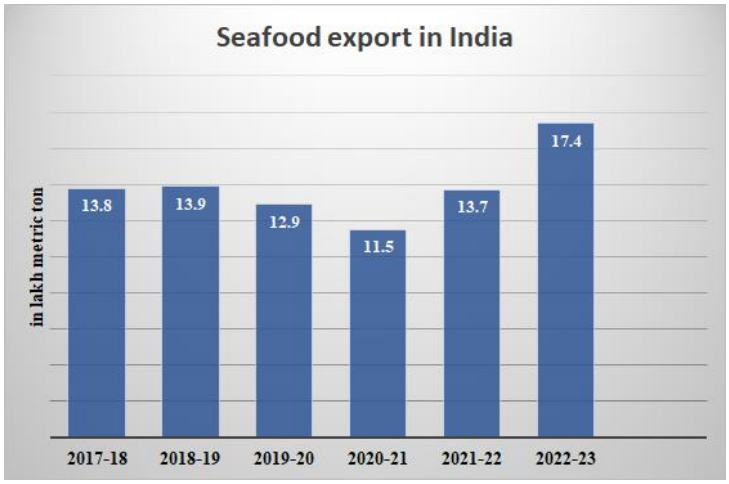

Figure 1.2 Seafood export by India in the last five years

And they are expected to be 61% more in 2029-30. The rate of seafood exported by India for the last five years is shown in **Figure 1.2**. In India, frozen shrimp contributes

significantly to seafood exports, which accounts for 40.98% of total seafood exports. Based on the 2022-23 report, approximately 0.7 million tons of frozen shrimp and 0.5 million tons of frozen crab were exported from India to various countries. The processing of shrimp and crab for exportation generates substantial waste, with chitin constituting a significant portion. It is noteworthy that approximately 20 and 30% of the total weight of crab and shrimp, respectively, corresponds to chitin, highlighting the considerable volume of this valuable resource within the waste generated by the seafood processing industry (Paulsen et al. 2016; Wang et al. 1999). Hence, in 2022-23, the global and India production of chitin waste amounted to over 2.1 million tons and 0.4 million tons, respectively, which is anticipated to rise annually. Chitin $(C_8H_{13}O_5N)n$ is a biopolymer found in a diverse array of organisms such as arthropods, shrimps, shellfish, Mollusca, coelenterate, protozoa, fungi, and crustaceans with a primary role of imparting mechanical strength to these organisms. The fundamental structure of chitin comprises a homopolymer of N-acetyl glucosamine (GlcNAc), connected by covalent (β-1,4) linkages and arranged in either an antiparallel (α-chitin) or parallel (β-chitin) form as shown in **Figure. 1.3**. In nature, α-chitin is more prevalent than other isomeric forms (Adrangi and Faramarzi 2013).

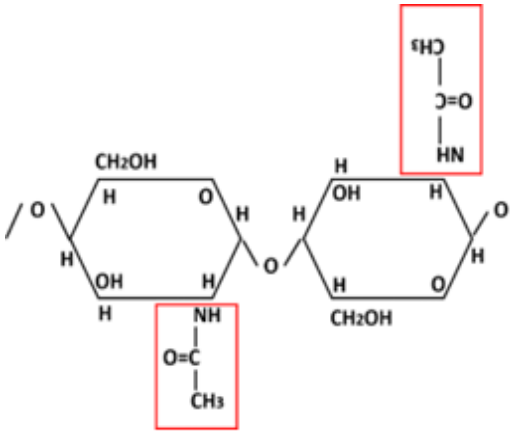

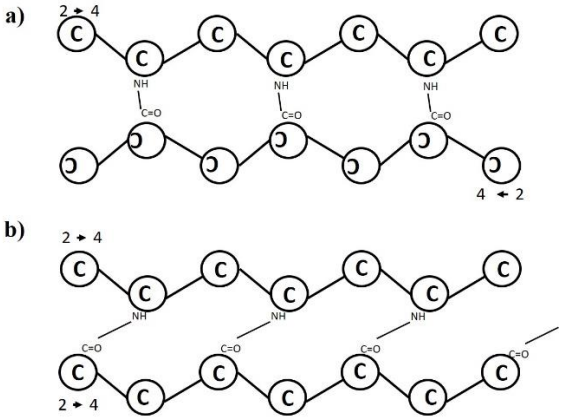

Figure. 1.3 Structure of Chitin. **Figure. 1.4 Structure of a) α and b) β chitin.** (Adrangi and Faramarzi 2013)

The arrangement of linear polymer chains by hydrogen bonds between amine groups differs from one form to another. In α chitin, chains are arranged anti-parallelly to each other, whereas in β chitin, it is arranged parallelly, as shown in **Figure. 1.4.** γ chitin comprises both parallel and antiparallel arrangements. In α chitin arrangements, hydrogen bonding is more stable, rigid and insensitive to hydration. Thus, the hard

shells of sea animals and fungal cell walls consist of α chitin for hard and rigid surfaces (Kim and Rajapakse 2005). Chitin, while biocompatible and biodegradable, poses a

Application	Description
Antibacterial and antifungal activity	In fungi and bacteria, CTOS reacts with negative groups in the cell wall, affects the cell wall's permeability, causes leakage of cell constituents and causes bacteria's death. CTOS works against various bacteria such as *Escherichia coli, Vibrio parahaemolyticus*, etc.
Antitumor activity	CTOS possess a positive charge and bind to negative charge moieties on the tumour cells, altering tumour cells' permeability.
Anti-inflammatory	CTOS suppresses the expression of the gene responsible for NF-κB associated inflammation in B cells by binding to the lipopolysaccharide (LPS) receptors.
Antioxidant	The amino groups of CTOS react with unstable free radicals and form stable products. DD and MW can alter the antioxidant activities of CTOS.
Immunostimulant and wound healing	CTOS interacts with macrophages' membrane receptors through their chemotactic effects and boosts macrophage migration and protein secretion of cytokines. Thus, the above mechanism stimulates an immune response that helps to heal wounds.
Food preservatives	The antifungal and antibacterial property of CTOS encourages their use in food preservation, like preservatives and packaging material.

Table 1.1. Different applications of CTOS (Liang et al. 2016; Vo et al. 2017)

challenge due to its high insolubility in water and solvents, attributed to its intricate and crystalline structure. To harness its potential, chitin must be converted into chitin oligomers (CTOS), which find diverse applications. Chitin oligomers have various applications. Chitin oligomers ranging from Monomer to Octamer have applications

in food packaging, drug delivery, immune stimulation, autoimmune suppression, malaria prevention, septic shock prevention, and controlling blood sugar levels in diabetic patients. Some applications of CTOS are summarized in **Table 1.1**. CTOS is the Chitin with DP (Degree of polymerization) in the range between 2 and 20 and an average Molecular Weight between 400 and 3000 Da. CTOS is produced with defined DP, Degree of acetylation (DA) and Degree of deacetylation (DD). Based on these DP, DA, and DD factors, the application of CTOS varies. Unlike Chitin, some advantages, such as high solubility, biocompatibility, easy cellular interactions, and ease of absorption by biological molecules, make CTOS extremely valuable (Vo et al. 2017)**.** Highlighting the production of CTOS from the chitin is that it is produced by hydrolysis of chitin using chemical, physical, and enzymatic methods. The physical method involves hydrolysis using Ultrasonic irradiation in which chitin is treated with ultrasound (20 kHz). The DP produced ranges between 2 and 11 (Liang et al. 2016). However, this method is unsuitable for a large scale because scaling up an ultrasonic setup is complicated. Hydrolysis of chitin to CTOS in industries is currently progressed by chemical methods using hydrochloric acid, nitrous acid, phosphoric acid, and hydrogen peroxide or persulfate. However, the complexity of reactions, chemical contamination formation, and product degradation are significant drawbacks in chemical methods (Lodhi et al. 2014). Consequently, enzymatic methods have gained a preference for chitin oligomer production. This preference is attributed to the advantages of the enzymatic approach, including specific product formation, reduced impurities, environmental friendliness, and overall sustainability. Chitinases, classified under EC number 3.2.1.14, are hydrolase family members. They play a crucial role in catalyzing the bioconversion of chitin into N-acetylglucosamine (NAG) and smaller chitin oligomers. This process involves the hydrolysis of the (1-4)-beta glycosidic linkages in chitin. Chitinase is produced by various organisms, including bacteria, fungi, plants, and even humans (Hamid et al. 2013). Based on the mechanism, Chitinases can be classified into endochitinases (EC 3.2.1.14) and exochitinases. Endochitinases possess the function of hydrolysis of chitin and produce soluble chitin oligomers of different DP (2 to 20). Exochitinases have two subcategories: first, chitobiosidase, classified under EC number EC 3.2.1.29, which releases dimer by acting at the non-reducing end of chitin, and second,

N-acetylglucosaminidase classified under EC 3.2.1.30, which cleaves chitin oligomers to monomers (Le and Yang 2019). The mechanism of each type is explained in **Figure. 1.5.** Based on amino acid sequence and 3D structure of the catalytic domain of chitinases, they have been classified into five classes (I, II, III, IV and V) which have been categorized into three families such as glycosyl hydrolases 18 (GH18), glycosyl hydrolases 19 (GH19) and glycosyl hydrolases 20 (GH20) (Kobayashi et al. 2002). Chitinases of the GH18 family are widely found in fungi, bacteria, animals, viruses, and certain plants. Even though chitinases are from different sources, lately, there has been a growing interest in chitinase sourced from marine environments.

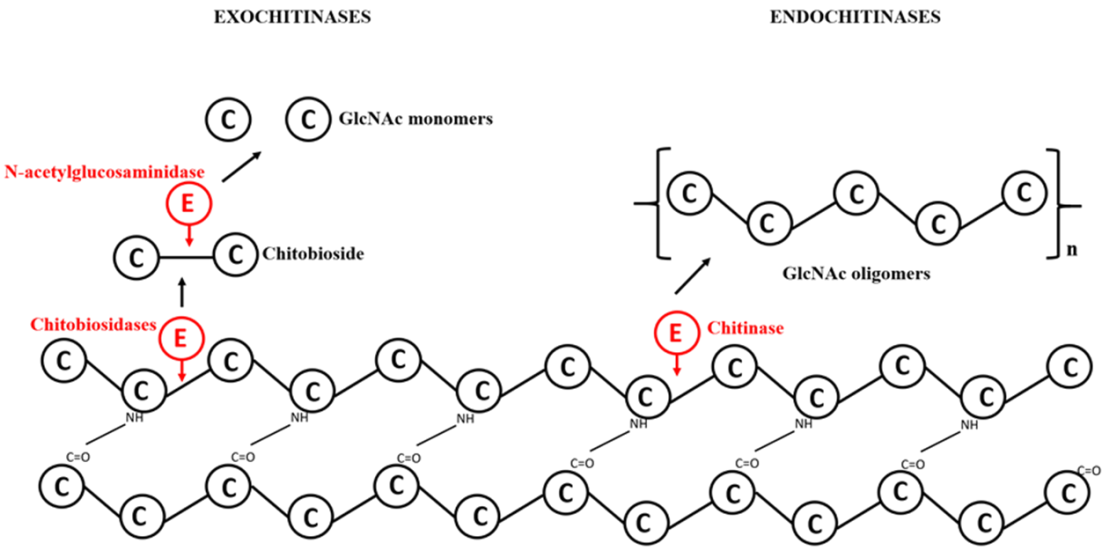

Figure. 1.5. Action mechanism of Exo and Endochitinases (Le and Yang 2019)

Given that the primary reservoir of chitin is in marine organisms, utilizing chitinase derived from these sources offers enhanced compatibility for chitin degradation. Chitinase-producing bacteria from marine sources play a fundamental role in oceanic nutrient cycling by transforming chitin waste into a beneficial form through biodegradation. Additionally, marine enzymes are frequently preferred in industries due to their superior operational characteristics compared to animal, plant, or bacteria counterparts (Ikeda et al. 2007; Makhdoumi et al. 2015; Stefanidi and Vorgias 2008). While biological methods exhibit specific activity, their effectiveness on insoluble and crystalline chitin presents a significant challenge. Partial acid degradation of chitin is often necessary before chitinase can effectively act on it. Improving the production of chitin oligomers from crystalline and insoluble chitin remains a

demanding task that requires further enhancement (Annamalai et al. 2011a; Fu et al. 2016; Tamadoni Jahromi and Barzkar 2018; Xie et al. 2021). In recent studies, chitinase was fused with the carbohydrate-binding domain (CBP) to enhance its activity upon insoluble chitin powder (Kidibule et al. 2018; Madhuprakash et al. 2015; Manjeet et al. 2013). The chitinase activity towards crystalline and insoluble chitin is still deficient and challenging (Liu et al. 2019). Thus, this study isolated and adapted a novel chitinase-producing marine bacterium, *Bacillus aryabhattai*, to grow on insoluble chitin-containing media. Growth and chitinase activity were studied against the insoluble chitin powder, flakes, and colloidal chitin. Media composition and process parameters were optimized using the Plackett Burman design (PBD) and Response surface method (RSM) to improve the bacterial growth and chitinase activity. An antifungal assay was performed to confirm the antifungal properties of chitinase. The TLC and LC-MS analysis was performed to determine the different CTOS produced by the *Ba*ChiA from different insoluble chitin substrates, such as chitin powder and flakes. Also, producing wild-type enzymes will significantly lead to less yield. The purification of enzymes of interest from wild-type crude products is more complicated (Ramli et al. 2011). Thus, the development of recombinant chitinase may overcome these challenges. Purificsation of Recombinant enzymes is more flexible than wild-type enzyme purification. In this study, a recombinant *E. coli PLysS Rosetta* strain containing pET23a plasmid with *Ba*ChiA gene is developed. This chitinase is expressed using the IPTG induction method and purified using Ni-NTA affinity chromatography. The optimization of chitinase expression is performed to improve the soluble chitinase formation. The characterization and kinetics study of purified chitinase are performed. The chitin oligomers produced from insoluble chitin substrates using purified chitinase are studied using TLC and LC-MS analytical methods.

CHAPTER 2
REVIEW OF LITERATURE

Chitinase is extensively produced by different organisms, including both micro and macro-organisms. As is familiar, bacteria and fungi dominate chitin recycling, converting it into carbon and nitrogen sources for survival (Keyhani and Roseman 1999). Besides bacteria and fungi, chitinases are also produced in mammals, plants, insects and viruses. In these organisms, chitinases are involved in various physiological functions such as cell wall and cell organelles development, defence against pathogens and parasites, and cellular activities (Funkhouser and Aronson 2007; Gortari and Hours 2008). In addition, it also involves antagonistic interactions (Adrangi and Faramarzi 2013; Swiontek Brzezinska et al. 2014). In the UniProt database, 3967 different chitinases were identified (https://www.uniprot.org/) (Bateman 2019). From this database, it is exciting that chitinase from bacterial sources contributed about 63% of the overall number of chitinases, with a count of 2779. The most significant chitinolytic bacteria include Proteobacteria phyla and terrabacteria such as Cyanobacteria, Actinobacteria, Tenericutes, Deinococci, Chloroflexi, etc.

2.1 Domain architecture

In general, chitinase domain architecture (**Figure. 2.1**) includes the signal peptide, S/T rich linker region, chitin-binding domain, PKD (Polycystic Kidney Disease) domain, FnIII (Fibronectin type III) domain and a catalytic domain (Kobayashi et al. 2002)**.** The signal peptide is required for the chitinases to be secreted extracellularly.

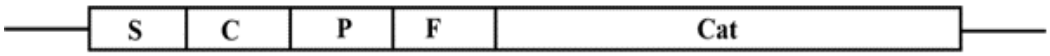

Figure. 2.1. Domain Architecture of Chitinase gene
(S- signal peptide, C- chitin-binding domain, P – PKD domain, F- FnIII domain Cat – Catalytic domain) (Kobayashi et al. 2002)

Most GH18 enzymes are extracellular with exceptional chitinase from *Serratia*, where chitinase is exported to periplasm without any processing (Funkhouser and Aronson 2007). The Serine/Threonine rich linker region is present either in the N/C terminal region of the chitinase gene. The length of the sequences varies in different organisms. The most extended S/T region is found in *D. melanogaster*, with approximately 3900 bases. The function of the region is to provide stabilization from the attack of proteases. The glycosylation of the S/T region provides stability for

chitinase from protease activity. The degree of glycosylation increases with the length of the linker region, increasing the chitinase stability against proteases (Huang et al. 2012). The catalytic domain is the kitchen of chitinase, which is responsible for chitin hydrolysis. Based on the vital residue in their amino acid sequences, they are classified into two types. GH18E, in which glutamate residue is present in their catalytic centre. Mutation of glutamate residue results in a complete loss of chitinase activity. Another type is the absence of glutamate residue, and chitinase is still active. The catalytic domain has a deep cleft-like structure, which is responsible for chitinase activity. PKD and FnIII domain function was initially unknown and thought to be present because of the horizontal gene transfer from human beings during evolution. Later mutation studies revealed that they help break the crystalline structure of chitin so that the chitinase can act. PKD and FnIII domains are more or less like each other structurally (Yan and Fong 2018). PKD domain is not predominantly present in chitinase like the FnIII domain. The experimental evidence for their structure was yet to be proven. Later, mutation studies suggested the FnIII domain is essential for the structure integrity of the enzyme rather than in enzymatic activity. Based on the position of the FnIII domain, their role varies, and they are found to have no role in chitinase activity**.** The last domain is the carbohydrate-binding module (CBM), which facilitates the chitinases' ability to act on the insoluble substrate. Based on the CAZy database, there are 73 different families of CBM. Depending upon the structural and functional relationship, they are classified as type A, B, and C. Type A CBM consist of a domain which can bind to the crystalline structure of the polymer due to the binding of the aromatic amino acid crystalline lattice of protein to the planar structure in the polymer. Type B CBM consists of protruding groves that can accommodate individual sugar units. The higher the degrees of polymerization, the better the binding efficiency. Type C CBM consists of a lectin-like binding site that can hold only disaccharides or trisaccharides(Pell et al. 2003). The catalytic domain includes some amino acids conserved for enzyme core formation. These signature sequences are found in the active site and include a Glu residue, which is crucial to the catalytic mechanism. A barrel structure is formed by eight strands of parallel β sheets, and α helices, forming a ring outside the β barrel. Family GH19 belongs to chitinase from plant sources, although there are some representatives from bacterial sources. Glu 67

and Glu 89 are essential residues in the mechanism of action of family GH19 chitinases (Chang et al. 1995). The members of each family are homologs, the two families are entirely dissimilar, and even 3D structures are different, which confirms that both families evolve from different ancestors. Family GH20 includes N-acetylglucosaminidases belonging to bacteria, certain fungi, and humans. Several organisms, such as bacteria, fungi, plants and even humans, produce chitinase. The function of chitinase is different for different organisms, which is highlighted below.

2.2 Chitinolytic bacteria

Recently, Bacterial chitinases have been widely preferred in several commercial applications since they gain many advantages, such as less doubling time, high thermostability, and ease of gene isolation and gene knocking study. So far, Chitinases of *Serratia marcescens*, *Bacillus sp.*, *Streptomyces sp*., *Paenibacillus sp*. IK-5 and FPU-7, *Vibrio sp*. and *Salinivibrio sp.*, etc., from different habitats were isolated (Kusaoke et al. 2017; Le and Yang 2018; Monreal and Reese 1968; Pan et al. 2019; Ralph Berger and Reynolds 1958; Tamadoni Jahromi and Barzkar 2018a; Tanakal and Phaff 1965). Recently, a pathogenic bacteria called *Listeria monocytogenes* was identified, influencing the listeriosis infection in humans. The study also reported that the bacteria produces chitinase (ChiA and ChiB), which helps the bacteria suppress the immune response and invasion of listeriosis in humans (Halbedel et al. 2019). Most bacterial chitinases fall within the GH18 family. Few actinomycetes and purple bacteria chitinases are within the GH19 family (Terrapon et al. 2017). The *S. marcescens* is the earliest isolated species that produced chitinases. It was also taken as a referee model for a chitinase study (Vaaje Kolstad et al. 2013). This bacteria produces five chitinases: ChiA, ChiB, ChiC1, ChiC2, and ChiD. Both ChiA and ChiB are involved in the production of chitin dimer by acting on chitin chains in reverse directions, whereas ChiC acts as an endochitinase and produces chitin oligomers by randomly acting on chitin chains (Tuveng et al. 2017; Vaikuntapu et al. 2016). However, the role of ChiD in chitin hydrolysis remains unknown (Madhuprakash et al. 2019). ChiA, ChiB, ChiC and ChiD are found in several bacteria. Nearly ten chitinases have been reported in *Bacillus circulans*, classified as *Bc*ChiA, *Bc*ChiC, and *Bc*ChiD (Watanabe et al. 1992). ChiD from *B. circulans* was identified, which involved cleavage of both the N and C-terminal domains to produce

ChiBl and ChiB2 (Gao et al. 2018; Take et al. 2018). Reports by Robbins *et al.,* and Yandigeri *et al.,* proved that the highest number of chitinases were identified from *Streptomyces spp* belongs to both GH18 and GH19 families (Robbins et al. 1988; Yandigeri et al. 2015). Also, In *Chromobacterium violaceum,* chitinases possessed activity at higher temperature (100°C) (Sousa et al. 2019). Usage of Thermostable chitinase for the production of chitooligosaccharides will be more benifecial in industries. Some of the reported bacterial chitinases are summarized in **Table 2.1.**

2.3 Chitinolytic fungi

Like bacterial chitinases, fungal chitinases also act as an immune response against other fungal attacks. However, it also plays other roles, such as attaining chitin, developing cell morphology, and developing cell division (Rathore and Gupta 2015). Chitinase from different fungal genera, such as *Myrothecium, Mucor, Trichoderma, Penicillium,* Aspergillus, etc., have been reported (Gomaa 2021). The chitinase genes are available in a wide variety of fungi. However, most chitinases fall under the GH18 family, except for *Nosema bombycis, the* first reported GH19 family chitinase (Han et al. 2016). Some of the reported Fungal chitinases are summarized in **Table 2.1.** Based on conserved amino acid sequence, fungal GH18 chitinases are categorised into five subfamilies: A to E (Junges et al. 2014). Though the conserved region of the GH18 fungal family was not similar to the bacteria, they displayed high similarity with class III plant chitinases (Duo-Chuan 2006). Chitinase synthesis is more common in filamentous fungi than in yeast (Stoykov et al. 2015). However, the role of each chitinase was unknown since it was more challenging to knock down genes to characterize morphological changes. In the study by Langer et al., three chitinases (*Um*ChiA, *Um*ChiB, and *Um*ChiC) were identified in *Ustilago maydis*. The *Um*ChiA and *Um*ChiB play the leading role in cell separation, while UmChiC is expected to play a role against invading microbiome (Langner et al. 2015). Silencing of the ChiA gene in Saccharomyces cerevisiae resulted in defective cell separation, leading to the formation of multicellular aggregates. The ChiA plays an essential role in the development and renewal of cell walls, while ChiB is responsible for spores formation (Giaever et al. 2002; Kurandas and Robbins 1975).

Organism name	Chitinases type	Glycoside hydrolase family (GH)	References
Bacteria			
Serratia marcescens BJL200	A, B, C1, and C2, D	GH18	(Monreal and Reese 1968; Tuveng et al. 2017; Vaaje Kolstad et al. 2013)
S. marcescens GPS5	D	GH18	(Madhuprakash et al. 2019; Vaikuntapu et al. 2016)
S. griseus HUT6037	C	GH19	(Ralph Berger and Reynolds 1958; Watanabe et al. 1992)
Streptomyces plicatus	Chitinase-63	GH19	(Robbins et al. 1988)
Bacillus circulans WL-12	A1, A2, B1, B2, C and D	GH18	(Tanakal and Phaff 1965; Watanabe et al. 1992)
Vibrio alginolyticus H-8	B	GH18	(Ohishi,' et al. 2000)
Listeria monocytogenes	B	GH18	(Halbedel et al. 2019)
Paenibacillus sp. IK-5	A and B D	GH18 GH19	(Kusaoke et al. 2017)
Bacillus sp.	Chisb	GH18	(Lee et al. 2007; Pan et al. 2019)
B. thuringiensis	A74	GH18	(Juarez-Hernandez et al. 2019)
S. albolongus ATCC 27414	A4	GH18	(Gao et al. 2018)

Chromobacterium violaceum ATCC 12472	Chi47	GH18	(Sousa et al. 2019)
S. thermodiastaticus HF 3–3	Chi1	GH18	(Take et al. 2018)
Paenibacillus sp. FPU-7	A, B, C, D, E, F, and W	GH18	(Itoh and Kimoto 2019)
Fungi			
Xenorhabdus nematophila HB310	Chi60 and Chi70	GH18	(Liu et al. 2019)
Trichoderma harzianum	Chit46	GH18	(Deng et al. 2019)
Coprinopsis cinerea	E1	GH18	(Zhou et al. 2018)
Ustilago maydis	Cts1, Cts2, and Cts3	GH18	(Langner et al. 2015)
Metarhizium anisopliae	A, B, C, D, and E	GH18	(Junges et al. 2014)
Beauveria bassiana	Chit1	GH18	(Pinnamaneni et al. 2010)
Saccharomyces cerevisiae	Cts1 Cts2	GH18 -	(Hurtado-Guerrero and van Aalten 2007; Kurandas and Robbins 1991)

Table 2.1 Reported Bacterial and fungal chitinases in previous studies.

Also, a study reported that mycoparasitic and entomopathogenic fungi can produce chitinases (Deng et al. 2019). Based on the report by Deng *et al.,* the growth of the plant pathogen (*Botrytis cinereal)* was inhibited by Chit46 chitinase derived from *Trichoderma harzianum*. In addition, this chitinase produced chitin dimer with an efficiency of 94.8%. Furthermore, the virulence of the chitinase was increased by developing recombinant chitinase of *Beauveria bassiana* and *Trichoderma harzianum* (Selenius et al. 2018). Thus, fungal chitinase is suggested for producing chitin oligomers and controlling the infection of harmful fungi in crops.

2.4 Marine chitinases

Lately, chitinase sourced from marine environments has been focused on. Given that the primary reservoir of chitin is in marine organisms, utilizing chitinase derived from these sources offers enhanced compatibility for chitin degradation. Chitinolytic bacteria from marine play a fundamental role in oceanic nutrient cycling by transforming chitinous waste into a beneficial form through biodegradation (Tamadoni Jahromi and Barzkar 2018b). The industrial processes are performed in extreme physicochemical conditions. Using enzymes from marine sources may be beneficial because they show maximum activity in a wide range of process parameters such as pH, temperature, and salinity (Stefanidi and Vorgias, 2008). Hence, marine bacterial chitinases are preferred for several applications of Food Technology, Healthcare, agriculture, and waste management, for activities such as antimicrobial, antiparasite food quality enhancers, anticancer, immune regulatory etc. (Gohel et al. 2006; Hee Kuk et al. 2005; Santhi 2016; Wang et al. 2015). Sara Skott Paulsen *et al.,* performed antifungal performance of 11 different marine chitinase-producing bacteria, such as *P. galatheae, V. coralliilyticus, V. nigripulchritudo* etc., revealed that marine chitinase possessed good activity than other source (Paulsen et al. 2016). In the past, different type of chitinases was reported from marine bacteria such as *Alcaligenes* (Annamalai et al. 2011a), *Streptomyces* (Han et al. 2009; Santhi 2016), *Bacillus* (Cheba et al. 2016, 2017), *Pseudoalteromonas* (Wang et al. 2014), *Vibrio* (Revathi et al. 2012; Vincy et al. 2014), *Moritella* (Stefanidi and Vorgias 2008), and *Acinetobacter* (Krithika and Chellaram 2016). The different marine bacterial chitinase reported in previous studies are shown in **Table 2.2**.

Marine Bacteria	Chitinase type	Substrate	Activity	Ref
Achromobacter xylosoxidans	Wildtype Chitinase	Colloidal Chitin	464.2 U· ml^{-1}	(Inamine et al. 2015a)
Photobacterium galatheae S2753,	Wildtype Chi-A like chitinases	Colloidal chitin	-	(Paulsen et al. 2016)
Paenibacillus macerans TKU029	Wildtype Chitinase	Squid pen powder	-	(Bateman and Bycroft 2000)
Paenibacillus chitinolyticus strain UMBR 0002	Recombinant chitinase	Colloidal chitin	750.64 mU· mg^{-1}.	(Kulichevskaya et al. 2019)
Paenicibacillus barengoltzii CAU904	Recombinant Chitinase	Colloidal chitin	30 U· mg^{-1}	(Gutiérrez-Román et al. 2014)
Vibrio rotiferianus	Recombinant Chitinase	Colloidal Chitin	41.14 U· mg^{-1}	(Subramanian et al. 2020a)
Pseudoalteromonas piscicida	Recombinant Chitinase	Colloidal Chitin	42.17 U· mg^{-1}	(Doan et al. 2018)
Micrococcus sp. AG84	Wildtype Chitinase	Colloidal chitin	93.02 U· mg^{-1}	(Chen et al. 2007)
Alcaligenes faecalis AU02	Wildtype Chitinase	Colloidal chitin	81.5 U· mg^{-1}	(Annamalai et al. 2011b)

Table 2.2. Enzymatic activity against different chitin substrates by different wild type chitinase-producing bacteria

Microbial source	Chitinase type	Host organisms	Substrate	Activity	Ref
Streptomyces sampsonii	Recombinant chitinase	*E. coli BL21 (DE3)*	Colloidal chitin	0.104 U· g^{-1}	(Wang et al. 2023a)
Bacillus velezensis	Recombinant chitinase	*E. coli BL21 (DE3)*	Colloidal chitin Chitin flakes Chitin powder	0.50 U· mg^{-1} 0.20 U· mg^{-1} 0.05 U· mg^{-1}	(Tran et al. 2022)
Aeromonas sp.	Recombinant chitinase	*E. coli BL21 (DE3)*	Colloidal chitin	10.7 U· mg^{-1}	(Yu et al. 2022)
Streptomyces alfalfae	Recombinant chitinase	*E. coli BL21 (DE3)*	Colloidal chitin Chitin powder	28.4 U· mg^{-1} 1.9 U· mg^{-1}	(Lv et al. 2021)
Paenibacillus xylanexedens	Recombinant chitinase	*E. coli BL21 (DE3)*	Colloidal chitin Glycol Chitin Chitin powder	16.1 U· mg^{-1} 5.4 U· mg^{-1} 0.4 U· mg^{-1}	(Zhang et al. 2021a)
Bacillus thuringiensis *Mamestra brassicae*	Extracellular fused recombinant chitinase	*E. coli BL21 (DE3)*	Colloidal chitin	133.9 U· mg^{-1}	(Paek et al. 2020)

Table 2.3. Enzymatic activity against different chitin substrates by different recombinant chitinase

Several recent studies reported recombinant chitinase from different marine bacteria such as *Streptomyces sampsonii, Chitinibacter tainanensis, Serratia marcescens, Bacillus thuringiensis, Paenibacillus xylanexedens, Aeromonas sp* etc. (Okay and Alshehri 2020a; Wang et al. 2023a; Wang and Wu 2020a; Zhang et al. 2021a) and from some fungal species such as *Rasamsonia emersonii* (Dwyer et al. 2023). However, recombinant chitinase developed from the above organisms performed activity against soluble chitin oligomers and colloidal chitin, partially solubilized using acids. No results were mentioned in these studies that these recombinant chitinase acted on insoluble chitin substrates. Moreover, few studies reported on recombinant chitinase from *Bacillus velezensis, Streptomyces alfalfae* (Lv et al. 2021; Tran et al. 2022), which were performed against insoluble chitin substrate. In the study performed by Nilpa *et al.,* (Nilpa et al. 2022), the fused chitinase gene of *Serratia marcescens* with the alkaline protease gene of *Bacillus circulans* was developed for better performance of enzyme against insoluble chitin substrates. In the study performed by Paek *et al.,* (Paek et al. 2020), a hybrid recombinant enzyme was developed by fusing the chitinase catalytic domain from *Bacillus thuringiensis* bacteria with the chitin-binding domain from *Mamestra brassicae* insect, which improved the binding efficiency of chitinase towards insoluble chitin. Some recombinant chitinase developed recently is also shown in **Tables 2.2 and 2.3**. However, the activity of wildtype and recombinant chitinase from marine sources against insoluble chitin substrates is challenging. The different applications of chitinases are explained below.

2.5 Applications of chitinases

Chitinases are essential in healthcare, food preservation, crop disease control, and chitin oligomer production due to their significant advantages: they are more specific, non-hazardous, and cost-effective.

2.5.1 Agricultural applications

In agriculture, the major problem emerging recently is the loss of crops due to infection by bacteria, fungi and insects. Fungi play a significant contribution in crop diseases of more than 70%. Common crop diseases include black mould, white rot, southern leaf blight, and basal stem rot. Some common fungal species involved in plant diseases are *Colletotrichum spp, Fusarium sp., Puccinia spp., Botrytis cincerea,*

Ustilago maydis, and *Penicillium*. Chitinase has been considered for protecting crops from fungal infection (Liu et al. 2019). The chitinase from *Bacillus thuringiensis* exhibits an antifungal effect against *Fusarium roseum,* responsible for dry rot in potato tubers (Sadfi et al. 2001). It also showed effect against *Urocystis tritici*, (Tao et al. 2014), *Botrytis cinerea*, (Martínez-Absalón et al. 2014), *Sclerotinia sp*. (Shrestha et al. 2015), *F. oxysporum* (Djenane et al. 2017). These fungal species are responsible for the majority of the crop diseases. In addition, an antifungal effect was observed against several species, such as *Ustilago maydis, Rhizopus oryzae, A. flavus* and *F. oxysporium* from the *Streptomyces macrosporeus* M1 chitinase. Also, chitinase from *Trichoderma viride* AUMC 13021 inhibited the infection by *Fusarium oxysporum* in tomatoes (Abu-Tahon and Isaac 2020). Furthermore, transgenic plants with overexpression of the chitinase gene showed a better resistance against fungal infection than crops with chitinase spray. This was due to the overexpression of chitinase in transgenic crops (A. H. Fahmy et al. 2018). For instance, in transgenic tobacco, the overexpression of *Th*Chi33 and *Th*Chi42 genes, which belong to *Trichoderma harzianum*, helped it to develop resistance against plant pathogens, high salinity, and high heavy metals contamination (De Las Mercedes Dana et al. 2006). Moreover, (Shin et al. 2008) reported that *Fusarium sp*., an infection causing head blight in wheat, was inhibited by expressing class II chitinase in transgenic barley. The above reports proved that chitinase is a promising tool for protecting crops from fungal infections.

2.5.2 Nutritional applications

2.5.2.1 Food preservation

The major problem experienced in food handling is fungal infection. It is tedious to control it. Recently, food preservation has been achieved through different methods, such as chemical or microbial coating. The usage of microbes showed more benefits because of time and cost reduction, no contaminants and eco-friendliness (Sharma et al. 2009). However, chitinase-producing bacteria showed added advantages and better effects against fungal contamination (Castillo et al. 2016). In a report, the chitinase (ChiC) from *Salinivibrio sp*. showed promising results in food preservation due to its antifungal properties. Another report confirmed that chitinase inhibited food contamination by *Botrytis cinerearom, Trichoderma harzianum* (De Las Mercedes

Dana et al. 2006). In a report, chitinase expression in cucumber hypocotyls was induced by fungal spore infection and gained resistance against fungal spore infection (Kästner et al. 1998). Thus, chitinases are preferred for food preservation due to their specific inhibition of fungal growth and spore formation.

2.5.2.2 Single cell protein (SCP) formation

Humans have recently consumed SCP for high-value protein sources instead of non-vegetarian sources(A. T. Nasseri et al. 2011). A study reported that the production of single-cell proteins could be achieved by chitinase and chitinous materials (Le and Yang 2018). In another study (Tom and Carroad Paul A 1981), it was confirmed that hydrolysis of chitin by chitinases from *Pichia kydriavzevii* and *Serratia marcescens* have resulted in the production of SCP (45 – 50% protein and 8–10% nucleic acids). In addition, SCP, with 61% protein and 3.1% nucleic acids, was produced by chitinase from *Saccharomyces cerevisiae* and *Myrothecium verrucaria* (Vyas and Deshpande 1991). In a report, the optimum SCP with 65 – 70% protein and 2.9 – 3.5% nucleic acids was produced by chitinase from *Penicillium ochrochloron* by utilizing 2% chitin (Patil and Jadhav 2014).

2.5.3 Medical applications

Chitinases play an essential role in healthcare applications (Halder et al. 2019) reported that consumption of chitinase and antifungal drugs enhanced treatment against various fungal infections. An outstanding antifungal effect on *Candida albicans* was achieved by the combination of chitinase with the lactic acid bacteria *Lactobacillus casei* (Allonsius et al. 2019). Chitinase has shown promising effects against some cancer diseases. For instance, (Pan Xing Q. et al. 2005) reported that the MCF-7 and B11–2 cancer cells were destroyed by chitinase from *Streptomyces griseus* and *Serratia marcescens* in mice. Additionally, the chitinase from *Trichoderma viride* AUMC 13021 showed a cytotoxic effect on different cell lines (Abu-Tahon and Isaac 2020). However, further investigation should be performed in mammalian tumour cells. Mediators of allergic inflammation are also an added-on property of chitinases (Goldman and Vicencio 2012).

CHAPTER 3
SCOPE AND OBJECTIVE

3.1 Scope:

The above findings suggest that developing an enzymatic process for producing chitin oligomers from insoluble chitin substrates can be an alternative to chemical methods. However, the chitinases discovered in the previous studies lack action against insoluble chitin substrates, which is still challenging. Chitinases from marine sources showed the best performance in extreme conditions.

No research was performed on the enzymatic production of chito oligomers using the marine bacteria *Bacillus aryabhattai.* The following objectives are framed based on the above scope for this research work.

3.2 Objective:

The objective framed for this research work is the enzymatic production of chito oligomers from insoluble chitin by recombinant Chitinase. Based on this, the following specific objectives are derived.

Objective I: Isolation, characterization, and optimization of chitinase production by marine bacterium *Bacillus aryabhattai*.

Objective II: Cloning, expression, and process optimization of recombinant chitinase expression and purification from *Bacillus aryabhattai* in *E. coli Rosetta pLysS.*

Objective III: Characterization of enzymatic reaction products of recombinant chitinase using insoluble chitin substrates.

CHAPTER 4

MATERIALS AND METHODS

A. WILDTYPE CHITINASE STUDY

All the experiments were performed in triplicate, and the graphs plotted in the thesis are their mean values indicated in the legend of the figures. Error bars were included in all graphs.

4.1 Chemicals used

Genomic DNA isolation kit (Himedia, India, CatLog No. MB505), 3 kDa Pall centrifugal membrane filters (Pall laboratory, USA, CatLog, MCP003C41), TLC silica plate (Merk, Germany, CatLog No. HX16775554), Bradford reagent (Himedia, India, CatLog No. ML106), Bovin serum albumin (Himedia, India, CatLog No. GRM105), N–acetyl glucosamine (TCI chemicals, India, CatLog No. A0092), Chitin powder (LOBA chemie, India, CatLog No. 1398-61-4), Chitin flakes (Himedia, India, CatLog No. GRM2356), Sodium Hydrogen Phosphate, Potassium hydrogen phosphate, Ammonium chloride, Sodium chloride, Potassium chloride, Calcium chloride, Magnesium chloride, Magnesium sulphate, Iodine, Potassium Iodide, Agar, Concentrated hydrogen chloride, Sodium hydroxide, Glucose, Sucrose, Glycerol, Yeast Extract, Peptone, Tryptone, Soybean, Copper sulphate, Cobalt chloride, Ferric sulphate, Potato dextrose Agar, 3,5 Dintrosalicylic acid, Sodium potassium Tartarate, Phenol, Sulphuric acid, Butanol, Methanol, Ammonia, Diphenylamine, Aniline, Acetone, Orthophosphoric acid.

4.2 Instruments used

SDS PAGE setup Mini PROTEAN tetra cell (Biorad, USA, Model No. 552BR 216528), Agarose gel Electrophoresis (Enertech, India, Model No. ENPS500 STD), Thermo cycler for PCR (Himedia, India, Model No. WEE32), UV-Visible Spectrometer (Thermo scientific, USA, Model No. G10S), Centrifuge (REMI, India, Model No. C24 plus), PH meter (LabMan, India, Model No. LMPH-9), Weighing balance (Wensar, India, Model No. MAB220), Incubator shaker (Scigenics biotech, India, Model. Orbitek), Magnetic stirrer (REMI, India, Model No. 1-ML), Hot air oven (KEMI, India, Model No. KOMS-4F), Water bath (Rotek, India, Model No. Rsw 30), Freeze dryer (Inkarp, India, Model No. FDS-2SE), Sonicator (Sonics, USA, Model No. VCX 500), -20℃ Deep freezer (Elanpro, India, Model No. PME139), BOD incubator (LEAD instruments, India), Laminar air flow chamber (Cleanair, India), -80℃ Deep freezer (Haier, India), UV transilluminator (Himedia, India, Model No. LA1067), LC-MS (Waters corporation, USA, Model, Acuity

UPLC and Xevo G2 QTOF MS).

4.3 Isolation and screening of chitinase-producing strain

The marine samples were collected from a depth of 12 m from the Arabian Sea, Dakshin Kannada (12º 48'N & 74º 40'E) with the help of Central Marine Fisheries Research Institute (CMFRI), Mangalore, India. A serial dilution of the marine samples was made. Undiluted and diluted samples (50 µL) were spread on plates containing 1% (w/v) colloidal chitin, 1.5% agar (w/v) and minimal salts (Na_2HPO_4 6.78 g. L^{-1}, KH_2PO_4 3 g. L^{-1}, NH_4Cl 1 g. L^{-1}, NaCl 0.5 g. L^{-1}) dissolved in artificial seawater (NaCl 26.29 g. L^{-1}, KCl 0.74 g. L^{-1}, $CaCl_2$ 0.99 g. L^{-1}, $MgCl_2.6H_2O$ 6.09 g. L^{-1}, $MgSO_4.7H_2O$ 3.94 g. L^{-1}) according to cold spring harbor protocol (Ferreira et al. 1998). The plates were incubated at 37℃ for 48 hours. After incubation, the plates were flooded with 2 mL of Lugol's iodine solution (5% iodine and 10% potassium iodide in distilled water), and the isolates showing zone of clearance were considered chitinase producers. Lugol's iodine was added to increase the contrast. The colonies which produced chitinase were purified by restreaking those colonies on colloidal chitin plates and incubated at 37℃ for 48 hours. As Bergey's systematic bacteriology manual mentioned, the chitinase-producing isolates were identified by biochemical characterization. Microscopic tests such as gram staining, endo-spore staining, and motility studies were performed to study the bacteria's morphology. Biochemical tests such as indole, MRVP, triple sugar, citrate utilization, catalase, starch hydrolysis, and casein hydrolysis tests were performed to identify the genus and species of the isolated bacteria. Finally, molecular-level identification was performed using 16S rRNA analysis. The genomic DNA of species was isolated using the Genomic DNA isolation kit. 16S rRNA gene was amplified using 27F: 5'-AGAGTTTGATCMTGGCTCAG-3' and 1492R: 5'-CGGTTACCTTGTTACGACTT-3' as forward and reverse primer, respectively (27F and 1492R were the universal primers for species-level identification in bacteria). 16S rRNA amplification was performed in the thermocycler. The PCR product was sequenced using Sanger sequencing performed by Eurofins Pvt Ltd, Bangalore, India. The 16S rRNA sequence was compared to the database using the BlastN algorithm to determine the relative position of strain in phylogeny. Multiple sequence alignment of the top 15 blast hits was done using the MUSCLE algorithm

by MegaX software (Kumar et al. 2018). The aligned sequences were encoded to a maximal parsimony algorithm, creating bootstrap values and a Phylogenetic tree.

4.4 Preparation of colloidal chitin as a substrate for chitinase

Colloidal chitin was prepared using the protocol described by Murthy et al. (Murthy and Bleakley 2012). 10 g of chitin flakes were subjected to acidic treatment using 120 mL of 37% (v/v) concentrated HCl in a 500 mL beaker. 120 mL HCl was added slowly at 40 mL every 5 minutes and stirred for 1.5–2 hours at 37℃ until visible homogeneity was achieved. The solution was filtered using a muslin cloth to remove the visible flake chunks, and the filtrate was obtained. Filtrate was added to the 800 mL of pre-chilled distilled water to achieve precipitation and stored at 4℃ overnight. After overnight incubation, the colloidal chitin precipitate was obtained by centrifugation at 10,000 rpm for 10 minutes. The colloidal chitin was washed with tap water by centrifuging at 10000 rpm for 5 minutes. The washing step was repeated till the pH of the solution reached above 5. Finally, the pellet was washed twice with distilled water. The pellet was dissolved in 400 mL of distilled water such that the final concentration of colloidal chitin became 2.5% (w/v) (2.5% was achieved by dissolving colloidal chitin prepared from 10-gram chitin flakes in 400 mL of distilled water). The final pH was adjusted to 7 by adding 4 N NaOH. The Colloidal chitin was autoclaved and stored in a brown bottle at 4℃ for further usage. The concentration of colloidal chitin was quantified using the Phenol Sulphuric acid method (***Refer to section 4.10.3 for protocol***).

4.5 *Bacillus aryabhattai* growth and chitinase activity on media containing different chitin substrates

The growth profile of *Bacillus aryabhattai* was investigated by inoculating the single loop in media containing different chitin substrates (1% chitin flakes, powder, and colloidal chitin) with minimal salts prepared in artificial seawater (pH 7) and incubating at 37℃ and 120 rpm. The biomass concentration at different time intervals was determined. Cell growth was determined at different time intervals by measuring optical density at 600 nm using a UV-VIS spectrometer. The biomass concentration was obtained from the optical density using the calibration curve. The calibration curve was plotted between Biomass concentration ($mg \cdot mL^{-1}$) as the X-axis and optical density at 600 nm as the Y-axis. (Standard equation was $y = 1.189x$,

x is biomass concentration (mg· mL^{-1}), and *y* is the optical density at 600 nm). To measure the optical density, 2 mL of bacterial culture was taken in 15 mL centrifuge tubes and undisturbed for 2 minutes. After chitin particles settled down, the supernatant was transferred to fresh tubes and optical density was measured at 600 nm. *Serratia marcescens*, a member of the Enterobacteriaceae, was used as the reference organism as it produces an array of chitin-degrading enzymes like Chitinase A, Chitinase B, Chitinase C, and CBP21 (Tanaka et al. 1999). A cell-free supernatant sample from bacterial culture was obtained by centrifugation at 10000 rpm for 5 minutes. The activity of crude chitinase present in the supernatant against different chitin substrates was evaluated. A 10 mM sodium phosphate buffer (0.138 gram of NaH_2PO_4 was dissolved in 100 mL of distilled water, and pH was adjusted to 7 using 4 M NaOH) was used for the assay. In the reaction mixture, 1 mL of 10 mM sodium phosphate buffer was mixed with 500 µL of supernatant and 500 µL of 1% (w/v) colloidal chitin and the mixture was incubated for 1 hour at 37℃ under shaking conditions at 100 rpm. Enzyme and substrate blanks were prepared and incubated using the same procedure for reaction samples. Substrate and enzyme blank samples were analysed to confirm that the products were formed only by a reaction between *Ba*ChiA and chitin substrates. The substrate blank sample had no chitin substrates (1.5 mL of 10 mM sodium phosphate buffer and 0.5 mL of crude chitinase). The enzyme blank sample had no chitinase (1.5 mL of 10 mM sodium phosphate buffer and 0.5 mL of chitin substrate). The concentration of the chitin oligomers produced by chitinase from different chitin substrates was determined by DNSA Assay. One unit of chitinase activity is defined as one micromole of chitin oligomers released per minute under the above-performed assay conditions. One unit of specific chitinase activity is defined as one micromole of chitin oligomers released per minute and mg of the chitinase under the above-performed assay conditions. Thus, it was required to quantify the crude enzyme concentration in the supernatant. Enzyme concentration was determined by performing a Bradford assay. (***Refer to sections 4.10.1 and 4.10.2 for DNSA and Bradford assay protocol***). To improve the *Ba*ChiA activity, the optimization of media components and different process parameters used to grow the bacteria was performed using statistical optimization such as Placket Burman design (PBD) and Response surface methodology (RSM).

4.6 Optimization of media components for chitinase production

The Placket Burman design method was performed to screen the significant components affecting the growth of *Bacillus aryabhattai* using Design Expert 11 (State-Ease, Minnesota, USA) software. Different carbon sources (glucose, sucrose, glycerol), nitrogen sources (yeast extract, tryptone, peptone, soybean meal), and minimal salts ($CuSO_4$, $CoCl_2$, $FeSO_4$, $MnSO_4$, $MgCl_2$, $CaCl_2$, KH_2PO_4, and Na_2HPO_4) were used to grow different bacteria in Industries. These components affected the growth of bacteria, and the change in growth rate affected the production of extracellular proteins by the bacteria. Thus, considering to ease the scale up of media solution the above components are used for media optimisation (Bonnet et al. 2020).Thus, the optimization study was performed with the above components to find the significance of achieving the maximum *Ba*ChiA activity.

Type	Component Name	High value (+1)	Low value (-1)
Carbon sources	Glucose	5 g. L^{-1}	1.5 g. L^{-1}
	Sucrose	5 g. L^{-1}	1.5 g. L^{-1}
	Glycerol	5% v/v	1.5% (v/v)
Nitrogen sources	Yeast Extract	5 g. L^{-1}	1.5 g. L^{-1}
	Peptone	5 g. L^{-1}	1.5 g. L^{-1}
	Tryptone	5 g. L^{-1}	1.5 g. L^{-1}
	Soyabean	5 g. L^{-1}	1.5 g. L^{-1}
Macronutrients	$MgCl_2.6H_2O$	100 mM	50 mM
	$CaCl_2.2H_2O$	100 mM	50 mM
	KH_2PO_4	100 mM	50 mM
	NaH_2PO_4	100 mM	50 mM
Micronutrients	$CuSO_4.5H_2O$	10 mM	5 mM
	$CoCl_2.6H_2O$	10 mM	5 mM
	$FeSO_4.7H_2O$	10 mM	5 mM
	$MnSO_4.H_2O$	10 mM	5 mM

Table 4.1. Placket Burman design Matrix with 15 variables

Fifteen variables with two levels, high (+1) and low (-1), were considered for this study, as shown in **Table 4.1**. Usually, this model does not describe the interaction between variables. However, this model explains the significance of each variable

towards the chitinase activity.

A two-level Plackett Burman Design based on a first-order model can be described as,

$$Y = \beta_0 + \Sigma \beta_i . X_i + \varepsilon$$

Y is the experimental response (chitinase activity), β_0 is the main effect of the factors, β_i is the regression coefficient, X_i is the level of the independent variable, and ε is a random error. This experiment, constituting 15 factors with 22 experimental runs with three centre points, was generated using Design Expert 11 (State-Ease, Minnesota, USA). According to the developed experimental design, media was prepared, and 1% (w/v) colloidal chitin was added to the media prepared in each experimental run. Each media was prepared using artificial Sea water and inoculated with 5% (v/v) of 24 hours aged pre-inoculum (initially, 5% (v/v) of 24 hours aged pre-inoculum was used. Later, optimization of inoculum size and age was performed) and incubated at 37℃ with 120 rpm for 48 hours. The media volume was 20% of the flask volume (250 mL flask). The chitinase activity was observed as the response Y. Significant components that enhance the growth were investigated further using the ANOVA table and Pareto chart. The experiments were carried out in triplicates.

4.7 Optimization of media concentration using RSM (Box-Behnken design)

The significant variables screened by the Placket Burman design were further subjected to response surface methodology to ascertain the best concentrations at which maximum chitinase activity was achieved.

Variable	Component	Level of Variable		
		-1	0	1
A	Glycerol (v/v)	1.5%	3.25%	5%
B	Yeast extract	1.5 g· L^{-1}	3.25 g· L^{-1}	5 g· L^{-1}
C	$MgCl_2$	50 mM	75 mM	100 mM
D	$MnSO_4$	5 mM	7.5 mM	10 mM

Table 4.2. Three-level Box-Behnken design Matrix with four variables

A three-level Box-Behnken design RSM method was performed with 27 runs (3 centre points) using Design Expert 11 (State-Ease, Minnesota, USA) software. The selected variables (Glycerol, Yeast extract, $MgCl_2$, and $MnSO_4$) were studied at three different concentration levels, as shown in **Table 4.2**. Since simple linear regression

models cannot accurately explain the complex influence of the above four parameters on chitinase activity, higher-level models, such as the quadratic model, were considered to explain the complexity of interactions between these factors. The response data generated was fitted using the quadratic model to suit the polynomial equation represented below.

$$Y = \beta_0 + \sum \beta_i . X_i + \sum \beta_{ii} . X_i^2 + \sum \beta_{ij} . X_{ij}$$

Y is the predicted response in chitinase activity, β_0 is the coefficient of fitted response, β_i is a linear coefficient, β_{ii} is a quadratic coefficient, β_{ij} is the coefficient of interaction, X_i represents significant variables, and X_{ij} represents interacting variables. According to the developed experimental design, media was prepared, and 1% (w/v) colloidal chitin was added to the media prepared in each experimental run. Each media was prepared using artificial seawater, inoculated using 5% (v/v) of 24 hours aged pre-inoculum, and incubated at 37℃ with 120 rpm for 48 hours. The media volume was 20% of the flask volume (250 mL flask). The chitinase activity was observed as the response Y. Significant process parameters that enhance the chitinase activity were investigated further using the ANOVA table and contour plots. The experiments were carried out in triplicates. Further, the process parameters were optimized using RSM.

4.8 Optimization of process parameters using RSM to improve chitinase activity

The media concentration obtained after the optimization was validated. Further optimization of process parameters such as temperature, pH, inoculum size, and inoculum age were performed, as shown in **Table 4.3** (Patidar et al. 2005a).

Parameters	Level of Variable		
	-1	0	1
Temperature (℃)	25	40	55
pH	5	7	9
Inoculum age (hour)	12	20	28
Inoculum size (%)	5	12.5	20

Table 4.3. Three levels Box-Behnken design Matrix with four variables

The response data generated was fitted using the quadratic model to suit the polynomial equation represented below.

$$Y = \beta 0 + \sum \beta i . Xi + \sum \beta ii . Xi\ 2 + \sum \beta ij . Xij$$

Where Y is the predicted response in chitinase activity, β_0 is the coefficient of fitted response, β_i is a linear coefficient, β_{ii} is a quadratic coefficient, β_{ij} is the coefficient of interaction, X_i represents significant variables, and X_{ij} represents interacting variables. The design matrix generated 27 runs with 3 centre points for four process parameters. According to the developed experimental design, optimized media was prepared, and 1% (w/v) colloidal chitin was added to each experimental run. Each media was prepared using artificial seawater and inoculated using different process parameters as designed experimental runs at 120 rpm for 48 hours. The Media volume was 20% of the flask volume (250 mL flask). The chitinase activity assay was performed to determine the best process parameters that enhance the yield and productivity of *Ba*ChiA. The optimized process parameters were validated.

4.9 Antifungal efficiency of *Ba*ChiA

The zone of inhibition method determined the antifungal activity of the chitinase. Cell-free spent media of *Bacillus aryabhattai* was obtained under two different conditions. One, the bacteria was grown in optimized media containing 1% (w/v) colloidal chitin, incubated in optimized process parameters, and spent media was obtained by centrifuging at 10000 rpm for 10 minutes. Other bacteria were grown in optimized media without 1% (w/v) colloidal chitin and collected after 48 hours of incubation (Since, at this time, maximum chitinase activity was obtained). The supernatant samples were used against plant pathogenic fungi such as *Candida albicans and Fusarium oxysporum*. Two Potato dextrose agar plates were prepared for two fungal cultures. Each fungus was spread in each plate, and three wells were made there. 100 µL of crude enzyme sample obtained from a culture grown in optimized media containing 1% colloidal chitin was added to **well 1**, and the crude enzyme sample from a culture grown in the optimized media without 1% colloidal chitin was added to **well 2**. The autoclaved medium was loaded to **well 3**, which serves as a negative control. The antifungal activity was measured after incubating two fungal plates at 25℃ for 48 hours. This measurement was based on the clearance zone obtained around the well containing the crude enzyme.

4.10 Analytical methods for wildtype chitinase study

4.10.1 DNSA Assay for chitin oligomers quantification

DNSA assay was performed by incubating 1 mL of DNSA reagent

(1 g of 3,5 Di-nitrosalicylic acid was dissolved in 20 mL of 2M NaOH with constant mixing (The solution was heated to 50℃ to dissolve completely). Then 30 grams of sodium potassium tartrate was added to the solution at the rate of 5 grams till it dissolved completely, and the solution was diluted to a final volume of 100 mL distilled water) with 1 mL of reaction sample and boiled at 95℃ for 10 minutes. After cooling, the absorbance of the solution was read at 540 nm using a UV-visible spectrometer (Mekasha et al. 2017). The final absorbance obtained was used to estimate the concentration of reducing sugars released with the help of a calibration curve. The calibration curve was plotted with standard N-acetyl glucosamine at different concentrations (2 – 10 mM) as the X axis against OD at 540 nm as the Y axis. (Standard equation was $y = 0.6309x$, where y is Optical density, and x is the N-acetyl glucosamine concentration (mM)).

4.10.2 Bradford Assay for Protein Quantification

In this assay, 0.2 mL of sample was added to 1.8 mL of Bradford reagent and incubated in the dark at room temperature for 5 minutes. After incubation, the absorbance was determined at 595 nm using a UV-visible spectrometer. The final absorbance was used to estimate the protein concentration with the help of a Calibration graph. The calibration graph used different concentrations (10–50 $\mu g \cdot mL^{-1}$) of Bovine serum albumin Protein (BSA). The graph was plotted between different concentrations of BSA as the X-axis and its absorbance at 595 nm as the Y-axis (Standard equation $y = 0.0089x$, whereas x is BSA concentration and y is Optical density at 595 nm.

4.10.3 Phenol Sulphuric acid method for colloidal chitin quantification

This assay was used to quantify the concentration of the colloidal chitin used in the activity assay. 200 µL of colloidal was added to the test tube. 200 µL of 5% (v/v) phenol solution was added to the colloidal chitin and mixed using a vortex mixer for 2 minutes. 1 mL of concentrated Sulphuric acid was added to the test tube and mixed for 2 minutes. The mixture was incubated at 25-30℃ for 20 minutes in the water bath. The final absorbance of the solution was determined at 490 nm using a UV-visible spectrometer. The final absorbance was used to estimate the concentration of colloidal chitin with the help of a Calibration graph. The calibration graph was performed using different weights of chitin powder (0 – 10 mg) added to 200 µL of distilled water. The

graph was plotted between the amount of chitin as the X-axis and its absorbance at 490 nm as the Y-axis. (Standard equation was $y = 0.0137x$, where y is Optical density, and x is the amount of chitin powder (mg)).

4.10.4 Thin layer chromatography (TLC) analysis of chitin oligomers produced by wildtype chitinase

For the TLC study, a silica aluminium plate (20 cm X 15 cm) was used as a stationary phase and 240 mL of mobile phase solvent was prepared at a ratio of 5:4:2:1 of water-saturated n-butanol, methanol, ammonia, and water, respectively. To prepare water-saturated n-butanol, 40 mL of n-butanol was mixed with 5 mL of water for 10 min using a vortex mixer and left undisturbed for an hour. Two layers formed in which the top butanol layer was obtained and stored at 4℃. A spraying solution containing diphenylamine reagent was used for signal development. The solution included Reagent A (4 g diphenylamine in 100 mL of acetone), Reagent B (4 mL of aniline was added to 96 mL of acetone and mixed well) and Reagent C (85% orthophosphoric acid). 100 mL of reagent A was mixed with 100 mL of reagent B, and 20 mL of reagent C was added to the above mixture before spraying. The samples were loaded to 1.5 cm above the bottom of the silica plate. Different samples such as 5 µL of Chitin (1 mg. mL^{-1}), Chitosan (1 mg. mL^{-1}), 1 µL of Chitin oligomers (20 mg. mL^{-1}), N-Acetylglucosamine (1 mg. mL^{-1}), Glucosamine (1 mg. mL^{-1}) and 10 µL of three enzymatic reaction samples for chitin powder, flakes, and colloidal chitin, treated with *Ba*ChiA were added. For substrate sample preparation, 10 mg of chitin powder was added to 10 mL of distilled water and suspended well with a vortex mixer. Then 5 microliters of the suspension were loaded onto the TLC plate. Chitin oligomers are soluble in water; hence, if they were present in the chitin suspension, they would appear in the TLC. The samples were run to three fourth distance of the TLC plate for 3 hours. The plate was dried, and the spraying solution was sprayed onto the plate. (The entire plate was sprayed evenly with delicate sprays, achieved by spraying the solution 10 cm away from the plate. Both spray bottle and plate were kept vertical on the flat surface and facing each other while spraying). For the best results, after spraying, the plates were dried at 100–120℃ in the hot air oven till the spots appeared.

4.10.5 LC-MS analysis of chitin oligomers produced by wildtype chitinase

Bacillus aryabhattai was grown in 1% insoluble chitin-containing optimized media for 48 hours at 37℃, pH 7.5, under constant shaking of 120 rpm. The media volume was 20% of the conical flask volume (25 mL flask). After 48 hours, the biomass and insoluble chitin substrates were removed by centrifuging the sample at 10000 rpm for 10 minutes. The supernatant was removed and filtered through a 3 kDa centrifugal membrane filter. The filtration was achieved by centrifuging the tubes at 10000 rpm for 20 minutes. The retentate, which contained crude enzyme, was discarded. The 1 mL of purified cell-free supernatant was incubated with 1% (w/v) chitin powder and flakes at 55℃ overnight to obtain the maximum concentration of chitin oligomers. Again, chitin substrates were removed by centrifuging the sample at 10000 rpm for 10 minutes. The supernatant containing chitin oligomer was separated from the other impurities by filtering the supernatant through a 3 KDa centrifugal membrane filter. Different chitin oligomers produced were identified using high-resolution liquid chromatography-mass spectrometry (HRLCMS). The Acquity UPLC Xevo G2 QTOF MS (Waters, USA) was used for LCMS analysis. In UPLC, the BEH amide column (100 mm X 2.1 mm, 1.7 µm particle size and pore size of 130 Å) was used. Two mobile phases, water and acetonitrile, were used at a 30:70 ratio at a 0.1 mL min^{-1} flow rate. The inlet method comprises 0 to 20 min, 30% water and 70% acetonitrile; at 21 to 31 min, 10% water and 90% acetonitrile. The injection volume used was 0.5 µL. PDA detectors were used at a UV wavelength range of 190 nm to 250 nm. In MS, QTOF analyzers were analysed in positive mode and a mass range of 100 to 1500 m/z. Capillary and Cone voltage were 3 kV and 30 V, respectively; Source and Desolvation gas temperatures were 150℃ and 450℃, respectively; Cone gas and Desolvation gas flow rates were 50 $L \cdot h^{-1}$ and 600 $L \cdot h^{-1}$. The retention time (RT) of peaks for different oligomers was identified using an LC chromatogram, and m/z values of corresponding RT peaks were analysed using the MS spectrum. Standard chitin oligomers, substrate and enzyme blank samples used for TLC were also subjected to LCMS analysis.

B. RECOMBINANT CHITINASE STUDY

4.11 Chemicals used

Genomic DNA isolation kit (Himedia, India, CatLog No. MB505), Lysozyme (Himedia, India, CatLog No. MB098), Proteinase K (Himedia, India, CatLog No. MB086), RNase A (Himedia, India, CatLog No. DS0003), HiElute miniprep spin column (Himedia, India, CatLog No. DBCA03), Genomic DNA elution buffer (Himedia, India, CatLog No. DS0040), Hi-proof DNA polymerase kit (Himedia, India, CatLog No. MBT069), Plasmid DNA isolation kit (Qiagen, Germany, CatLog No. 12123), NcoI restriction enzyme (NEB, UK, CatLog No. R3193S), XhoI restriction enzyme (NEB, UK, CatLog No. R0146S), Cut smart restriction buffer (NEB, UK, CatLog No. B6004S), T4 DNA ligase kit (NEB, UK, CatLog No. B6004S), Ni-NTA agarose (Qiagen, Germany, CatLog No. B6004S), Pre stained Protein ladder (Himedia, India, CatLog No. MBT092), SDS running buffer (Himedia, India, CatLog No. ML042), TAE running buffer (Himedia, India, CatLog No. MBT016), Chitin oligomers (TCI chemicals, CatLog No. C2762), Bradford reagent (Himedia, India, CatLog No. ML106), Bovin serum albumin (Himedia, India, CatLog No. GRM105), N–acetyl glucosamine (TCI chemicals, India, CatLog No. A0092), Chitin powder (LOBA chemie, India, CatLog No. 1398-61-4), Chitin flakes (Himedia, India, CatLog No. GRM2356), TLC Silica gel (Merk, Germany, CatLog No. HX16775554), LB broth (Himedia, India, CatLog No. G557), LB Agar (Himedia, India, CatLog No. M557), IPTG (Himedia, India, CatLog No. MBT072), Ampicillin (Himedia, India, CatLog No. MD068) and Chloramphenicol (Himedia, India, CatLog No. CMS218). 3 kDa Pall centrifugal membrane filters (Pall laboratory, USA, CatLog, MCP003C41), Phenol, Chloroform, Isoamyl alcohol, Sodium Acetate, Isopropanol, Calcium chloride, Glycerol, Acrylamide, Bis-acrylamide, SDS, Ammonium persulphate, TEMED, Tris Base, Tris HCl, β – mercaptoethanol, Bromophenol blue, Coomassie blue, Methanol, Glacial acetic acid, Ammonia, Butanol, Magnesium chloride, Cobalt chloride, Sodium chloride, Manganese chloride, Nickel chloride. All the chemicals used above are analytical grade.

4.12 Cloning of chitinase gene into recombinant *E. coli Rosetta PLysS*

4.12.1 Gene sequence annotation and 3D structure modelling and validation of *Ba*ChiA

The 3D structure of the *Ba*ChiA was developed by Homology modelling

(using Maestro software, Schrodinger, New York, USA). The modelling was performed using the amino acid sequence of the chitinase, which was obtained from the Uniport database. The developed model was validated using EXPASY SWISS-MODEL online tools, which explains the Ramachandran plot of the developed protein model. The PDB structure of the chitinase of *Serratia marcescens* was obtained from the RCBS PDB database for comparison with the developed *Ba*ChiA structure. Different domains in the chitinase of *Serratia marcescens* and *Bacillus aryabhattai* were analysed using their structure and sequence. The amino acids involved in active sites of the catalytic domain were identified, and the mechanism of chitin hydrolysis using identified amino acids was studied.

4.12.2 Genomic DNA isolation from *Bacillus aryabhattai*

A single colony of *Bacillus aryabhattai* was inoculated with 10 mL of LB broth. The inoculated culture was incubated at 37℃ for 16 hours at 120 rpm in an incubator shaker. 2.0 mL of *Bacillus aryabhattai* culture was centrifuged at 10000 rpm for 10 minutes at room temperature. The genomic DNA from the bacteria was isolated using a Genomic DNA isolation kit. The pellets were obtained and suspended in 200 µL of lysozyme solution (45 mg. mL^{-1}) and incubated at 37℃ for 30 minutes. Then, 20 µL of proteinase K (20 mg. mL^{-1}) and 20 µL of RNase A (20 mg. mL^{-1}) were added and incubated at room temperature for 5 minutes. 200 µL of lysis solution C1 was added, mixed by inverting the tubes 5 to 6 times and incubated at 55℃ for 30 minutes. 200 µL of ethanol (95%) was added to the lysate and mixed by inverting the tubes. The lysate was transferred to the HiElute miniprep spin column and centrifuged at 10000 rpm for 1 minute. The flow-through was discarded, and 500 µL diluted prewash solution was added to the column and centrifuged at the same speed and time. After discarding the flow-through, the empty column was centrifuged at the same speed for 1 minute. Then, the DNA was eluted by adding a Genomic DNA elution buffer to the column and centrifuged at the same speed and time. Flow through containing genomic DNA was subjected to further experiments. Genomic DNA was visualized in agarose gel under UV light. DNA concentration and purity were determined using a UV-visible spectrophotometer at 260 and 280 nm.

4.12.3 pET 23a plasmid isolation

pET23a plasmid DNA was isolated from *E. coli DH5α* using Qiagen Spin Miniprep Kit. A single colony of bacteria was inoculated with 20 mL of LB broth with 100 μg. mL^{-1} ampicillin and incubated at 37℃ for 16 hours and at 120 rpm. The media volume was 20% of the flask volume (100 mL conical flask). Once the Optical density (OD) of culture reached 1.5 – 1.8, 2 mL of culture was added to a 2 mL tube and centrifuged at 10,000 rpm for 10 minutes at room temperature. The pellet was suspended in 250 μL of P1 Buffer. 250 μL of P2 Buffer was added to the tube and mixed by inverting the tubes 4-6 times until the solution became clear. 350 μL of N3 Buffer was added to the tube, mixed, and centrifuged at 10,000 rpm for 10 minutes. The supernatant was transferred to the QIAprep spin column and centrifuged for 2 minutes at 10000 rpm. After discarding Flow through, 750 μL of wash buffer was added to the column and centrifuged at the same speed and time. Flow through was discarded, and the empty column was centrifuged at the same speed and time. The column was transferred to a new 1.5 mL centrifugal tube. Plasmid DNA was eluted by adding 50 μL of elution buffer and centrifuging at 10000 rpm for 5 minutes. The plasmid concentration and purity were determined by UV-visible spectrometer at 260 and 280 nm.

4.12.4 Polymerase chain reaction (PCR) for chitinase gene isolation

PCR was performed to isolate the chitinase gene from the *Bacillus aryabhattai* genome and to amplify the gene with higher concentrations. PCR was performed using a Hi-proof DNA polymerase kit. The different components used in the kit are shown in **Table 4.4**. The PCR cycle condition for gene isolation is shown in **Table 4.5**. The primers were designed using snap gene software (GSL Biotech LLC, Boston, USA)**.** The primers were designed to insert the restriction site for NcoI and XhoI to both ends of the chitinase gene. The Primer details are shown below

Forward Primer: 5'-CCC**GGATCC**ATGGGCATGAGTAAAG -3'

NcoI restriction site

Reverse Primer: 5'-GTCTGCTAAGGTG**CTCGAG**AAAGTTG-3'

XhoI restriction site

Components	Volume used for 50 µL Reaction	Final concentration
10 X Reaction buffer	5 µL	1X
10 mM dNTPs	5 µL	1 mM
10 µM Forward Primer	2.5 µL	0.5 µM
10 µM Reverse Primer	2.5 µL	0.5 µM
Template DNA	5 µL	>145 ng
Q5 DNA Polymerase	0.5 µL	0.02 U· μL^{-1}
Nuclease free water	29.5 µL	-

Table 4.4. Components required for PCR experiments

No. of cycles	Step	Temperature	Time
1	Initial Denaturation	95℃	10 Minutes
10	Denaturation	95℃	30 Seconds
	Annealing	56.5℃	20 Seconds
	Extension	72℃	90 Seconds
30	Denaturation	95℃	30 Seconds
	Annealing	69℃	20 Seconds
	Extension	72℃	90 Seconds
1	Final Extension	72℃	10 Minutes

Table 4.5. PCR cycle for Chitinase gene isolation

4.12.5 Restriction Digestion of pET23a plasmid and gene

Based on standard NEB protocol, restriction digestion of pET23a plasmid and isolated chitinase gene was performed using NcoI and XhoI restriction enzymes. Different components used in the reaction are shown in **Table 4.6.**

The reaction mixture was incubated at 37℃ for 2 hours. After 2 hours, the reaction was stopped by incubating the sample at 65℃ for 20 minutes. Restricted products

Component	For Gene digestion	For Plasmid digestion	Final concentration
10X Cut smart buffer	5 µL	5 µL	1X
Template DNA	12 µL	8 µL	1 µg
NcoI-Enzyme	1 µL	1 µL	10 units· mL^{-1}
XhoI-Enzyme	1 µL	1 µL	10 units· mL^{-1}
Water	31 µL	35 µL	-

Table 4.6. Reaction condition for Restriction digestion of Plasmid/Gene

were visualized in agarose gel, and concentration was estimated by measuring absorbance at 260 nm using a UV-visible spectrometer.

4.12.6 Ligation of restricted plasmid and gene

T4 DNA ligase (New England Biolabs, India) was used to ligate the restricted pET 23a plasmid and chitinase gene. A ligation reaction was performed using a molar ratio of 1:3 of plasmid to insert and incubated at 16℃ for 16 hours. Different components used in the ligation experiment are shown in **Table. 4.7**.

Components	Volume for 20 µL reaction	Final Concentration
Ligase Buffer (10X)	2 µL	1X
T4-DNA ligase (400 units· μL^{-1})	1 µL	20 units· μL^{-1}
pET 23a plasmid (40 ng· μL^{-1})	3 µL	120 ng
Chitinase gene (30 ng· μL^{-1})	3.5 µL	105 ng
Water	10.5 µL	-

Table 4.7. Reaction Condition for Ligation

After 16 hours, the Ligation reaction was stopped by incubating the sample at 65℃ for 10 minutes. The ligated sample was used for transformation experiments. The ligated plasmid was transformed to *E. coli Rosetta PLysS.*

4.12.7 Competent *E. coli Rosetta pLysS* preparation

E. coli Rosetta pLysS cells were made competent for transforming cloned pET 23a plasmid into it using the standard calcium chloride method. The starter culture was

prepared by inoculating a single *E. coli Rosetta pLysS* colony in sterile LB media containing chloramphenicol (35 µg· mL^{-1}) and incubated at 37℃ overnight. 100 ml LB Broth was inoculated with 1% starter culture and incubated at 37℃ at 120 rpm till the OD reached 0.4 to 0.6. After the OD reached 0.4 to 0.6, the cells were immediately transferred to 50 mL centrifugal tubes and incubated in ice for 30 minutes. The culture was centrifuged in a prechilled 50 mL centrifuge tube at 5000 rpm for 10 minutes at 4℃. The supernatant was discarded, and the pellet was suspended in 20 mL of prechilled and 0.45 µm filter sterilized 0.1M $CaCl_2$, incubated on ice for 30 minutes and centrifuged at 4℃, at 5000 rpm for 10 minutes. After discarding the supernatant, the pellet was resuspended in 5 mL of prechilled and 0.45 µm filter sterilized ice-cold 0.1M CaCl2 with 15% glycerol. 100 µL of cells were aliquot in a 1.5 ml centrifuge tube and could be used for transformation or stored at -80℃.

4.12.8 Transformation of Cloned pET 23a to *E. coli Rosetta pLysS*

Ligated pET 23a plasmid with chitinase gene was transformed into *E. coli Rosetta pLysS* using heat shock method. 100 µL Competent cells were thawed on ice for 45 minutes. 10 µL of ligation sample was added to the competent cell (The ratio of plasmid and competent cells should be 1:10) and incubated on ice for 30 minutes. The sample was incubated at 42℃ for 90 seconds, transferred to ice, and incubated for 10 minutes. 1 ml of sterile LB media was added to the tube and incubated at 37℃, 160 rpm for 3 hours. Transformed cells were spread on the LB agar plate containing Chloramphenicol (35 µg· mL^{-1}) and Ampicillin (100 µg· mL^{-1}). The plate was incubated at 37℃ overnight and screened for positive colonies.

4.12.9 Confirmation of cloned plasmid transformation into *E. coli Rosetta pLysS*

A random colony was picked from the agar plates and incubated in 10 mL LB broth containing chloramphenicol (35 µg· mL^{-1}) and ampicillin (100 µg· mL^{-1}) antibiotics at 37℃, 120 rpm for 16 hours. Plasmid DNA was isolated from *E. coli Rosetta PLysS* using a Qiagen Spin Miniprep Kit. The restriction digestion of isolated plasmid was performed with BamHI and XhoI restriction enzymes to confirm the transformation of the cloned plasmid into *E.coli Rosetta PLysS*. For further confirmation, the cloned plasmid was subjected to PCR. The chitinase gene in the plasmid was amplified using primers designed to isolate the chitinase gene from the *Bacillus aryabhattai* genome.

The sequence of the cloned plasmid was also obtained by Sanger sequencing, which Eurofins Scientific, Bangalore, India, performed.

4.13 Expression of Chitinase in *E. coli Rosetta pLysS* cells by IPTG induction method

Two different bacterial cultures were used to perform the expression study of the *Ba*ChiA. First, a single colony of *E. coli* containing a cloned plasmid was added to 50 mL LB broth (containing ampicillin (100 $\mu g \cdot mL^{-1}$) and chloramphenicol (35 $\mu g \cdot mL^{-1}$)) in a 250 mL conical flask. The culture was incubated at 37℃ at 120 rpm until the culture's optical density (OD) reached 1.5. Then, the culture was induced by 1.5 mM Isopropyl β-D-1-thiogalactopyranoside (IPTG) and incubated at 16℃ at 120 rpm for 48 hours. Second, a single colony of *E. coli* containing uncloned plasmid was added to 50 mL of LB broth (containing ampicillin (100 $\mu g \cdot mL^{-1}$) and chloramphenicol (35 $\mu g \cdot mL^{-1}$)) in a 250 mL conical flask and incubated in the same condition. After 48 hours, the cell pellets from two cultures were isolated by centrifugation at 6000 rpm for 10 minutes. The cell pellets were resuspended in 50 mM Tris buffer at pH 8.0 containing 0.5 M PMSF (Phenyl methyl sulfonyl fluoride). PMSF is a protease inhibitor added to lysis buffers to prevent the degradation of recombinant chitinase by protease enzymes. Then, the cells were lysed by sonication using a probe Sonicator (Power: 500 watts and Frequency: 20 KHz). The conditions for sonication were as follows: pulse ON and OFF time was 10 seconds. The pulse amplitude was 60%. And the time of sonication was 90 seconds. The lysed sample was centrifuged at 10000 rpm for 20 minutes.

SDS PAGE protocol:

Biorad SDS PAGE set-up was used to carry out SDS PAGE.

Components	**Volume**
Molecular grade water	3.4 mL
Acrylamide (30%)	4 mL
1.5 M Tris-Cl buffer (pH 8.8)	2.5 mL
SDS (20%)	50 µL
APS (10%)	100 µL
TEMED	10 µL

Table 4.8 Composition of Separating gel (Final acrylamide concentration was 12%)

The supernatant containing chitinase enzyme was subjected to 12% SDS-PAGE gel for analysis. The protocol for preparing SDS PAGE gel and sample is shown below. The SDS PAGE gel and loading buffer composition are shown in **Tables 4.8, 4.9, and 4.10**.

Components	Volume
Molecular grade water	2.7 mL
Acrylamide (30%)	0.8 mL
1M Tris-Cl buffer (pH 6.8)	0.5 mL
SDS (20%)	20 µL
APS (10%)	40 µL
TEMED	10 µL

Table 4.9 Composition of Staking gel (Final acrylamide concentration was 10%)

30% Acrylamide solution was prepared by dissolving 29 grams of Bis acrylamide and 1 gram of acrylamide in 100 mL of distilled water. 1.5 M Tris-Cl buffer (pH 8.8) was prepared by dissolving 18.15 grams of Tris Base in 100 mL of distilled water. The solution pH was adjusted to 8.8 using 4N HCl (Do not use NaOH). 20% SDS was prepared by dissolving 0.2 gram of SDS in 1 mL of distilled water.

Components	Volume
1M Tris-HCl, pH 6.8	2.5 mL
10% SDS	1.0 mL
14.3M β-mercaptoethanol	2 mL
0.1% Bromophenol blue	0.8 mL
100% Glycerol	4 mL
Distilled water	Make the total volume up to 10 mL.

Table 4.10 Composition of sample loading buffer.

10% Ammonium Per Sulphate (APS) was prepared by dissolving 0.1 grams of APS in 1 mL of distilled water.10 µL of supernatant and Pellet sample was mixed with 50 µL loading dye. The sample was then heated for 10 min at 95℃ to denature the proteins.

Once the sample was prepared, 10 µL of the sample and 5 µL of pre-stained protein ladder were loaded onto the gel. The Electrophoresis setup was subjected to 110 V. Gel was immersed in the staining solution in a plastic box (0.1 gram Coomassie blue, 40 mL methanol, 50 mL distilled water and 10 mL glacial acetic acid) and incubated in a shaking rocker for two hours. Then, the gel was immersed in a destaining solution (45 mL methanol, 45 mL distilled water and 10 mL glacial acetic acid) and incubated for 16 to 24 hours until the bands were visible. After destaining, the gel was viewed under visible light.

4.14 Optimization of processing parameters of IPTG induction method

High-level recombinant protein expression in *E. coli* often aggregates the expressed protein into inclusion bodies. The formation of inclusion bodies imposes a significant hurdle in the production and purification of recombinant proteins. The secretion of inclusion bodies can be reduced by reducing the protein expression rate, which can be achieved by restricting bacterial growth. Thus, optimization of process parameters such as growth phase to add IPTG for induction, IPTG concentration, temperature, incubation time, and glycerol concentration plays an essential role in producing soluble recombinant protein forms. Two phases of growth were followed. In the first phase, bacteria were grown in LB broth at 37℃, 120 rpm till the optical density of culture reached 1.5, and in the second phase, IPTG was added to the culture and bacteria were grown at 10-20℃, 120 rpm for 48 hours (At 48 hours, bacterial growth reached maximum). After incubation, the cell pellets were isolated by centrifugation at 6000 rpm for 10 minutes. The cell pellets were resuspended in 50 mM Tris buffer pH 8.0. Then, the cells were lysed by sonication. The lysed sample was centrifuged at 10000 rpm for 20 minutes. Both pellet and supernatant were subjected to SDS PAGE analysis.

4.14.1 Effect of IPTG induction at different growth phase

In four 250 mL conical flasks, 50 mL of *E. coli* culture was incubated at 37℃, 120 rpm. In each flake, 1.0 mM IPTG was induced at different optical densities: 0.6 OD (early log phase), 1.2 OD (mid-log phase), 1.5 OD (early stationary phase), 1.7 OD (late stationary phase) and then incubated in 16℃ for 24 hours to express recombinant protein. The effect of IPTG induction at different growth phases to

minimize the inclusion body formation was investigated. The supernatant and pellets containing soluble recombinant chitinase and inclusion bodies were separated and subjected to SDS-PAGE analysis. The enzyme activity of soluble crude chitinase was quantified (***Refer to section 4.18 for chitinase activity assay protocol***).

4.14.2 Effect of IPTG concentration on Inclusion Bodies Formation

In eleven different 250 mL conical flasks, 50 mL of *E. coli* culture was incubated in an orbital shaker at 37℃, 120 rpm under observation until the optical density (O.D) of the culture reached 1.5 (log phase), which was optimized in the previous method. Then, each flask was induced with different IPTG concentrations ranging from 0.2 mM to 4.0 mM and incubated at 16℃ for 48 hours. After 48 hours, the cells were lysed, and the supernatant and pellets were separated. The supernatant and pellet were subjected to SDS-PAGE analysis, and enzyme activity was quantified.

4.14.3 Effect of incubation time after IPTG induction

In four 250 mL conical flakes, 50 mL of *E. coli* culture was incubated in an orbital shaker at 37℃, 120 rpm under observation until the Optical density (O.D) of the culture reached 1.5 (log phase). Each flask was induced with 1.5 mM IPTG and was incubated at 16℃, 120 rpm for different times, such as 24, 36, 48 and 60 hours. After incubation, the cells were lysed, and the supernatant and pellets were separated. The supernatant and pellet were subjected to SDS-PAGE analysis, and enzyme activity was quantified.

4.14.4 Optimization of Glycerol-Based Media

After optimizing the physical parameters, the LB broth was supplemented with glycerol as a carbon source to enhance biomass and chitinase production. The concentrations ranging from 1 – 4% v/v of glycerol were added to the 50 mL of LB broth in a 250 mL conical flask and incubated at 37℃, 120 rpm under observation until the Optical density (O.D) of the culture reached 1.5 (log phase). Flasks were then induced with 1.5 mM IPTG and incubated at 16℃ at 120 rpm for 48 hours. After 48 hours, the cells were lysed, and the supernatant and pellets were separated. The supernatant and pellet were subjected to SDS-PAGE for analysis, and the enzyme activity of chitinase was determined.

4.15 Expression of chitinase by autoinduction media for higher yields

The expression was performed using Terrific Broth (TB) to increase biomass concentration and protein yield. 100 mL of TB media (Tryptone 12 g. L^{-1} (1.2%), Yeast Extract 24 g. L^{-1} (2.4%), Glycerol 0.5 mL (0.5%)) was prepared. TB salts (0.17 M KH_2PO_4 and 0.72 M K_2HPO_4) were measured for 10 mL and were autoclaved separately. After the autoclave, 45 mL of TB media and 5 mL of TB salts were mixed in a 250 mL conical flask. Further, the remaining carbon sources, i.e., 0.05% glucose (10% stock solution) and inducer 0.2% lactose (8% stock solution), were sterilized using 0.22 μm syringe filters and added to 50 mL culture. Also, filter-sterilized ampicillin (100 μg· mL^{-1}) and chloramphenicol (25 μg· mL^{-1}) was added along with 5% inoculum in a 250 mL conical flask, and the culture was incubated at 16℃, 180 rpm for 48 hours (At 48 hours the cell growth was maximum). After incubation, cells were lysed, and both soluble enzyme and inclusion bodies were analysed using SDS PAGE. The enzyme activity of soluble chitinase was also determined.

4.16 Statistical optimization of chitinase expression using the Taguchi method

Genichi Taguchi first developed the Taguchi method to determine the effect of process parameters in biodiesel production. Unlike other factorial designs, this method requires minimal experiments to perform optimization, even for a more significant number of process parameters. This design considers the S/N ratio to determine the interaction of parameters and response. Here, the 'signal' represents the desirable value, whereas 'noise' represents the undesirable value. There are three types of the S/N ratio: the smaller the-better, the bigger the-better, and the nominal the-better. The type of S/N ratio preferred depends on the desirable response. The SN ratio for this criterion is shown below:

$$\frac{S}{N} = -10log_{10}\left(\frac{\sum\left(\frac{1}{y_i^2}\right)}{n}\right)$$

Y_i is the response value, and n is the number of experiments.

In this study, using the autoinduction method, a 5-level for different physical parameters and media components was considered to reduce the inclusion bodies formation in chitinase expression. Physical parameters such as Temperature,

incubation time, shaking speed, Lactose and glucose concentration were optimized using the Taguchi method. The experiment, constituting five factors with 25 experimental runs, was generated using Minitab software (UK). The different levels of parameters are shown below in **Table 4.11**.

Parameters	**Level of Variable**				
	1	**2**	**3**	**4**	**5**
Temperature (℃)	10	12.5	15	17.5	20
Incubation time (hours)	12	24	36	48	60
Shaking speed (Rpm)	120	130	140	150	160
Glucose concentration (%)	0	0.025	0.05	0.075	0.1
Lactose concentration (%)	0.5	1.0	1.5	2.0	2.5

Table 4.11 Five levels Taguchi design Matrix with five variables

4.17 Purification of chitinase by Ni-NTA affinity chromatography

The expressed chitinase was purified by affinity chromatography using the Ni-NTA agarose. The chitinase has 6X histidine tags in the C terminal end, explicitly bound to nickel metal in the Ni-NTA column. Initially, 2 mL of Ni-NTA slurry (1 mL bed volume) was added to the 15 mL tube and centrifuged at 3000 rpm for 2 minutes. The supernatant was removed. The column (pellet) was equilibrated by adding 5 mL of Lysis buffer (50 mM Tris pH 8.0, 300 mM NaCl, 10 mM Imidazole) and centrifuged at the same speed and time as above, and the supernatant was discarded. The above step was repeated. Lysate (supernatant obtained after sonication) was added to the pellet (Agarose bed) and transferred to the flow tube. The lysate and agarose were incubated at 4℃ for 2 hours. After incubation, the lysate sample was collected and marked as flow through sample. To the column**,** 10 mL of wash buffer (50 mM Tris pH 8.0, 300 mM NaCl, 25 mM Imidazole) was loaded to remove the non-specific bound proteins and collected through the flow tube. The above step was repeated. Pure chitinase was eluted with 2 mL of elution buffer (50 mM Tris pH 8.0, 300 mM NaCl, 250 mM Imidazole, 10% (v/v) glycerol). All collected samples were subjected to 12% SDS-PAGE analysis. Purified chitinase concentration was determined by performing a Bradford assay (***Refer to section 4.10.2 for Bradford assay protocol***).

4.18 Chitinase activity assessment

Chitinase activity assay was performed by incubating 1 mL of 1% (w/v) of chitin

substrates with 1 mL of purified chitinase prepared in 50 mM Tris buffer (pH 8.0) and incubated at 55℃ for 1 hour. After incubation, the reaction mixture was centrifuged at 10000 rpm for 10 min to remove the unused chitin substrates. The supernatant containing chitin oligomers was obtained. The 1 mL supernatant was subjected to DNSA assay to determine the product concentration and chitinase activity. One unit of chitinase activity is defined as one micromole of chitin oligomers released per minute under the assay conditions. One unit of specific chitinase activity is defined as one micromole of chitin oligomers released per minute and mg of the chitinase under the above-performed assay conditions. Thus, it was required to quantify the chitinase concentration in the supernatant. Chitinase concentration was determined using Bradford assay (***Refer to section 4.10.1 for DNSA assay protocol***).

4.19 Chitinase Characterisation Study

Chitinase activity was characterized by various parameters such as the pH of the buffer, reaction temperature, buffer components, and reaction time. Metal ions, and since the source of this chitinase was marine, the NaCl could alter chitinase activity. Thus, chitinase activity was also characterized by the presence of sodium metal ions.

4.19.1 Effect of pH, Buffer, and Temperature on chitinase activity

Initially, chitinase activity was performed in different pH ranges from 5 to 9 to determine the optimum pH and buffer. Different buffers with overlap at different pH levels were considered to study the effect of buffer and pH in a single experiment. The different buffer solutions considered were 50 mM citrate buffer (pH 5, 6), sodium phosphate buffer (pH 6, 7), Tris base buffer (pH 7, 8), and Borate buffer (pH 8, 9). For chitinase activity assessment at different pH and buffers, 1 mL of chitinase prepared in different buffers and pH was added to 1 mL of 1% (w/v) colloidal chitin and incubated at 37℃ for 30 minutes. To determine the optimum temperature for the highest chitinase activity, the chitinase activity assay was performed in different temperature ranges (40℃, 45℃, 50℃, 55℃, 60℃ and 65℃) at optimised pH, and buffer for 30 minutes. DNSA assay was performed on all the above samples to determine the enzyme activity.

4.19.2 Effect of Metal ions and NaCl on Enzyme Activity

Effects of different metal ions on the chitinase activity were determined by adding

metal ions such as Manganese ion (Mn^{2+}), Magnesium (Mg^{2+}), Nickle (Ni^{2+}), Cobalt (Co^{2+}), Calcium (Ca^{2+}) and Sodium (Na^{+}) in the form of 5 mM chloride salts to the reaction mixture. The reaction mixture was prepared by mixing 1 mL of the chitinase with 1 mL of 1% (w/v) colloidal chitin and the above metal ions. The reaction mixture was incubated at optimized pH and temperature for 30 minutes. Since the source of the chitinase is marine, the primary salt present in the seawater is NaCl. Thus, the effect of Na^{+} on chitinase activity was also determined.

4.20 Michaelis Menten kinetic parameters estimation

The enzyme kinetic parameters (*Km*, *Vmax*, *Kcat*, and catalytic efficiency) were determined by performing a chitinase activity assay for different colloidal chitin concentrations ranging from 0.1 mg. mL^{-1} to 50 mg. mL^{-1}. The chitinase velocity was determined by performing a DNSA assay for the above samples. The line graph was plotted for chitinase velocity (*v*) as the Y axis and substrate concentration (*S*) as the X axis to confirm whether the chitinase obeys Michaelis-Menten kinetics. The Michaelis-Menten kinetics parameters (*Km*, *Vmax*) were obtained by plotting Lineweaver-Burk plots in which *1/v* was the Y axis, *1/S* was the X axis, slope and intercept were *Km/Vmax* and *1/Vmax* respectively. The *Kcat* and catalytic efficiency were determined using the following formula:

$$Kcat = \frac{Vmax}{[E]}$$

Kcat is turnover number (min^{-1}), *Vmax* = maximum chitinase velocity (µmole min^{-1}) and *[E]* = chitinase concentration (µmole).

$$Catalytic\ efficiency = \frac{Kcat}{Km}$$

Kcat is turnover number (mL. mg^{-1}. $second^{-1}$), Km is Michaelis-Menten constant (mg. mL^{-1}). Moreover, the chitinase activity assay was performed against 1% (w/v) insoluble chitin substrates such as chitin powder and chitin flakes obtained from shrimp shells.

4.21 Antifungal activity of recombinant chitinase

The primary component responsible for the fungal cell wall is chitin. Thus, the developed recombinant chitinase could be used as an antifungal agent. The zone of inhibition method determined the antifungal activity of the recombinant chitinase.

Fungal pathogens such as Candida albicans, Fusarium solani and Penicillium chrysogenum were used in this study. Three Potato dextrose agar plates were prepared for three fungal cultures. Each fungus was spread in each plate, and three wells were made there. 100 µL of purified chitinase was added to **well 1**, the uninduced crude lysate sample was added to **well 2**, and autoclaved LB broth was added to **well 3** as a control. The antifungal activity was measured after incubating three fungal plates at 25℃ for 48 hours. A clearance zone around the well was assessed to confirm the antifungal property of the chitinase.

4.22 Analytical Methods for recombinant chitinase study

4.22.1 TLC and LC-MS analysis of chitin oligomers produced by *Ba*ChiA

As a result of incubating chitin substrates with chitinase, different chitin oligomers were released. Thus, the different chitin oligomer products formed from the reaction of the purified recombinant chitinase with the different chitin substrates were identified using TLC and LC-MS. Enzyme reaction was performed against colloidal Chitin and insoluble Chitin substrates such as chitin powder and flakes. 1% (w/v) of chitin powder and flakes were added to the 1 mL of purified chitinase with 5 mM cobalt chloride and 400 mM NaCl and then incubated at 55℃ and pH 8 for 30 minutes. After incubation, the reaction sample was centrifuged at 10000 rpm for 10 minutes, and chitin substrates were removed. The chitin oligomers from the reaction mixture were purified through a 3 kDa centrifugal filter membrane by centrifuging the filter at 10000 rpm for 20 minutes. Flow through, which contained chitin oligomer products with a concentration of 50 mg. mL^{-1}, was used for TLC analysis. The above experiments were performed on substrate and enzyme blank samples. In the substrate blank, the chitin substrates were absent (1 mL of purified chitinase with 5 mM cobalt chloride and 400 mM NaCl was present). In the enzyme blank, the chitinase was absent (1% (w/v) chitin substrates in 20 mM Tris buffer with 5 mM cobalt chloride and 400 mM NaCl was present). The standard chitin oligomers of concentration 20 mg. mL^{-1} (chitin monomer till hexamer) were also analysed. ***(For TLC and LC-MS protocol, refer to sections 4.10.4 and 4.10.5)***.

CHAPTER 5
RESULTS AND DISCUSSION

A. WILDTYPE CHITINASE STUDY

5.1 Isolation and screening of chitinase-producing strain

A total of 57 closely spaced colonies were visible after the first isolation. A second serial dilution and subsequent growth on the chitin-containing agar plate revealed nine distinguished colonies. Four rounds of purification of these colonies were carried out, and these purified colonies were further screened for their ability to hydrolyze chitin. After 48 hours of incubation, the plates of the isolates were later flooded with Lugol's iodine. The zone was visible in one of the isolates, SED 1, as shown in **Figure 5.1**.

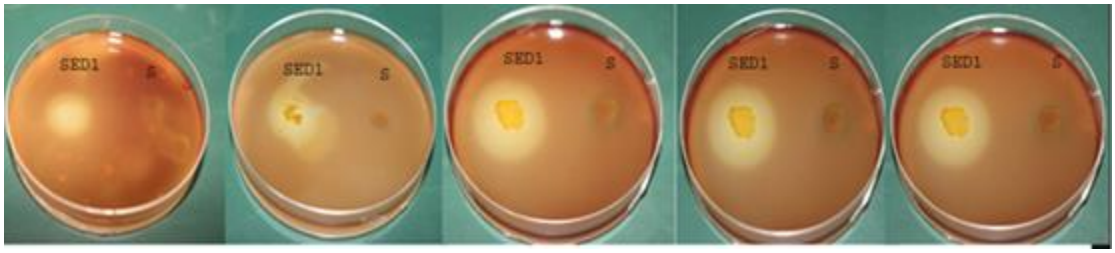

Figure 5.1 Screening of SED1 isolate for chitinase activity in the colloidal chitin plates flooded with Lugol's iodine.

A similar observation was reported (Kumar et al. 2018a) in *Paenibacillus sp*. which was isolated from the seafood dumping waste for chitin degradation in shrimp waste. The biochemical tests for primary identification revealed that the SED1 strain was a motile, gram-positive bacterium. It was amylase producer, catalase, MR-VP, glucose, lactose, and fructose positive.

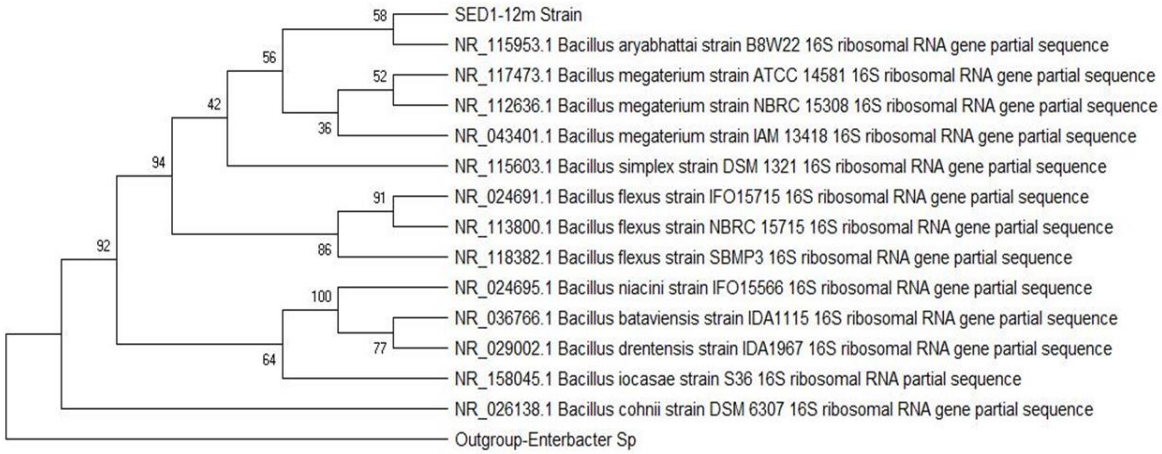

Figure 5.2 Phylogenetic tree of SED1 isolate, Enterobacter species, was taken as an out-group.

The isolate was fermentative without H_2S gas production and negative for the indole

test. The initial biochemical characterization of the isolate hinted at it being *Bacillus*. To find the species of the isolate, the 16S rRNA gene analysis was performed for the genome of the isolate. The phylogenetic positioning of the isolate is shown in **Figure 5.2**. The results confirmed that the strain SED1 was *Bacillus aryabhattai* (16S rRNA Genbank Accession number: NR_118442). The isolate SED 1 has been submitted to the National Culture for Microbial Resource (NCMR), India, with the accession ID MCC 3987.

5.2 Growth of *Bacillus aryabhattai* and its chitinase activity on different chitin substrates

The growth profile of *Bacillus aryabhattai* and *Serratia marcescens* in a growth media containing chitin flakes, powder, and colloidal chitin are shown in **Figures 5.3a, b and c,** respectively. The line plot and left horizontal axis represent both bacteria's growth profiles until the 72nd hour. The growth rate of *Bacillus aryabhattai* (μ = 0.16 h^{-1}) was high compared to *Serratia marcescens* (μ = 0.097 h^{-1}) in chitin powder, which confirmed that *Bacillus aryabhattai* efficiently utilized the chitin powder for its growth. *Bacillus aryabhattai* (μ = 0.043 h^{-1}) also grew in the medium containing chitin flakes, whereas no growth was observed for *Serratia marcescens*. These results confirmed that *Bacillus aryabhattai* was adapted to grow in insoluble chitin substrates. *Bacillus aryabhattai* (μ = 0.23 h^{-1}) and *Serratia marcescens* (μ = 0.17 h^{-1}) had similar growth rates in the colloidal chitin medium. The activity profile of chitinase present in the cell-free spent media of *Bacillus aryabhattai,* and *Serratia marcescens* against chitin flakes, powder, and colloidal chitin is shown in **Figures 5.3a, b and c,** respectively. The bar graphs and right horizontal axis explain the chitinase activity variation of *Ba*ChiA (*Bacillus aryabhattai* chitinase) and *Serratia marcescens* chitinase. Both *Ba*chiA and *Serratia* chitinase achieved highest activity of 27.1 U· mL^{-1} (Specific activity is 71.9 U· mg^{-1}) and 14.6 U· mL^{-1} (53.6 U· mg^{-1}), respectively against chitin powder at 36^{th} hour. Upon changing the substrate from chitin powder to flakes, the *Ba*ChiA maximum activity observed was 23.8 U· mL^{-1} (33.9 U· mg^{-1}). In contrast, there was no enzyme activity in *Serratia marcescens.* Against colloidal chitin, the *Ba*ChiA activity was 32.4 U· mL^{-1} (80.9 U· mg^{-1}), whereas *Serratia marcescens* chitinase activity was 22.1 U· mL^{-1} (61.7 U· mg^{-1}).

These results proved that crude chitinase from *Bacillus aryabhattai* developed activity against insoluble chitin substrates.

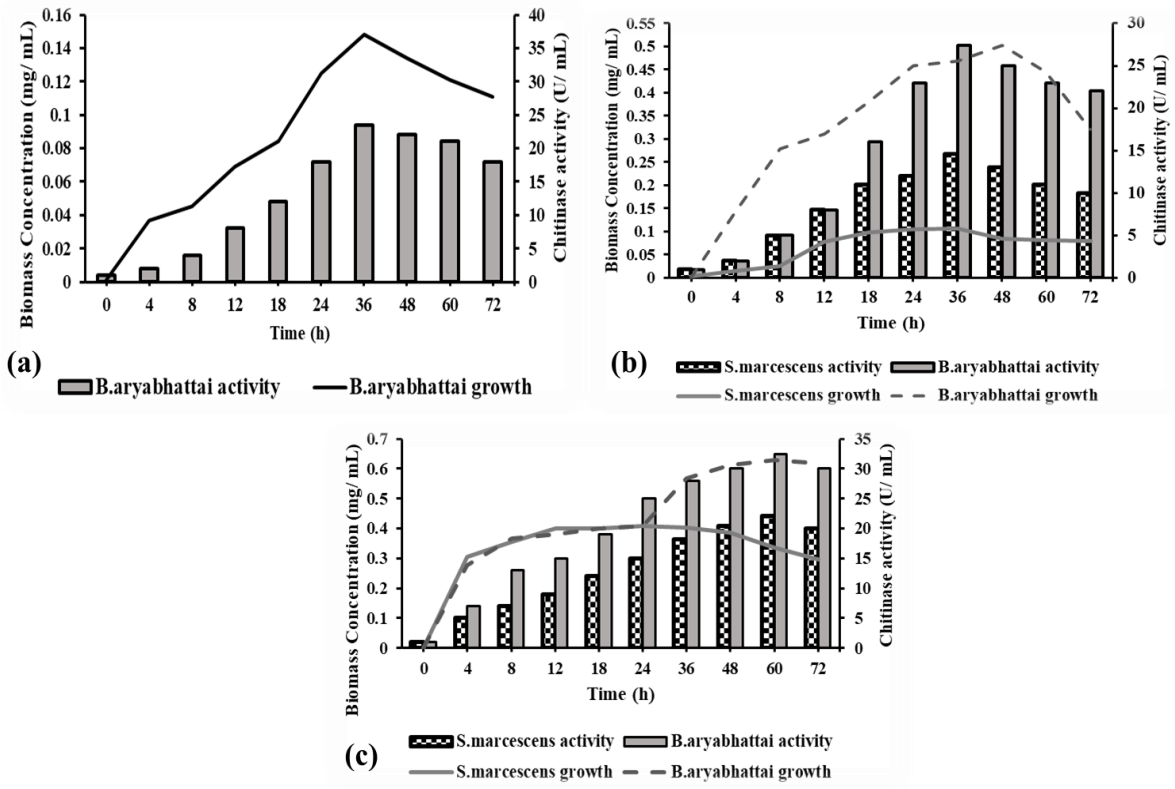

Figure 5.3 Growth profile and chitinase activity of *Bacillus aryabhattai* and *Serratia marcescens* in minimal salt medium containing 1% (a) Chitin flakes, (b) Chitin powder, and (c) Colloidal chitin.

However, the growth rate and chitinase activity were less. So those were improved by optimizing media composition and process parameters used to grow the *Bacillus aryabhattai* using statistical tools.

5.3 Optimization of media components to improve chitinase activity

Placket Burman design (PBD) based on ANOVA (Analysis of Variance) was performed to screen important media components using Design Expert 11 (State-Ease, Minnesota, USA) software. The ANOVA results are shown in **Table 5.1**. The responses were statistically evaluated, and the variables with a p-value less than 0.05 were considered significant for high chitinase activity. The model was highly significant ($p<0.0001$), and the regression coefficient R^2 was 0.98. The p-values for most variables were less than 0.0001; thus, the F value and factor coefficient were considered to define the most significant variable for the best response.

Source	Factor coefficients	F-value	p-value
Model		955.30	< 0.0001
A-Glucose	-0.078	701.51	< 0.0001
B-Sucrose	-0.005	3.63	0.1294
C-Glycerol	0.189	3432.56	< 0.0001
D-Peptone	0.155	2263.03	< 0.0001
E-Yeast extract	0.181	3402.71	< 0.0001
G-Tryptone	-0.064	334.74	< 0.0001
H-$MgCl_2$	0.030	81.82	0.0003
J-$CaCl_2$	-0.085	585.31	< 0.0001
K-KH_2PO_4	-0.096	744.83	< 0.0001
L-Na_2HPO_4	0.013	17.33	0.0088
M-$CuSO_4$	0.106	1078.25	< 0.0001
N-$CoCl_2$	-0.023	43.73	0.0012
O-$FeSO_4$	0.088	1218.83	< 0.0001
P-$MnSO_4$	0.128	1584.77	< 0.0001
Curvature		15.94	0.0104
Lack of Fit		1.72	0.5121
R^2 - 0.98	Adjusted R^2 - 0.97	Predicted R^2 - 0.85	

Table 5.1. ANOVA table of model and 15 variables, which includes p-value, F-value, and coefficients for all the variables

Table 5.1 confirms the glycerol (F value = 3432.56) (coefficient = +0.19), yeast extract (F value = 3402.71) (coefficient = +0.18), $MgCl_2$ (F value = 81.82) (coefficient = +0.03) and $MnSO_4$ (F value = 1584.77) (coefficient = +0.13) as the significant carbon source, nitrogen source, macronutrients, and micronutrients, respectively. Other macronutrients, such as KH_2PO_4 and $CaCl_2$, have higher F values; however, these variables possessed negative coefficients, which means these factors suppress the *Bacillus aryabhattai* growth. These results were also confirmed by the Pareto chart, as shown in **Figure 5.4**. The Pareto chart consists of two essential limits that help to screen the crucial factors. A higher t-limit, also called the Bonferroni limit, and a lower t-limit are represented in the Pareto chart.

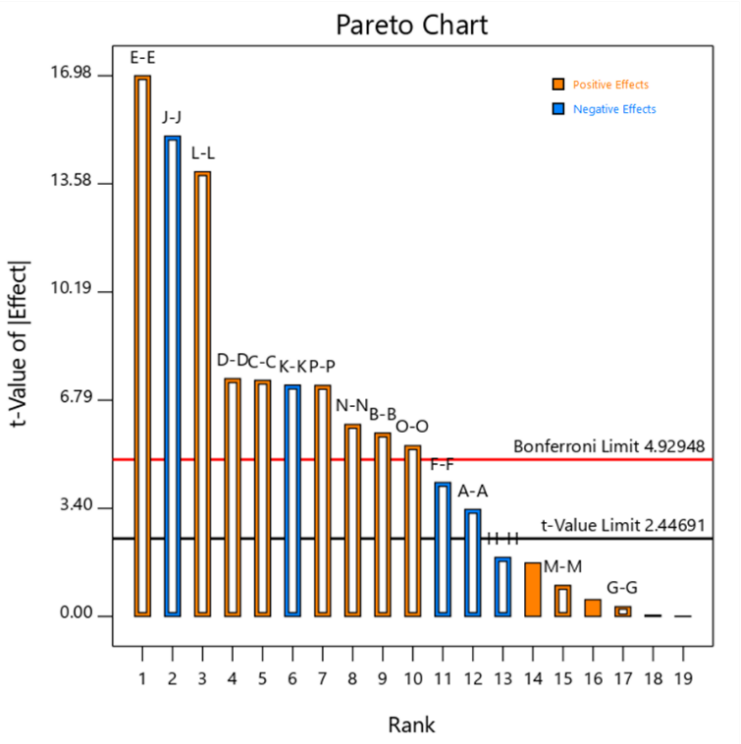

Figure 5.4. Pareto chart showing the positive and negative variables along with the Bonferroni and lower standard t-limit.

(A-Glucose, B-Sucrose, C-Glycerol, D-Peptone, E-Yeast extract, G-Tryptone, H- Na_2HPO_4, J-$CaCl_2$, K-KH_2PO_4, L- $MgCl_2$, M-$CuSO_4$, N-$COCl_2$, O-$FeSO_4$, P-$MnSO_4$)

Factors that emerged from the Bonferroni threshold limit are considered significant. The factors below the threshold of the lower t-limit are considered insignificant, and those found between both limits are moderately significant. From the Pareto chart, the values of the Bonferroni limit and a lower t-limit were found to be 5.54 and 2.57, respectively. Further optimization of the concentration of selected media constituents (Glycerol, Yeast extract, $MgCl_2$ and $MnSO_4$) was performed to improve chitinase activity.

5.4 Optimization of concentration of media components using response surface methodology (RSM)

RSM using the Box Behnken design (BBD) was applied to optimize the concentration of selected variables to improve chitinase activity. The ANOVA results are shown in **Table 5.2**, designed using Design Expert 11 (State-Ease, Minnesota, USA) software. The F-value of the quadratic model was 922.67, which confirmed that the model

selected for analysis was significant, and the lack of fit was insignificant, which also confirmed that the model was significantly fit. The model's goodness of fit was checked using the regression values.

Source	Factor coefficients	F-value	p-value
Model		922.67	< 0.0001
A-Glycerol	0.001	17.61	0.0008
B-Yeast extract	-0.013	826.84	< 0.0001
C-$MgCl_2$	0.005	120.67	< 0.0001
D-$MnSO_4$	-0.009	441.91	< 0.0001
AB	-0.008	100.82	< 0.0001
AC	0.006	68.94	< 0.0001
AD	-0.007	97.13	0.0001
BC	0.001	5.18	0.0712
BD	0.009	138.56	< 0.0001
CD	0.007	76.73	0.0008
A^2	-0.045	5389.68	0.0465
B^2	-0.018	892.01	0.8284
C^2	-0.050	6839.59	< 0.0001
D^2	-0.021	1184.89	< 0.0001
Lack of Fit		4.19	0.0636
R^2 - 0.98	Adjusted R^2 - 0.96		Predicted R^2 - 0.81

Table 5.2 ANOVA table of model and four media components, including p-value and F-value of model.

The R^2 value of the model was 0.98, showing that the data points were fitted, and the adjusted R_2 value was 0.96. Further, the F and p values of interactions of selected variables such as A, B, C, D, AB, AC, AD, BC, BD, CD, A^2, B^2, C^2, and D^2 are shown in the ANOVA table. The 3D surface plots represent the interactions between the factors chosen, highlighting their influence on chitinase activity. The optimal concentration of 4 factors within the given limit for the highest chitinase activity was

determined from this 3D plot. **Figure 5.5** shows the 3D plot of the interactions of four factors towards chitinase activity.

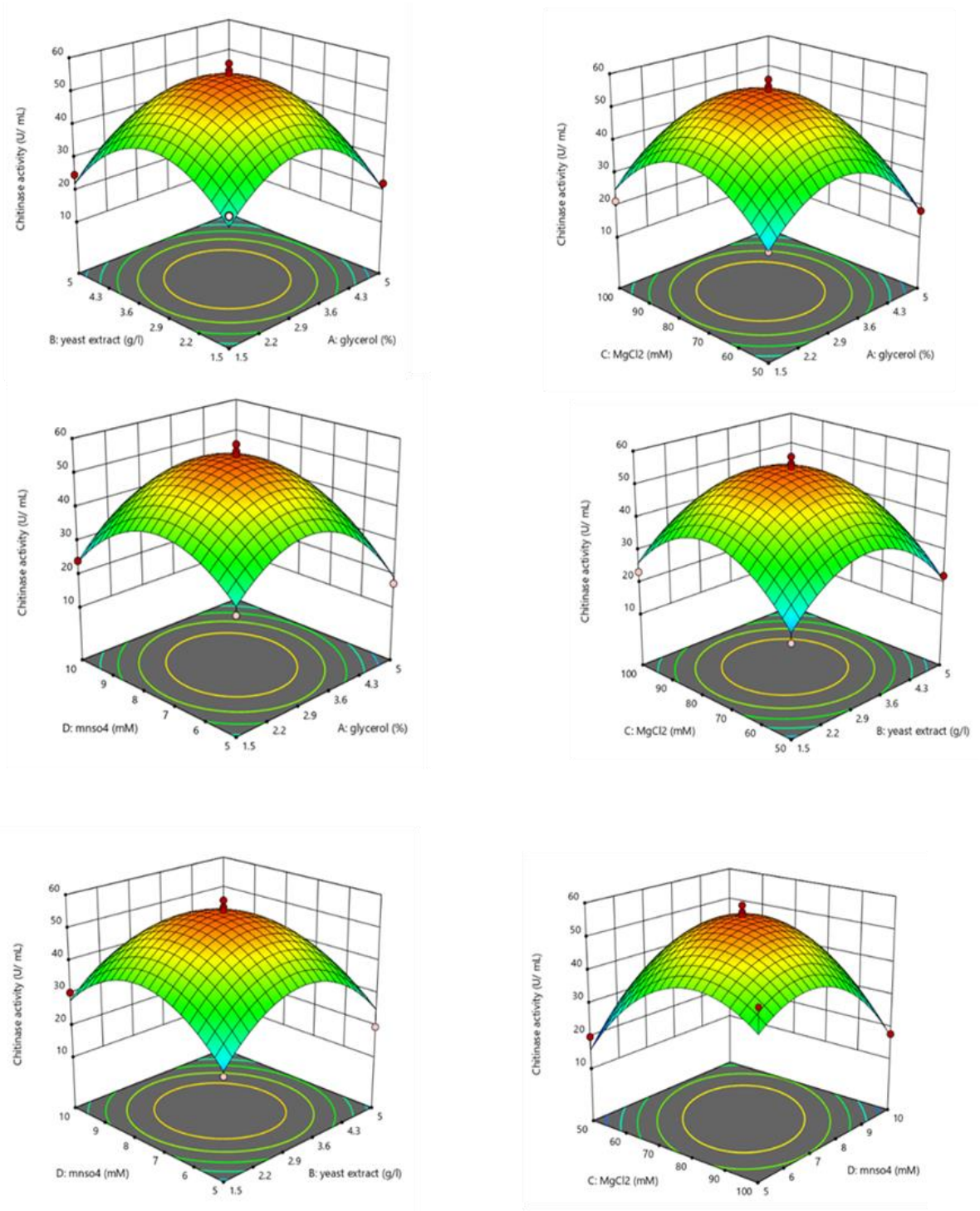

Figure 5.5 Response surface plot displaying four media components' optimized point and effect on chitinase activity.

The highest specific chitinase activity was observed as 106.9 U· mg^{-1} by using 3% (v/v) glycerol, 3.0 g· L^{-1} yeast extract, 75mM $MgCl_2$, and 7.5mM $MnSO_4$ in the growth media for *Bacillus aryabhattai*. The optimization of the concentration of media components increased specific chitinase activity from 80.98 U· mg^{-1} to 106.9 U· mg^{-1}. Further optimization of process parameters was performed using RSM.

5.5 Optimization of process parameters using RSM to improve chitinase activity

The essential process parameters chosen for the study were temperature, pH, inoculum size, and inoculum age. The ANOVA results are shown in **Table 5.3,** which was developed using Design Expert 11 (State-Ease, Minnesota, USA) software.

Source	Factor coefficients	F-value	p-value
Model		19.17	< 0.0001
A-pH	-8.47	6.01	0.0305
B-Temperature	9.15	7.01	0.0213
C-Inoculum age	3.33	9.87	0.0118
D-Inoculum size	2.44	7.46	0.0208
AB	-22.05	13.58	0.0031
AC	-14.88	6.18	0.0286
AD	13.11	4.80	0.0490
BC	-6.67	8.14	0.0141
BD	1.26	6.84	0.0243
CD	-0.9141	7.85	0.0189
A^2	-56.86	120.33	< 0.0001
B^2	-67.49	169.49	< 0.0001
C^2	-41.93	65.44	< 0.0001
D^2	-42.31	66.63	< 0.0001
Lack of Fit		6.31	0.1444
R^2 = 0.957	Predicted R^2 = 0.907. Adjusted R^2 = 0.758		

Table 5.3. ANOVA table of model and four physical parameters, including p-value and F-value and coefficients value

A quadratic model provided the best fit for the response obtained, validated using ANOVA and regression analysis. The F-value of the Model was 19.17, and the p-value was less than 0.05, confirming that the model selected was significant. The Lack of Fit F-value was 6.31, which confirmed that the Lack of Fit was insignificant relative to the pure error. The model showed an R^2 value of 0.96, and the predicted and adjusted R^2 values were 0.91 and 0.76, respectively. Interactions of four variables, A, B, C, D, AB, AC, AD, BC, BD, CD, A^2, B^2, C^2, and D^2, were analysed using 3D surface plots. **Figure 5.6** shows 3D plots of the interaction between four parameters.

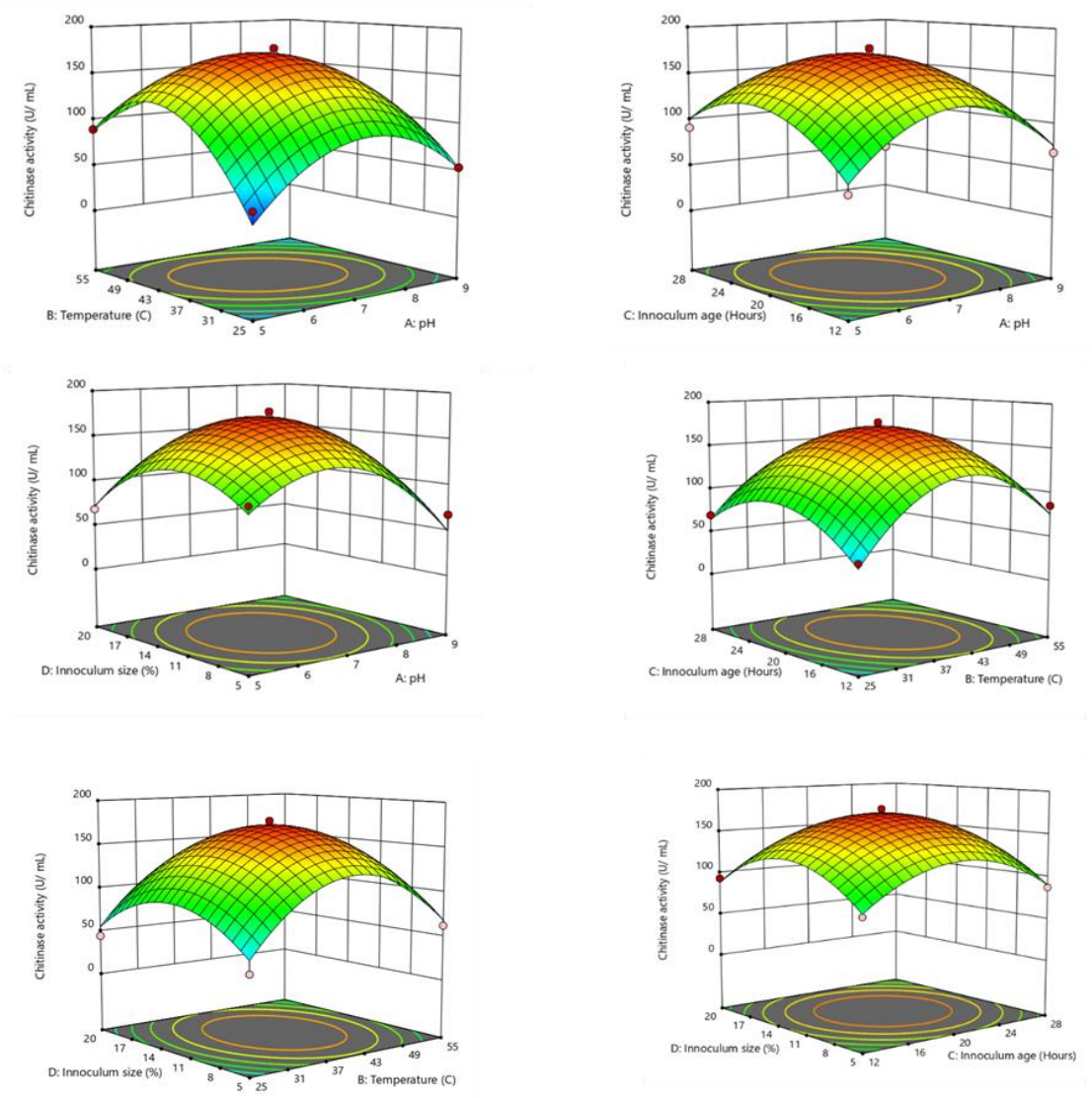

Figure 5.6. 3D response surface plot displaying interactions of temperature, pH, inoculum size, and inoculum age.

The highest specific chitinase activity obtained was 146.14 U· mg^{-1} at the temperature of 40℃, pH 7, inoculum size of 12.5% (v/v), and inoculum age of 24 hours. The statistical optimization resulted in the enhancement of specific chitinase activity from 80.98 U· mg^{-1} to 146.14 U· mg^{-1}, which was one of the highest activities of wild-type bacterial chitinase against insoluble chitin substrates reported till now (Doan et al. 2018; Paulsen et al. 2016; Subramanian et al. 2020a). Various research in breaking the crystalline form of chitin has been reported, such as the maximum increase in affinity toward insoluble chitin was shown in 2015 by the fusion of ChiD from *Serratia marcescens* with the PDK domain (CBM and CBP21). The synergistic effect of two or more chitinases also provides higher degradation efficiency with insoluble chitin, a reported maximum of 3.0 U· mL^{-1}, and heterologous expression (Madhuprakash et al. 2015).

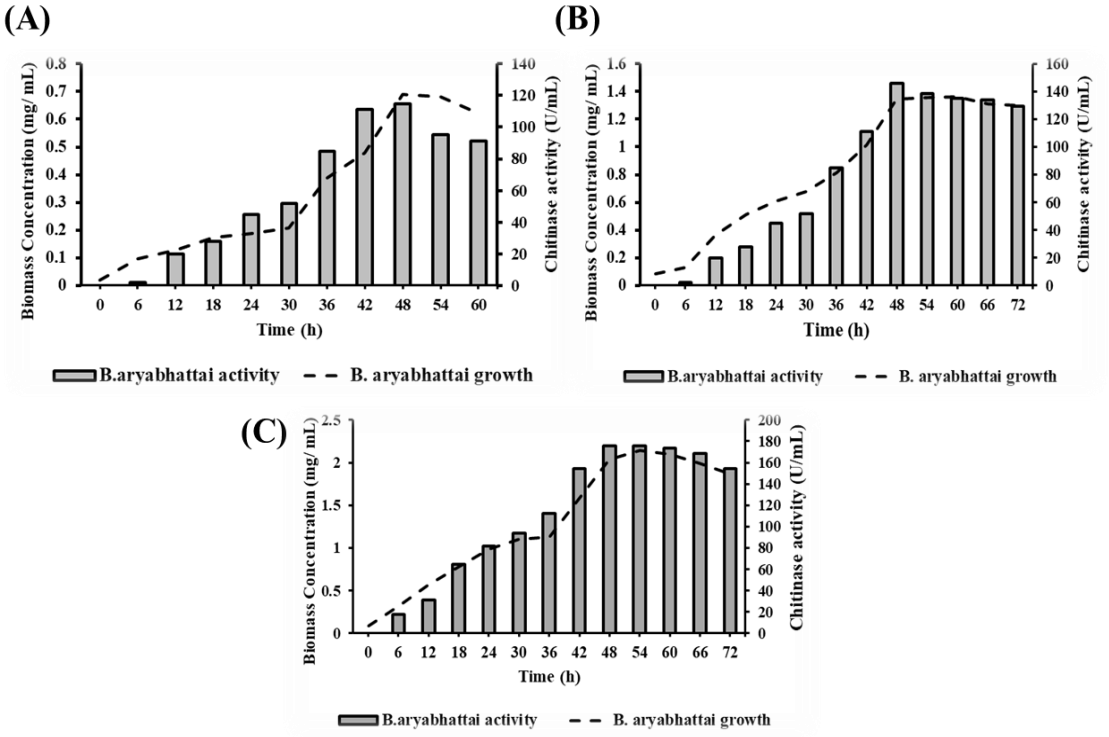

Figure 5.7. Growth profile and chitinase activity of *Bacillus aryabhattai* in optimized medium containing 1% (a) chitin flakes, (b) chitin powder, and (c) colloidal chitin.

The best-studied chitinase producer, *Serratia marcescens*, acts on insoluble chitin only in the presence of all the cocktails of chitinase (ChiA, ChiB, and ChiC) (Gutiérrez-Román et al. 2014). ChiA remains inactive in the absence of ChiB and

ChiC. LPMO (Lytic polysaccharide mono-oxygenases) was reported to break the glycosidic bond in crystalline chitin, yet they acted on insoluble chitin with the additional requirement. On the contrary, the chitinase from the screened *Bacillus aryabhattai* acted on insoluble chitin with LysM domains in its structure. The yield of enzyme activity was improved from 3200 U· g^{-1} of colloidal chitin to 17,400 U· g^{-1} of colloidal chitin after optimization. Moreover, chitin oligomers' yield improved from 10.8 g· g^{-1} of colloidal chitin to 61.3 g· g^{-1} of colloidal chitin. Moreover, the growth profile of *Bacillus aryabhattai* and *Ba*ChiA activity profile against different chitin substrates after optimization is shown in **Figure 5.7a, b and c**. The bar graph and right horizontal axis explain the variation of chitinase activity of *Ba*ChiA, and the line graph and left horizontal axis explain the growth profile of *Bacillus aryabhattai*. *Bacillus aryabhattai's* growth rate and highest achieved activity against chitin flakes were 0.045 h^{-1} and 114.9 U· mL^{-1} (63.02 U· mg^{-1}), respectively **(Figure 5.7 a)**. *Bacillus aryabhattai's* growth rate and highest achieved activity against chitin powder were 0.19 h^{-1} and 146.2 U· mL^{-1} (115.2 U· mg^{-1}), respectively (**Figure 5.7 b**). *Bacillus aryabhattai's* growth rate and highest achieved activity against colloidal chitin were 0.25 h^{-1} and 175.4 U· mL^{-1} (146.1 U· mg^{-1}), respectively (**Figure 5.7 c**). Thus, the specific activity of *Ba*ChiA was improved sixfold after optimization. The activity of recently isolated chitinase from marine bacteria and recombinant chitinase was tabulated in the Table 2.1 and 2.2 respectively. Moreover, chitinase isolated in this study possess highest activity against insoluble chitin substrates compared to chitinase mentioned in the Table 2.1 and 2.2.

5.6 Antifungal efficiency of *Ba*ChiA

The presence of chitin in the fungal cell wall is essential for its development and survival. This property of fungus helped explore the antifungal properties of chitinase. Research reported the antifungal activity of chitinases from the *Carica papaya* was achieved against *Alternaria brassicicola*[42]. The antifungal activity results of wildtype against two fungi are shown in **Figures 5.8a and b**. The antifungal effect on the two-plant pathogenic fungi, *Candida albicans* and *Fusarium oxysporum*, was determined. The antifungal effect was observed as a halo zone on the plates. ***Well 1*** with the crude enzyme produced by growing *Bacillus aryabhattai* in optimized media with 1% (w/v) colloidal chitin resulted in a zone of clearance. However, ***well 2*** with

the supernatant of the *Bacillus aryabhattai* grown in media without 1% (w/v) colloidal chitin failed to produce a clearance zone. Autoclaved medium in ***well 3*** served as a control for the experiment. The zone of clearance of 14 mm diameter was noted in *Candida albicans* and *Fusarium oxysporum* growth plate around well 1.

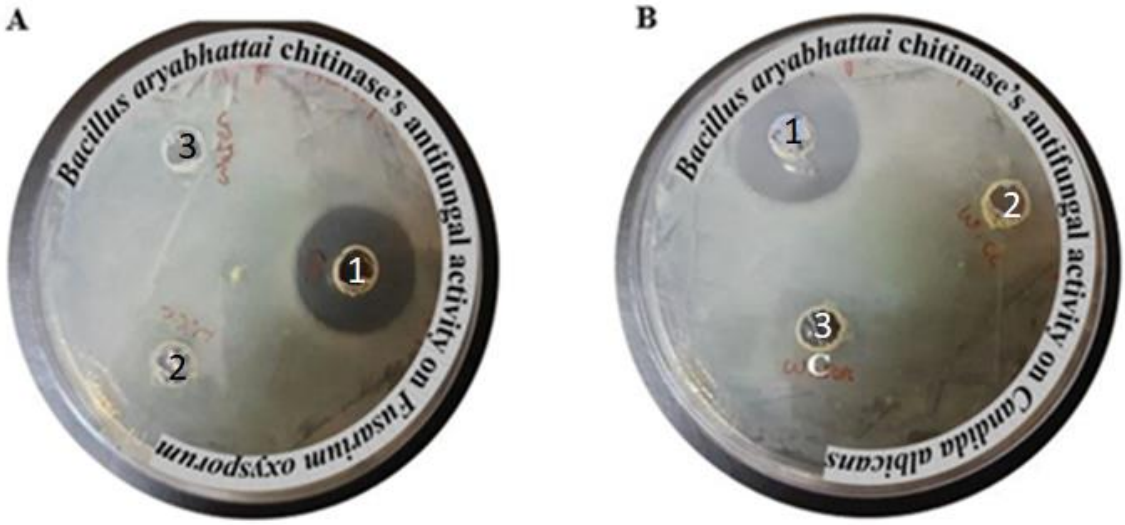

Figure 5.8 Antifungal activity of *Ba*ChiA against (a) *Candida albicans* and (b) *Fusarium oxysporum*.

The above results confirmed the antifungal property of chitinase from *Bacillus aryabhattai*.

5.7 TLC analysis of chitin oligomers produced by *Ba*ChiA

Chitin oligomers were the primary product produced from the chitin substrates by chitinase. Thus, this study analysed the chitin oligomers produced from different chitin substrates by wildtype *Ba*ChiA. The assessment was performed using thin-layer chromatography, as shown in **Figure 5.9**. Seven samples were added to the TLC plate, marked as 1 to 7. In lane 1, N-acetylglucosamine (GlNAc) was added as a standard marker. In Lanes, 2, 3, and 4, different chitin substrates, such as chitin powder, flakes and colloidal chitin, were added. Since chitin is insoluble, no bands were visible in these three samples. In lane 5, a chitin powder sample treated with *Ba*ChiA was loaded. A smear corresponding to the oligomers along with the monomer was observed. Similarly, in lanes 6 and 7, chitin flake and colloidal chitin treated with *Ba*ChiA were added. In both these lanes, the release of GlNAc is visible.

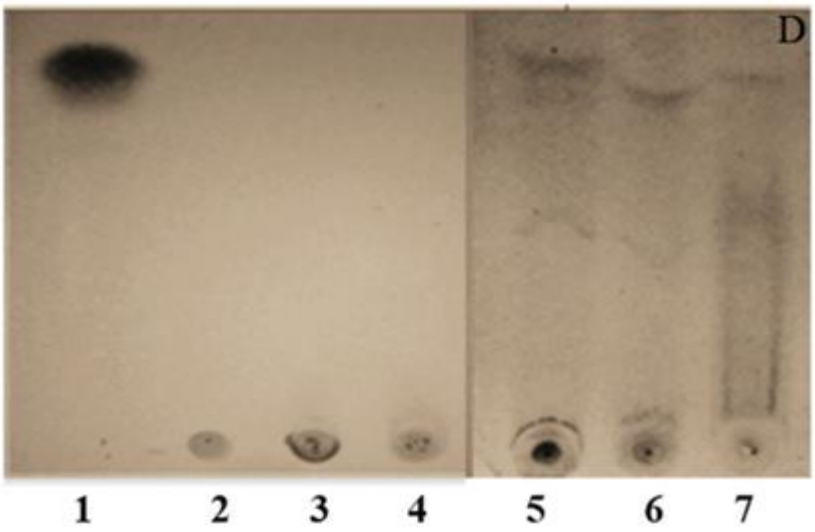

Figure 5.9 TLC of various chitin oligomers (1 – N-acetylglucosamine (GlNAc), 2, 3, 4 untreated chitin powder, flakes and colloidal chitin samples, respectively and 5, 6 and 7 – chitin powder, flakes and colloidal chitin samples treated with *Ba*ChiA respectively).

Apart from the chitin monomer, producing other chitin oligomers was possible. Since the resolution of TLC was poor, the presence of other oligomers due to their lesser concentrations was challenging to confirm. Thus, LC-MS analysis was performed for the reaction samples subjected to TLC.

5.8 LC-MS analysis of Chitin oligomers produced by wildtype *Ba*chiA from different chitin substrates

Initially, LC-MS analysis of the standard chitin oligomers was performed. 500 ppm of a standard chitin oligomer mixture (monomer to hexamer) was prepared and analysed using LC-MS.

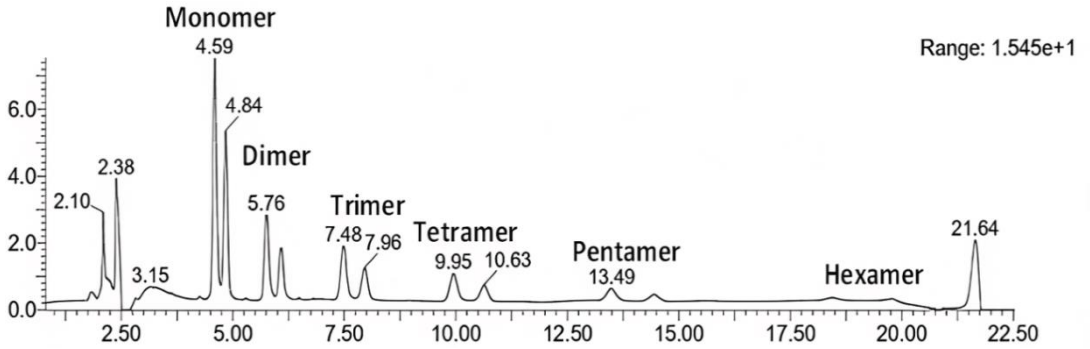

Figure 5.10a. LC Chromatogram of standard chitin oligomer mixture

Retention time and m/z peaks of all the oligomers were obtained and used to confirm the presence of oligomers in the reaction samples. LC chromatogram and MS spectrums for the standard sample are shown in **Figures 5.10 a and b**, respectively.

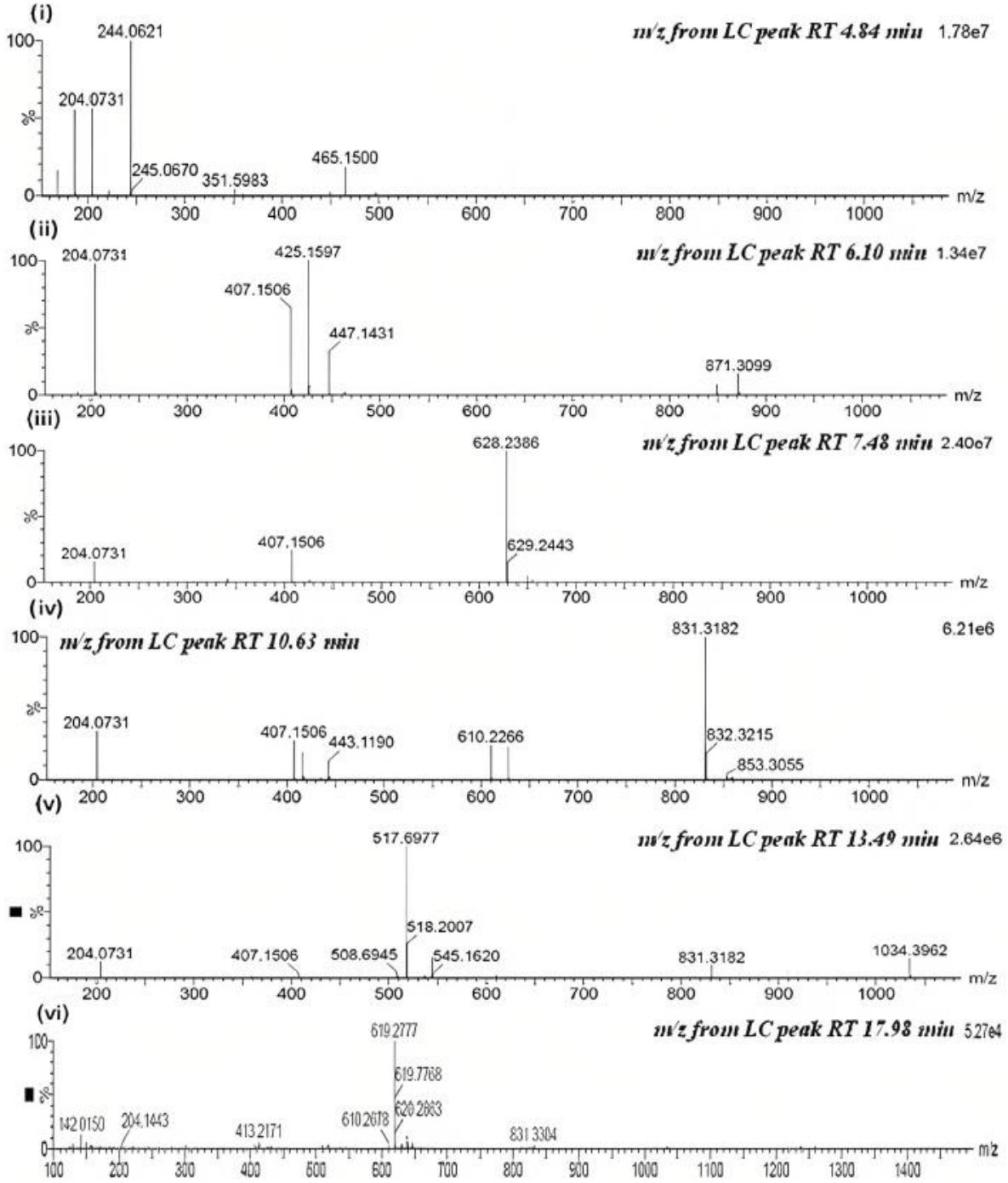

Figure 5.10b. MS spectrum of the chitin oligomer standard (i) Monomer (ii) Dimer (iii) Trimer (iv) Tetramer (v) Pentamer (vi) Hexamer.

LC-MS analysis of the chitin oligomer produced after incubating the 1% chitin powder and flakes with cell-free spent media of *Bacillus aryabhattai* is shown in **Figures 5.11 and 5.12**. LC chromatogram of chitin oligomers produced from chitin powder and flakes are shown in **Figures 5.11 a and b**, respectively. The MS spectrum of peaks obtained for different chitin oligomers from chitin powder and flakes are shown in **Figures 5.12 a and b**, respectively.

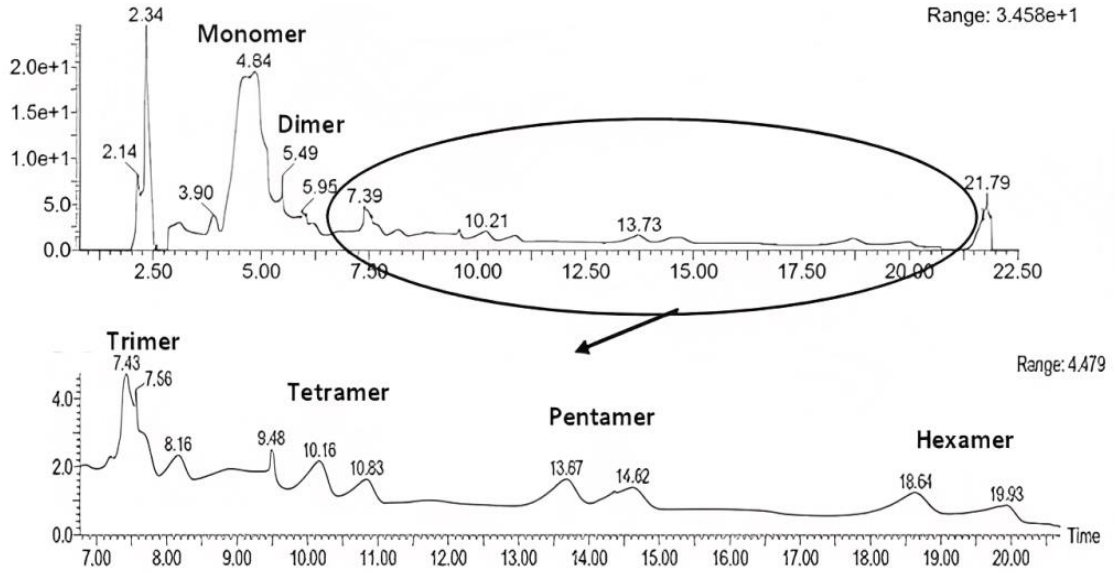

Figure 5.11a LC Chromatogram of reaction sample from Chitin powder

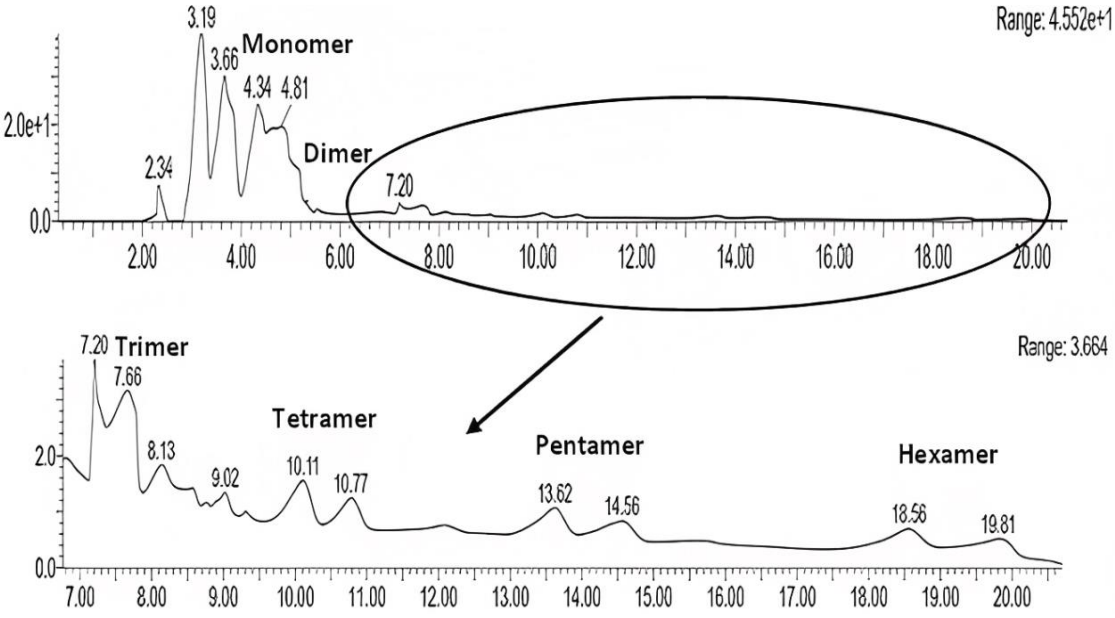

Figure 5.11b LC Chromatogram of reaction sample from Chitin flakes

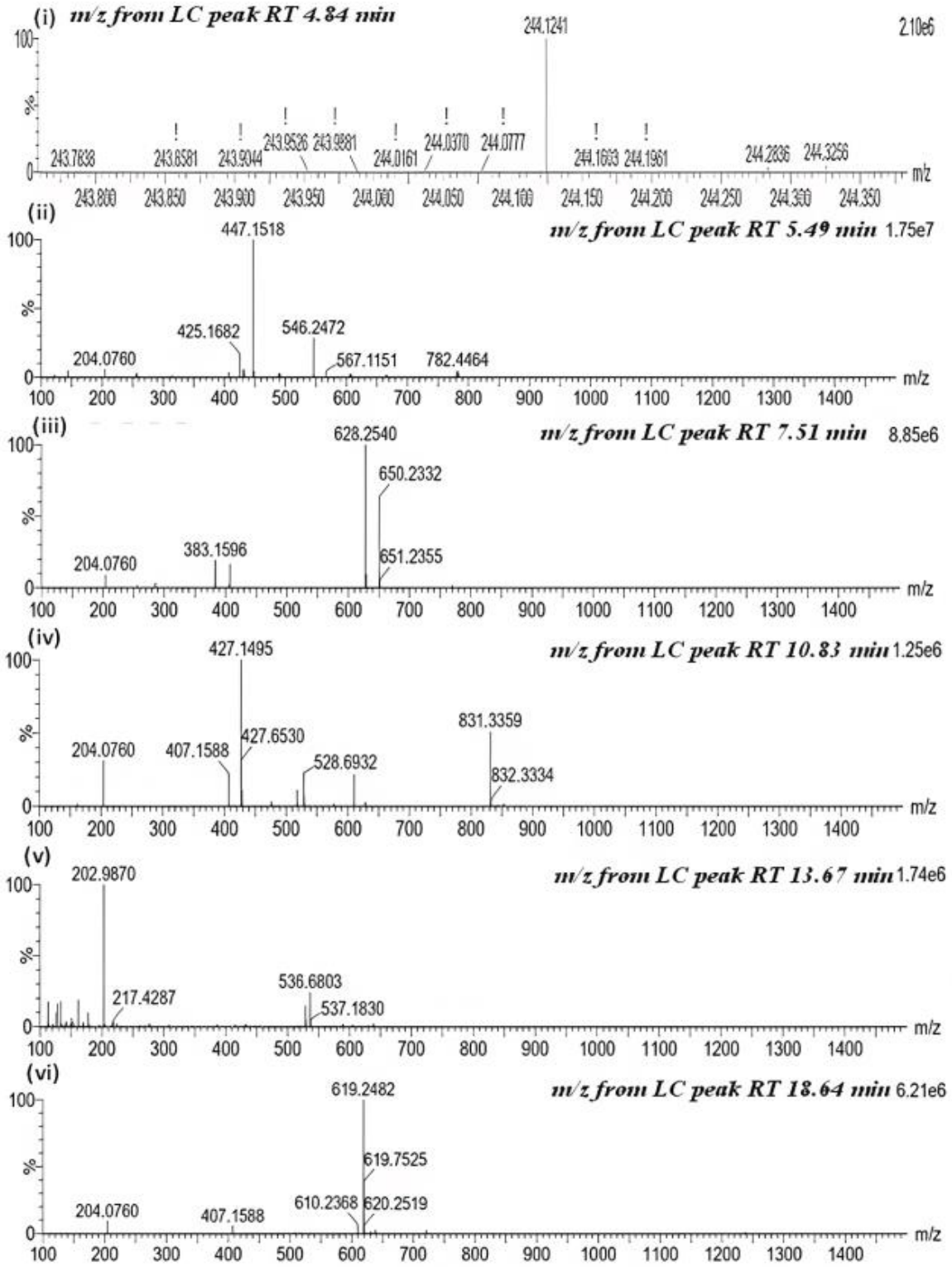

Figure 5.12a MS spectrum of chitin oligomers such as (i) Monomer (ii) Dimer (iii) Trimer (iv) Tetramer (v) Pentamer (vi) Hexamer from 1 % Chitin powder.

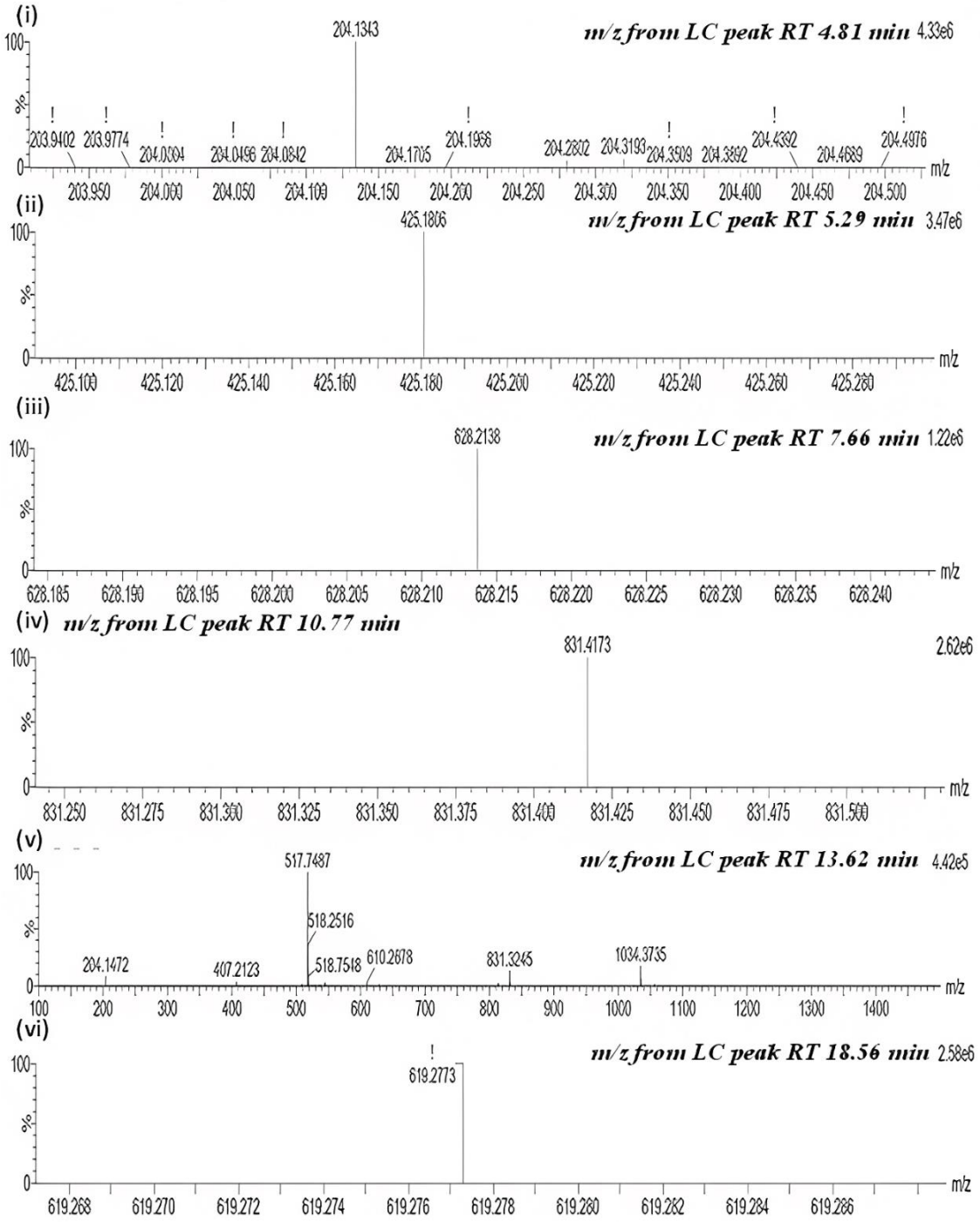

Figure 5.12b MS spectrum of chitin oligomers such as (i) Monomer (ii) Dimer (iii) Trimer (iv) Tetramer (v) Pentamer (vi) Hexamer from 1 % Chitin flakes.

LC-MS analysis of the substrate and enzyme blank sample was performed. The substrate blank sample contained only cell-free spent media of *Bacillus aryabhattai* without chitin substrates. The enzyme blank sample contained only chitin substrates without cell-free spent media. LC chromatogram and MS spectrums of the substrate

blank sample are shown in **Figures 5.13 a and b**, respectively. LC chromatogram of the enzyme blank is shown in **Figure 5.14**.

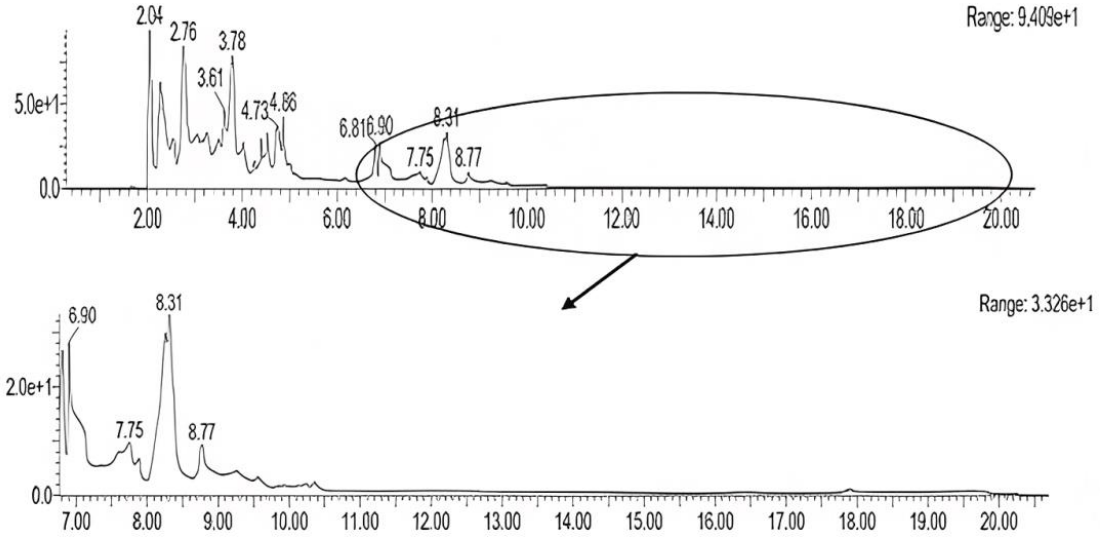

Figure 5.13a LC Chromatogram of Substrate Blank

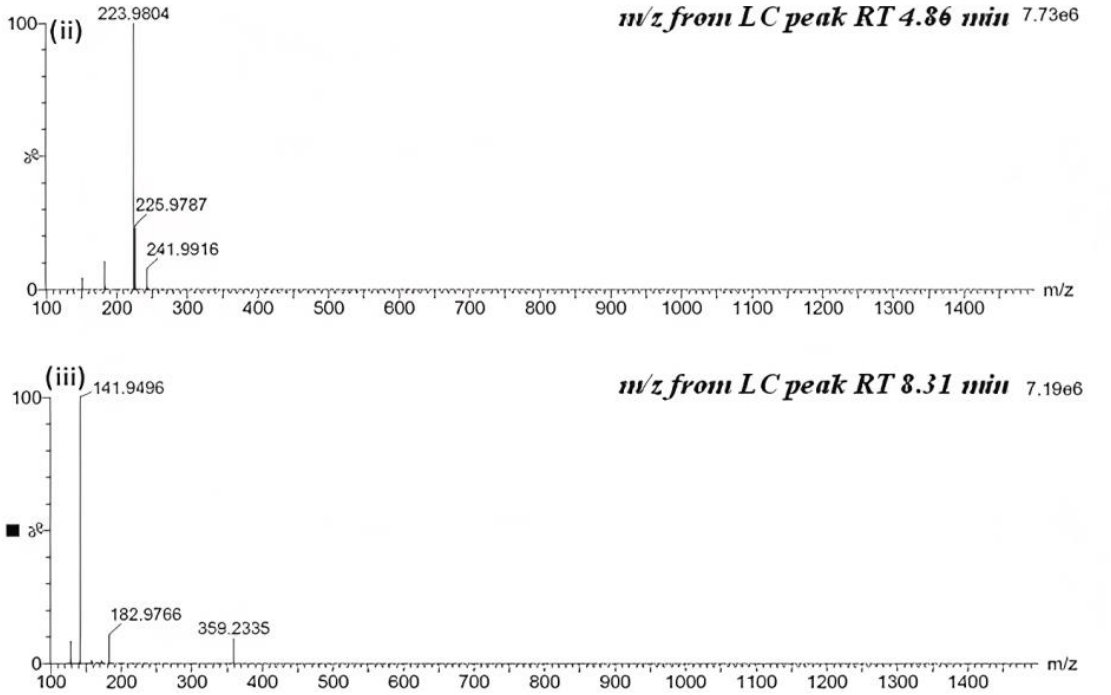

Figure 5.13b. MS spectrum for peak with retention time at (i) 4.86 min and (ii) 8.31 min of substrate blank sample.

The obtained LC peak at 4.86 min for the substrate blank sample was same as the retention time of the monomer peak from the standard sample. The obtained LC peak at 8.31 min for the substrate blank sample was predominant. So, the m/z spectrum of the above two peaks was analyzed. The m/z spectrum obtained from the 4.86 min

peak was 223.98, different from the m/z of the monomer. The m/z spectrum from the 8.31 min peak was 141.94, different from the peaks obtained in the reaction samples. These results confirmed no chitin oligomers were present in the substrate blank sample. The LC chromatogram of the Enzyme blank sample showed no peaks similar to those of the reaction sample.

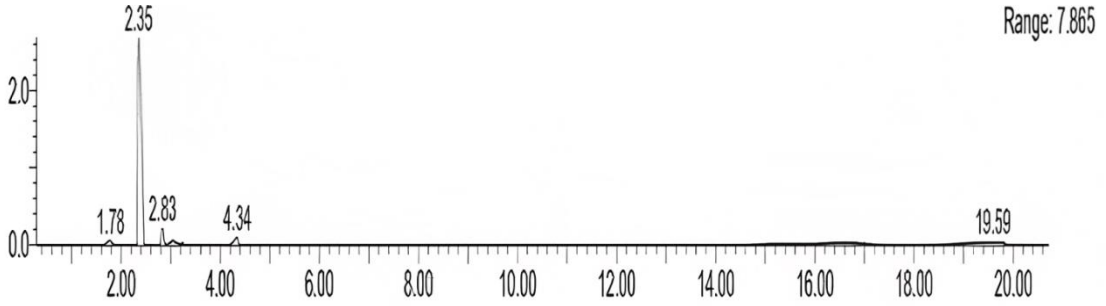

Figure 5.14. LC Chromatogram of Enzyme Blank

The explanation and comparison of the LC chromatogram and the MS spectrum for the reaction and standard samples are explained in **Table 5.4**. The chitin monomer's (N-acetyl glucosamine) molecular weight is 221 g/mol. These molecules can lose one or more water molecules. Thus, the molecular weight of each compound differs, which is also explained in **Table 5.4.**

Chitin oligomer	Standard Chitin Oligomer		Chitin powder Reaction sample		Chitin Flakes Reaction sample		Molecular formula and mass NAG mol weight (M = 221)
	MS peak (m/z)	LC peak (min)	MS peak (m/z)	LC peak (min)	MS peak (m/z)	LC peak (min)	
Monomer	204, 244	4.56, 4.84	244	4.84	204	4.81	$(M - H_2O) + H$ ion, $(221 - 18) + 1 = 204$ m/z $(M + Na$ ion$)$, $(221 + 23) = 244$ m/z
Dimer	407, 425, 447	5.76, 6.10	447	5.49	425	5.29	$(2M - H_2O) + H$ ion, $(442 - 18) + 1 = 425$ m/z $(2M - 2H_2O) + H$ ion, $(442 - 36) + 1 = 407$ m/z (2M – H2O) + Na ion, (442 – 36) + 23 = 447 m/z
Trimer	628	7.48, 7.96	628	7.51	628	7.66	$(3M - 2H_2O) + H$ ion, $(663 - 36) + 1 = 628$ m/z
Tetramer	831	9.97, 10.63	831	10.83	831	10.77	$(4M - 3H_2O) + H$ ion, $(884 - 54) + 1 = 831$ m/z
Pentamer	517.5, 528.5, 1034	13.49, 14.36	528.5	13.67	517.5	13.62	$(5M - 4H_2O) + H$ ion, $(1105 - 72) + 1 = 1034$ m/z $((5M - 4H_2O) + Na$ ion $+ H$ ion$) / 2$, $(1033 + 23 + 1) /2 = 528.5$ m/z $((5M - 4H_2O) / 2 + H$ ion$)$, $(516.5 + 1) = 517.5$ m/z
Hexamer	619, 1237	17.98, 19.19	619	18.64	619	18.56	$(6M - 5H_2O) + H$ ion, $(1326 - 90) + 1 = 1237$ m/z (6M – 5H2O) / 2 + H ion, (618 + 1) = 619 m/z

Table 5.4: MS and LC peaks for different chitin oligomers from standard and reaction samples.

B. RECOMBINANT CHITINASE STUDY

5.9 Sequence analysis and domain architecture of chitinase

The specificity of *Ba*ChiA against insoluble and crystalline chitin substrates was understood by studying amino acid sequences and domains present in the *Ba*ChiA. The sequence of *Ba*ChiA consists of 481 amino acids obtained from the Uniport database.

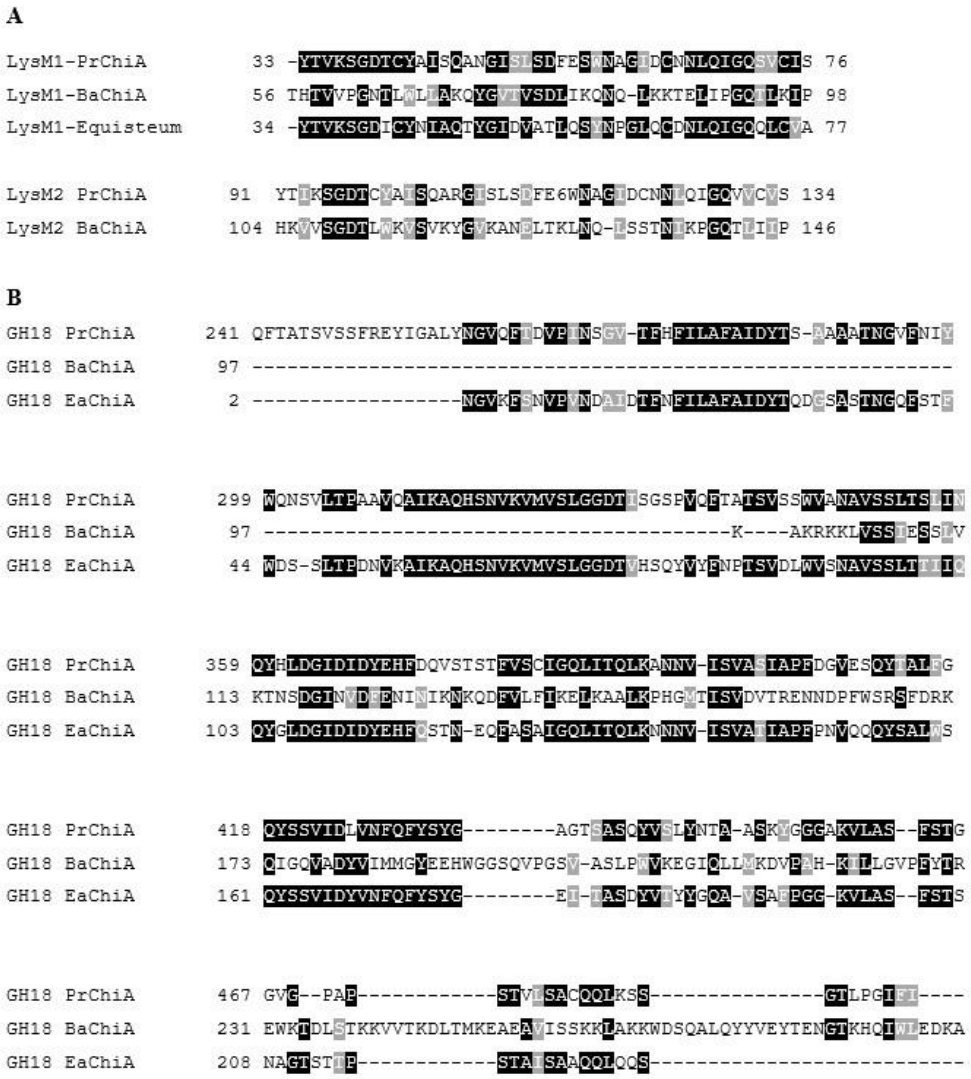

Figure 5.15 Alignment of amino acid sequences from domains of *Ba*ChiA with those from corresponding regions of higher organisms chitinase. (a) Alignment of sequences of LysM domains of *Ba*ChiA. (b) Alignment of the sequence from a catalytic domain of *Ba*ChiA.

The domain architecture of chitinase usually includes the catalytic domain, chitin-binding domain, S/T rich linker region, polycystic kidney disease (PKD) domain, and Fn3 region. In this study, multiple sequence alignment was performed, and the results

revealed that *Ba*ChiA had two N-terminal LysM domains and one ClassIIIb catalytic domain. The LysM motif is a substrate-binding domain of about 50 amino acids belonging to the carbohydrate-binding module family 50 (CBM 50). The primary role of the LysM domain is to anchor the enzyme to crystalline chitin structure, which helps the glycosyl hydrolase (GH) 18 catalytic domains to act on chitin and hydrolyze it (Kulichevskaya et al. 2019; Meriem and Mahmoud 2017; Patidar et al. 2005b).

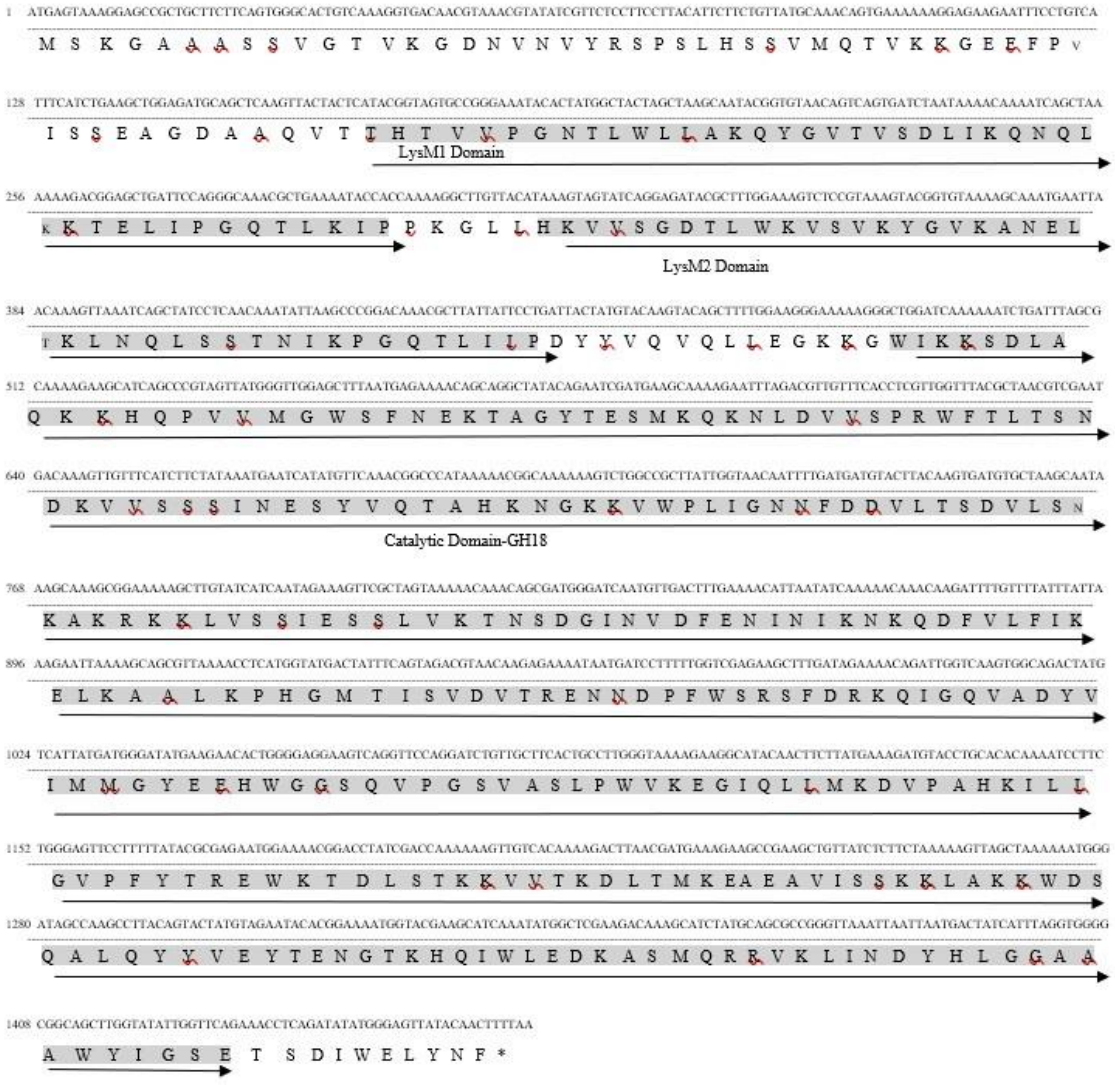

Figure 5.16 Protein sequence of *Ba*ChiA with its domain position.

This domain had been identified only in eukaryotic systems (Bateman and Bycroft 2000; Inamine et al. 2015b; Kitaoku et al. 2017; Ohnuma et al. 2017). The multiple sequence alignment results of *Ba*ChiA against chitinase of higher organisms such as *Pteris ryukyuensis* (*Pr*ChiA) and *Equisetum arvense* (*Ea*ChiA) are shown in

Figures 5.15 a and b. The amino acid sequence of 1st LysM domain region of *Ba*ChiA had high similarities to *Pr*ChiA and *Ea*ChiA sequence (Ohnuma et al. 2017),and amino acid sequence of *Pr*ChiA (Inamine et al. 2015c) had high similarities to the sequence of 2nd LysM domain of *Ba*ChiA. The amino acid sequence of the GH18 catalytic domain of *Ba*ChiA had high similarities to the sequence of *Pr*ChiA and *Ea*ChiA. *Ba*ChiA had a signature sequence as DGIXXDX, also present in PrChiA and EaChiA protein sequences. DGI is supposed to be a catalytic triad required for the chitinase also present in *Ba*ChiA. The conserved sequence for the LysM domain (XTVXSGDTXX) was also observed in *Ba*ChiA. The complete sequence of *Ba*ChiA and domain representation based on those sequences are shown in **Figure 5.16**.

The domain analysis was also performed for the chitinase of *Bacillus aryabhattai* and *Serratia marcescens* using NCBI conserved domain online tools. The domain analysis results for the chitinase from both organisms are shown in **Figures 5.17 and 5.18,** respectively. The domain architecture analysis revealed the presence of the two Lys domains (Carbohydrate binding domain) between 56th and 98th amino acids and 104th and 145th amino acids. The glycosyl hydrolase (GH18) domain (Catalytic domain) was present between 226th and 466th amino acids. Based on amino acid sequence and domain analysis, it was clear that chitinase from *Bacillus aryabhattai* belongs to the Glycoside hydrolase 18 family (GH18) of Endo-chitinase. Thus, the sequence and domain analysis confirmed that the presence of two LysM domains enhanced the binding efficiency of *Bacillus aryabhattai* chitinase towards insoluble chitin, which was absent in *Serratia*. The 3D structure of the chitinase enzyme was developed to study the structure of LysM domains and amino acids involved in catalytic activity.

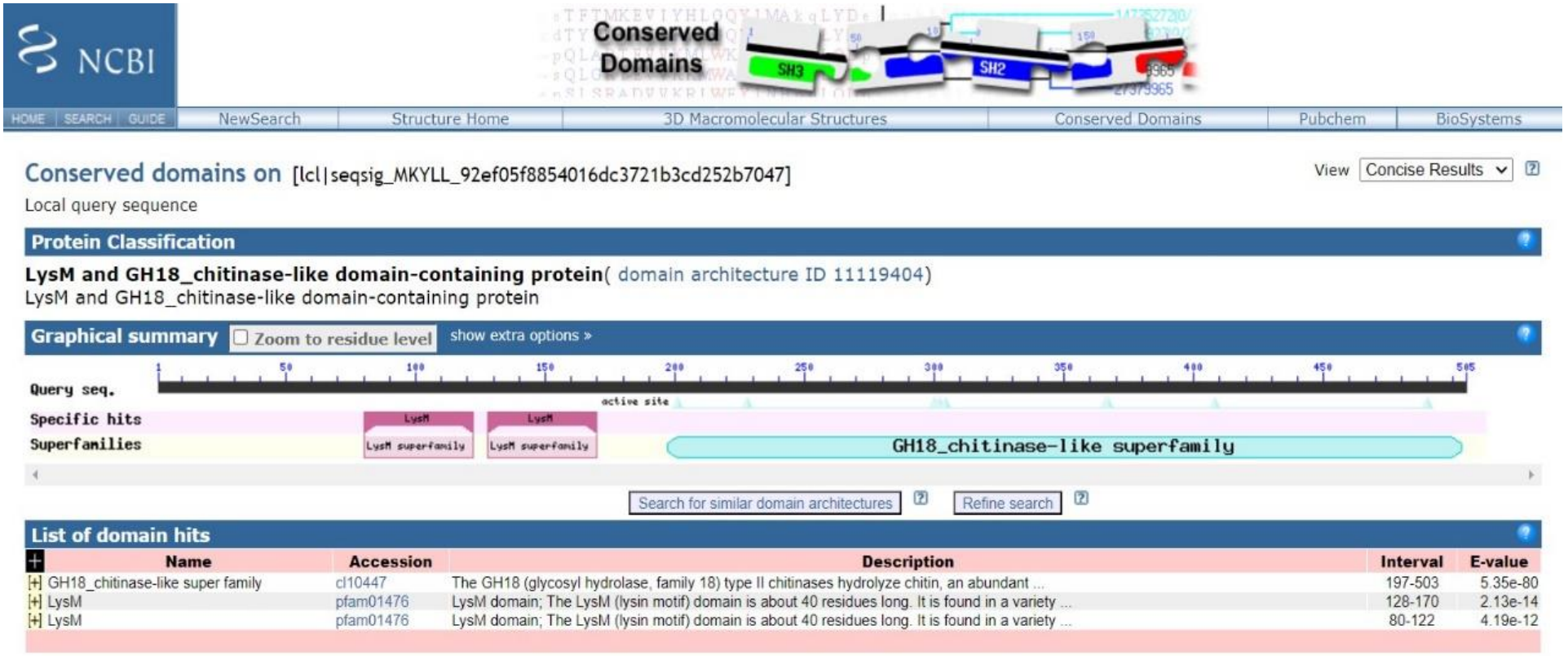

Figure 5.17 Conserved domain analysis of chitinase sequence of *Bacillus aryabhattai.*

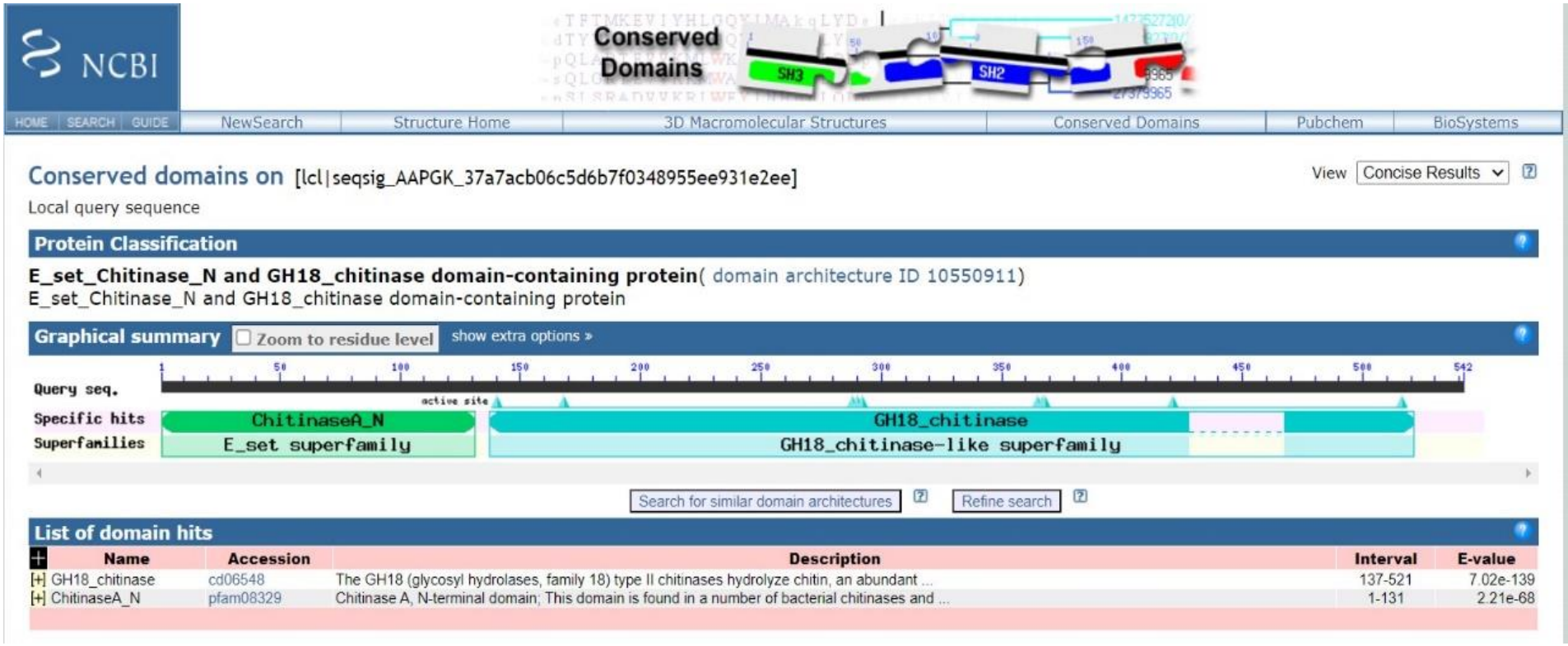

Figure 5.18 Conserved domain analysis of chitinase sequence of *Serratia marcescens*

5.10 3D structure modelling and validation of chitinase

The 3D structure of chitinase from *Bacillus aryabhattai* was developed by homology modelling using Maestro software (Schrodinger, USA). The 3D structure of chitinase from *Serratia marcescens* was obtained from the RCBS PDB database. Structural analysis of these enzymes confirmed the presence of the two LysM domains in *Bacillus aryabhattai* chitinase again, which was absent in *Serratia marcescens.*

Figure 5.19 3D structure of *Bacillus aryabhattai* chitinase

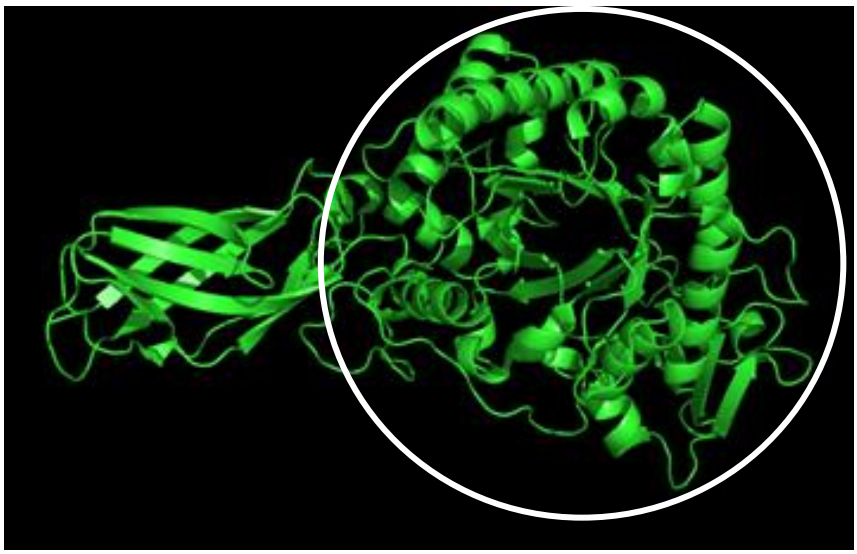

Figure 5.20 3D structure of *Serratia marcescens* chitinase.

The 3D structure of *Bacillus aryabhattai* chitinase is shown in **Figure 5.19**. The two N terminal LysM domain is highlighted inside the white circle in the figure. **Figure 5.20** shows the 3D structure of the *Serratia marcescens* chitinase, which contained catalytic domain GH18 (inside the white circle), but no N terminal LysM domain was present.

The developed 3D structure of *Ba*ChiA was validated using the SWISS-MODEL online tool. The Ramachandran plot was used to validate the developed 3D structure. The plot has three regions: most favoured, less favoured, and unfavored. If the modelled protein structure is perfect, the maximum amino acids of that enzyme should be in the most favoured region. The Ramachandran plot of the modelled *Bacillus aryabhattai* chitinase 3D structure is shown in **Figure 5.21**. In the image, there are three coloured regions: dark green represents the most favoured region, light green represents the less favoured region, and white region represents the unfavored region. The blue dots represent the amino acids of *Bacillus aryabhattai* chitinase. It was confirmed that 98.13 % of amino acids fell under the most favoured region, which proved that the 3D structure of *Bacillus aryabhattai* chitinase developed was valid.

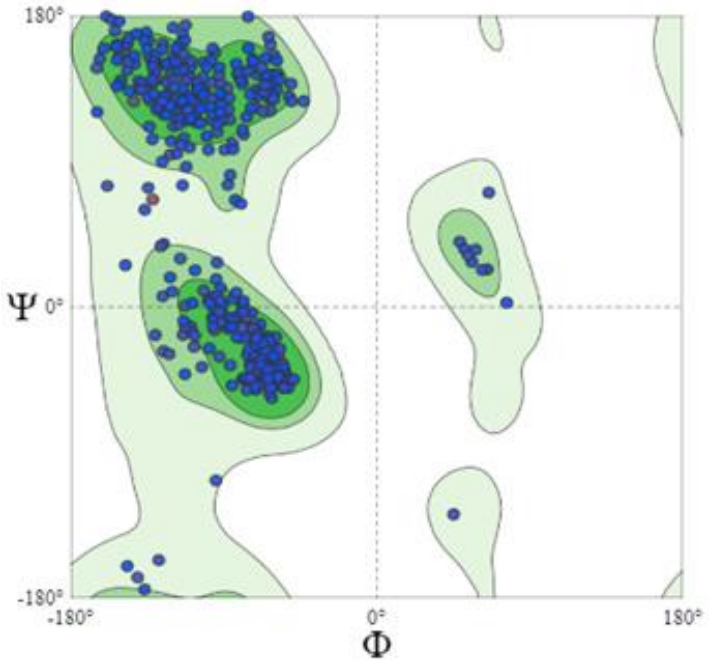

Figure 5.21 Ramachandran plot of the modelled *Bacillus aryabhattai* chitinase

When speaking about the 3D structure of the LysM domain, the general structural configuration of the LysM domain has two beta sheets and two alpha helix arranged alternatively. The structure of the LysM domain of the *Bacillus aryabhattai* chitinase is shown in **Figure 5.22a**. In the Figure, we can view the alternative arrangement of two beta sheets and an alpha helix. The schematic representation of the interaction of the LysM domain to chitin tetramer is shown in **Figure 5.22b**. This figure shows the

amino acids involved in interaction with chitin tetramer. The amino acid back bone of serine at the 60th position and the R group of aspartic acid at the 62nd position may form a hydrogen bond with OH groups of the chitin tetramer. The amino acid backbone of valine at the 25th, 27th, and 69th positions and Lysine at the 70th position may form a hydrogen bond with the OH groups of the chitin tetramer backbone. R group of Lysine and tryptophane at 66th and 17th position may form hydrogen bonds with chitin tetramer back bone.

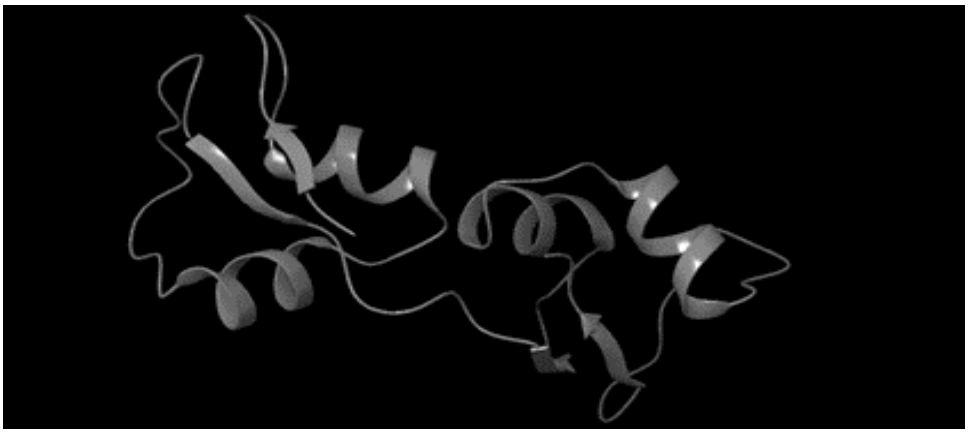

Figure 5.22a N terminal LysM domain of *Bacillus aryabhattai* chitinase

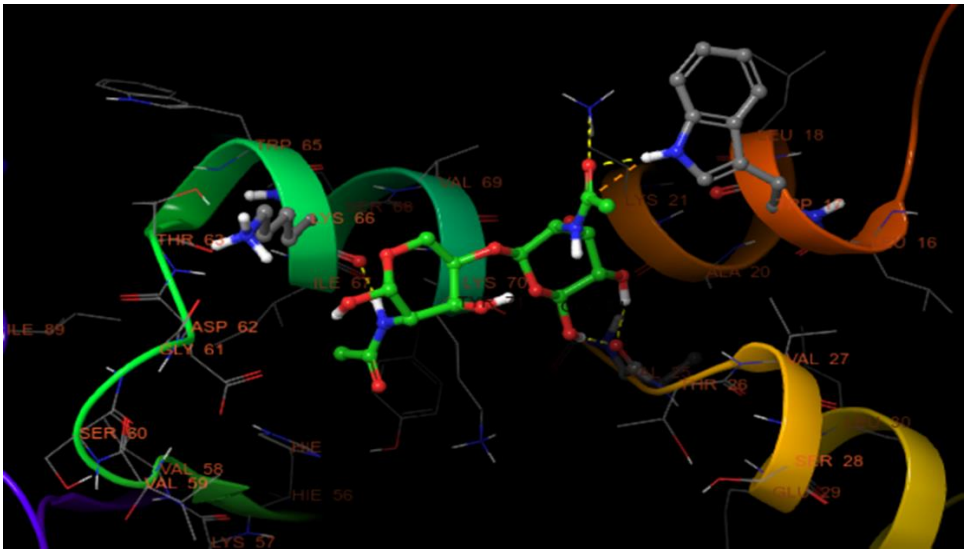

Figure 5.22b schematic representation of the interaction of LysM domain with chitin tetramer

There were maximum possibilities of charged interaction between the Lys domain and chitin tetramer. The study performed by Jolles P et al. in 1999 (Jolles et al. 1999) also explained the possible interaction of amino acids of chitinase from *Dioscorea*

opposita with chitin hexamer, which also confirmed that the lysine and tryptophan might play a significant role in binding to chitin backbone. The study also revealed the amino acids from *Serratia marcescens* chitinase might be involved in the hydrolysis of the chitin chain. It showed that glutamic acid and aspartic acid at the 315th and 391st positions were involved in chitin hydrolysis.

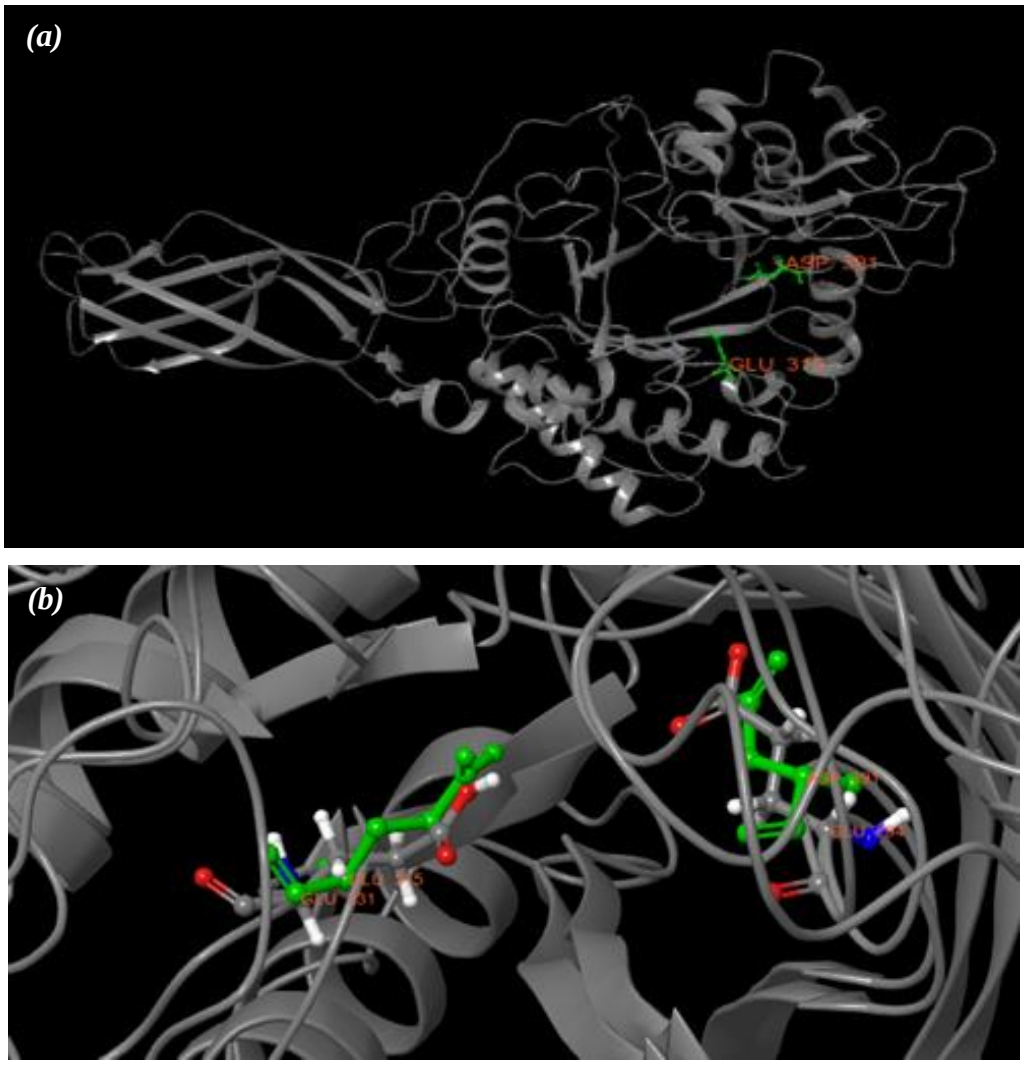

Figure 5.23 (a) Amino acids (Glu 315 and Asp 391) involved in catalytic activity in *Serratia marcescens* and (b) superimposed structure of chitinase of both organisms

The position of both the amino acids in the 3D structure of the *Serratia marcescens* chitinase is shown in **Figure 5.23a.** Thus, with reference to that structure, both 3D structures of *Bacillus aryabhattai* and *Serratia marcescens* chitinase were superimposed using Schrodinger software and amino acids in *Bacillus aryabhattai*

chitinase might be involved in hydrolysis activity were found as shown in **Figure 5.23b**. The green amino acids represent *Bacillus* chitinase, which may involve catalytic activity. Glutamic acid at the 231st and 294th positions were arranged in the same orientation of catalytic amino acids (grey colour) of *Serratia* chitinase. The schematic representation of the mechanism of the hydrolysis of chitin by these two active amino acids is shown in **Figure 5.24**. A 3D representation of the interaction of active amino acids of *Bacillus* chitinase with the chitin substrates is shown in **Figure 5.25.**

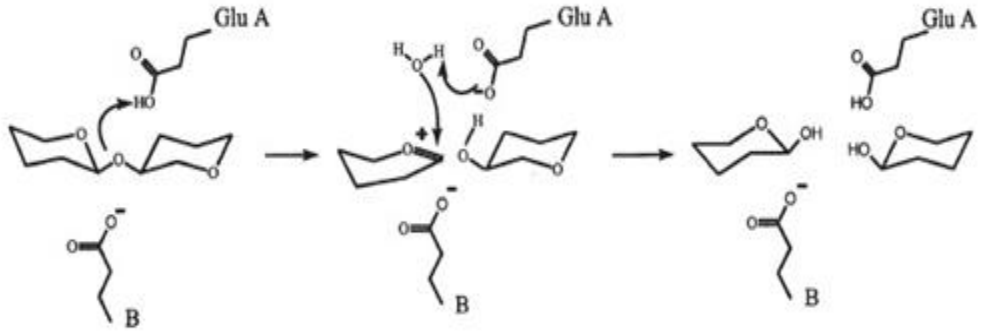

Figure 5.24 Mechanism of chitin hydrolysis by chitinase (Jolles et al. 1999)

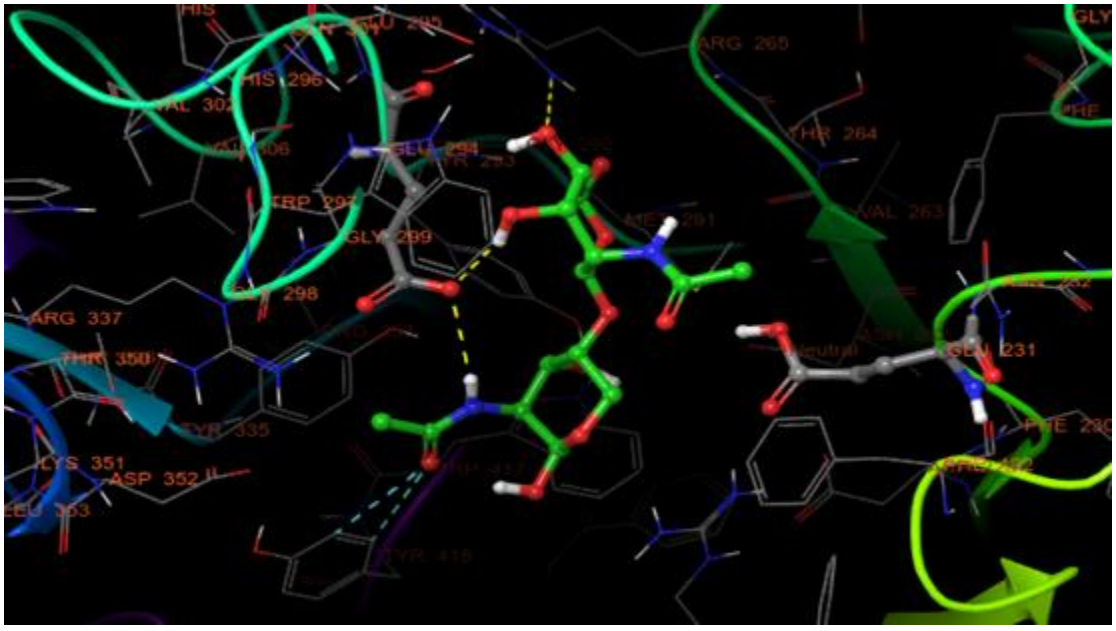

Figure 5.25 3D representation of the interaction of active amino acids of *Bacillus aryabhattai* chitinase with the chitin dimer.

In hydrolysis of β-1,4 bond between two chitin monomers, the Glu at 231st position acts as a base, which polarises the attacking water molecules. Glu at 294th position

acts as an acid to protonate O of the leaving sugar. Thus, the β-1,4 bond of the chitin substrates was hydrolysed. **Figure 5.25** illustrates the chitin dimer arrangement between two active amino acids.

5.11 Cloning of chitinase gene from *Bacillus aryabhattai* into *E. coli Rosetta pLysS*

5.11.1 Genomic DNA isolation from *Bacillus aryabhattai*

Genomic DNA from *Bacillus aryabhattai* was successfully isolated using the HiPurA genomic DNA Purification kit and then analyzed by agarose gel electrophoresis. Isolated DNA had no smear in agarose gel; the DNA yield was 145 ng· μL^{-1}. The absorbance ratio of 260 nm to 280 nm was 1.9, confirming that the isolated DNA was free of RNA and protein contamination. The agarose gel image of genomic DNA is shown in **Figure 5.26**. Isolated genomic DNA was further used as a template in PCR to isolate the chitinase gene.

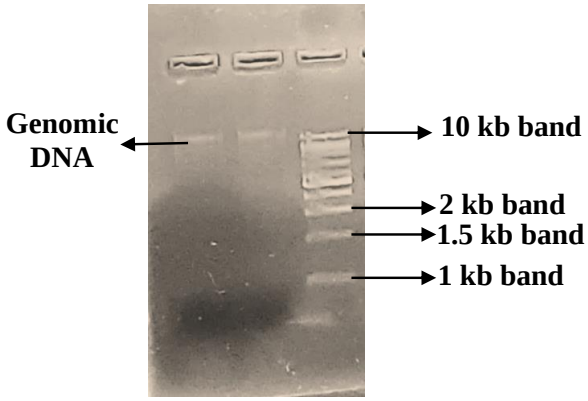

Figure 5.26 Genomic DNA isolation from *Bacillus aryabhattai*

1, 2 – Genomic DNA and 3 – 1kb DNA Ladder

5.11.2 pET 23a Plasmid isolation

Plasmid DNA exists in three conformations: supercoiled, open circular and linear. In supercoiled DNA, both strands are covalently closed and twisted, making the DNA more compact. In linear DNA, both strands of DNA have been cut; therefore, the DNA is linearized and less compact than supercoiled DNA. In open circular DNA, a nick is in one of the strands, and it relaxes the tension. This property makes the open circular DNA less compact than linear DNA. The order of these conformations is from the more compact to the least compact. In agarose gel, the more compact DNA takes less time to pass through the pores. Supercoiled DNA runs farther than linear

DNA, followed by open circular DNA. Using a Qiagen Miniprep kit, the pET 23a Plasmid was isolated from the *E. coli BL21* strain. This pET23a plasmid is an expression vector used to express the chitinase from *Bacillus aryabhattai* in *E. coli Rosetta pLysS*. The agarose gel image of the Isolated plasmid is shown in **Figure 5.27**. DNA yield was 200 ng· μL^{-1}. The absorbance ratio of 260 nm to 280 nm was 1.8, confirming that the isolated DNA was free of RNA and protein contamination.

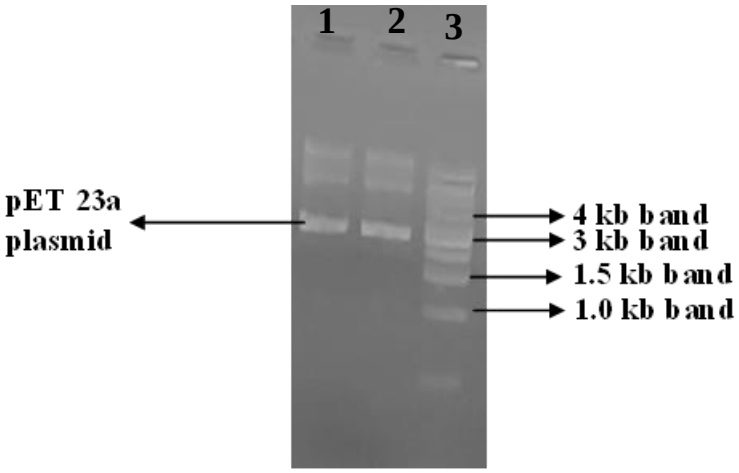

Figure 5.27 pET23a plasmid isolation

(1, 2 – Isolated pET23a plasmid, 3- 1kb DNA Ladder)

5.11.3 PCR amplification of chitinase gene

The primers for PCR were designed using the Snap gene software, USA and synthesized by Sigma Aldrich Corporation using the Phosphoramidite Method.

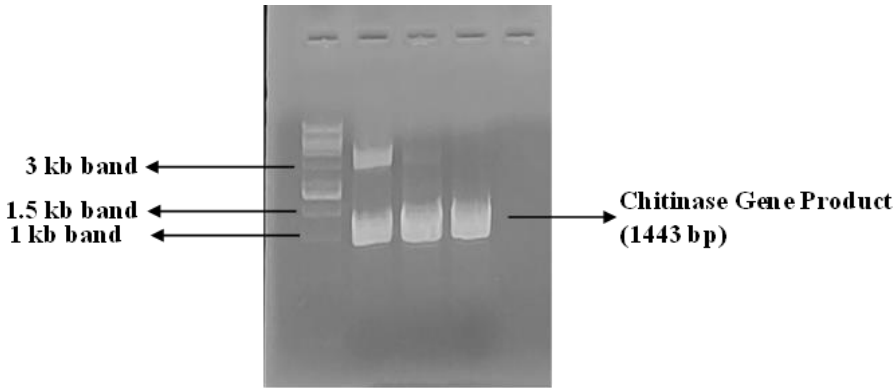

Figure 5.28 Amplified gene product by PCR

(1 – 1kb Ladder, 2, 3 & 4 – PCR product)

Gradient PCR was performed in different annealing temperatures such as 57℃, 58℃ and 59℃ with a constant second annealing temperature of 69℃. It was done to

identify the best annealing temperature for specific primer binding to the template DNA. The temperature which allowed specific binding was used further to amplify the chitinase gene on a large scale. **Figure 5.28** shows the amplified chitinase gene with BamHI and XhoI restriction sites. In the 2nd and 3rd lanes, for 57 and 58℃ due to non-specific binding, there were some other bands apart from the chitinase gene band. In the 4th lane, for 59℃, the specific binding of primers resulted in a single band of chitinase with high concentration.

5.11.4 Restriction Digestion of pET 23a plasmid and chitinase gene

The plasmid DNA and the chitinase gene were subjected to double digestion using the BamHI and XhoI enzymes. This process reduced the supercoiled and open-circular conformations of the plasmid DNA to a linear conformation. The restricted products were then visualized using agarose gel electrophoresis.

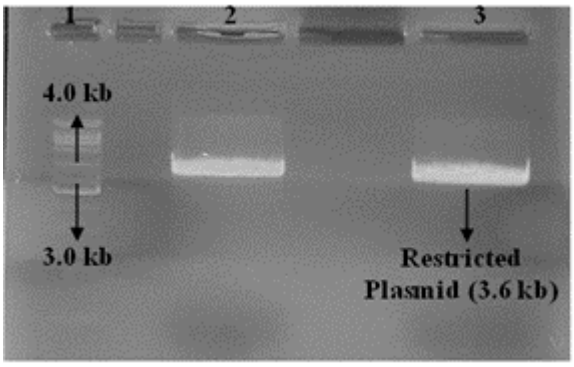

Figure 5.29 Double digestion of pET23a by Xho1 and BamH1

(1 - 1kb DNA Ladder, 2, 3 - Double digested pET23a)

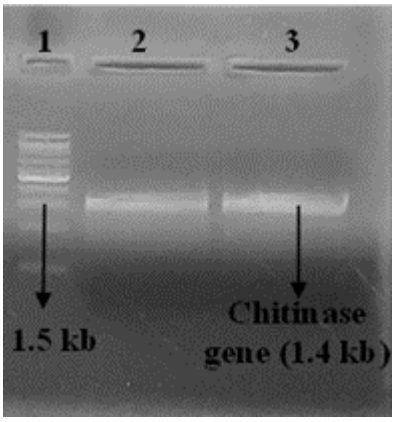

Figure 5.30 Double digestion of chitinase gene by XhoI and BamHI

(1 – 1kb DNA, 2, 3 –double digested chitinase Gene)

Figures 5.29 and 5.30 show the results of the plasmid and chitinase gene restriction

digestion, respectively. In **Figure 5.30**, a single band of the gene in lanes 2 and 3 confirmed the restriction of the gene. In **Figure 5.29**, the single band of the plasmid in lanes 2 and 3 confirmed the plasmid restriction.

5.11.5 Ligation and transformation into *E. coli Rosetta pLysS*

The restricted pET 23a plasmid and chitinase gene were ligated by the T4 ligase. The ligated sample was transformed into *E. coli Rosetta pLysS* competent cell and streaked in the ampicillin and chloramphenicol agar plate. For positive control, the *E. coli* transformed with uncloned pET 23a plasmid was streaked to an agar plate with ampicillin and chloramphenicol. Untransformed E. coli was streaked to an agar plate with ampicillin and chloramphenicol for negative control. **Figures 5.31a, b and c** show the agar plates with transformed, positive, and negative control bacteria.

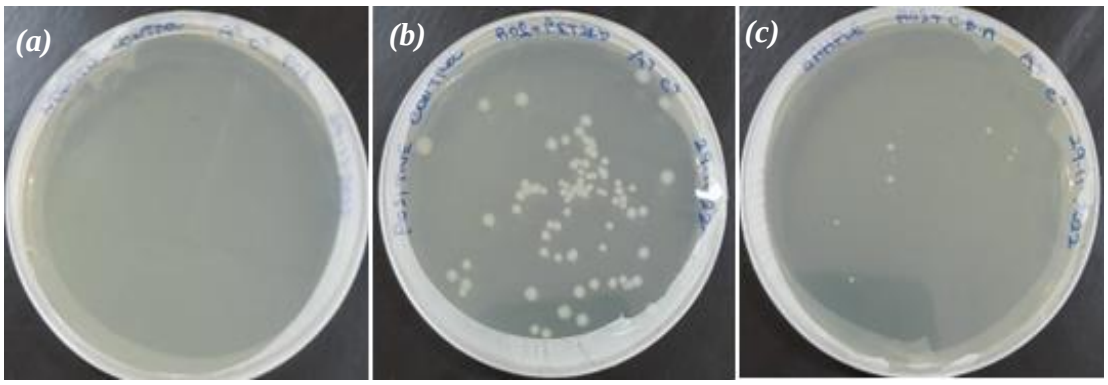

Figure 5.31 (a) Negative control, (b) Positive control and (c) Transformed sample (LB agar plate containing Chloramphenicol (35 µg. mL^{-1}) and Ampicillin (100 µg. mL^{-1} was used)

Some bacterial colonies were grown in the sample agar plates. This result confirmed the transformation of the cloned plasmid into *E. coli Rosetta pLysS.* If the Plasmid were transformed to *E.coli*, it would gain ampicillin resistance properties. Thus, bacteria were successfully grown in agar plates containing ampicillin and chloramphenicol. In the positive control sample, the *E. coli* with pET 23a plasmid gained ampicillin resistance properties and grew in agar plates. In the negative control sample, *E. coli* without any Plasmid did not gain ampicillin resistance property, so it could not grow in agar plates. Thus, the above explanation confirmed the successful transformation of the cloned plasmid.

5.11.6 Transformation confirmation

The cloned plasmid was isolated and restricted by BamH1 and Xho1 restriction

enzymes, and restricted samples were viewed in agarose gel, as shown in **Figure 5.32**. PCR confirmed the presence of the chitinase gene in the plasmid.

In PCR, the chitinase gene in the plasmid was amplified by primers used to isolate the chitinase gene from the *Bacillus aryabhattai* genome. The PCR products were verified by agarose electrophoresis, shown in **Figure 5.33.**

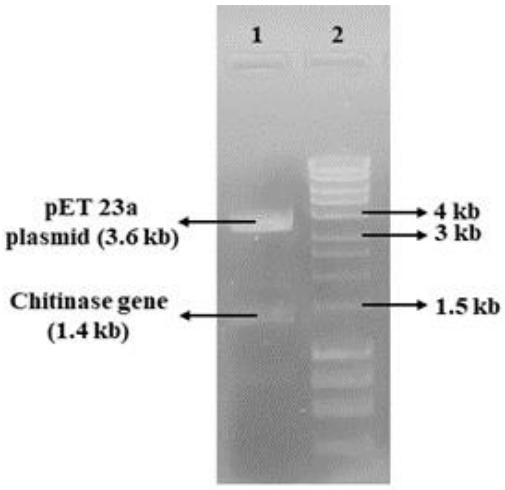

Figure 5.32 Restriction of plasmid by BamH1 and Xho1

(1 – DNA marker, 2 –Restricted cloned plasmid)

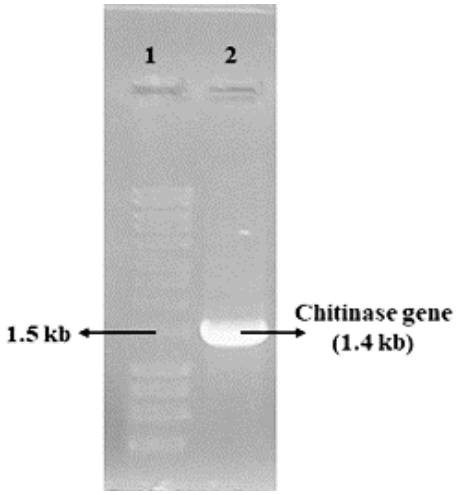

Figure 5.33 PCR method confirmation

(1 – DNA marker, 2 – Chitinase gene (1.4 kb))

The two bands of 3.6 and 1.4 kb size were in the double-digested sample. 3.6 kb band represented the size of pET 23a plasmid without gene, and 1.4 kb represented the size of the chitinase gene. This result confirmed the transformation of the cloned plasmid. PCR of isolated plasmid resulted in one band with the size of 1.4 kb, representing the size of the chitinase gene. Both results confirmed the insertion of the chitinase gene

from *Bacillus aryabhattai* to the pET 23a plasmid and the transformation of the cloned plasmid to *E. coli Rosetta pLysS*. The presence of the chitinase gene in the transformed plasmid was also confirmed by sequencing the cloned plasmid. The amino acid sequence of chitinase from *Bacillus aryabhattai* is shown below.

MKYLLPTAAAGLLLLAAQPAMAMGMSKGAAASSVGTVKGDNVNVYRSPSLHSSIV
QTVKKGEEFPAISSEAGDAAQVITHKVVPGNTLWLLAKQYGVTVSELIKQNQLKTTE
LTPGQTLKIPPKGLLHKVVSGDTLWKISVKYGVKATELTKLNQLSSTNIKPGQMLIIP
DYYVQVQLLEGKKGWIKKSDLAQKKHQPVVMGWSFNEKTAGYAESMKQKNLDVV
SPRWFTLTRSDKVVSSSINPSYVQTAHKNGKKVWPLIGNNFDDVLTSDVLGNKAKR
QKLVSSVESSLVKTNSDGINVDFENINIKNKQDFVLFIKELKGALKPHGMTVSVDVTR
ENNDPFWSGSFDRKQIGQVADYVIMMGYEEHWGGSQVPGSVASLPWVKEGTELLM
KDVPAHKILLGVPFYTREWKTDLSTKKVVTKDLTMKEAEAIISSKKLTKKWDSQASQ
YYVEYTENGTKHQIWLEDKASMQRRVKLINDYHLGGAAAWYIGSETSDIWELYNF.

The above protein sequence was blasted against the NCBI protein database, and it showed top identity with the protein sequence of LysM peptidoglycan-binding domain-containing protein from *Bacillus aryabhattai* (GeneBank Id: MBY0074003.1). Thus, the results confirmed that the cloned gene belongs to the chitinase gene of *Bacillus aryabhattai*.

5.12 Expression of Chitinase in *E. coli Rosetta pLysS* using IPTG induction method

The *Ba*ChiA was expressed using transformed *E. coli Rosetta pLysS*. The recombinant chitinase expressed were intracellular products, so cell lysis was performed to extract the expressed chitinase. SDS PAGE analysis of chitinase expression is shown in **Figure 5.34**.

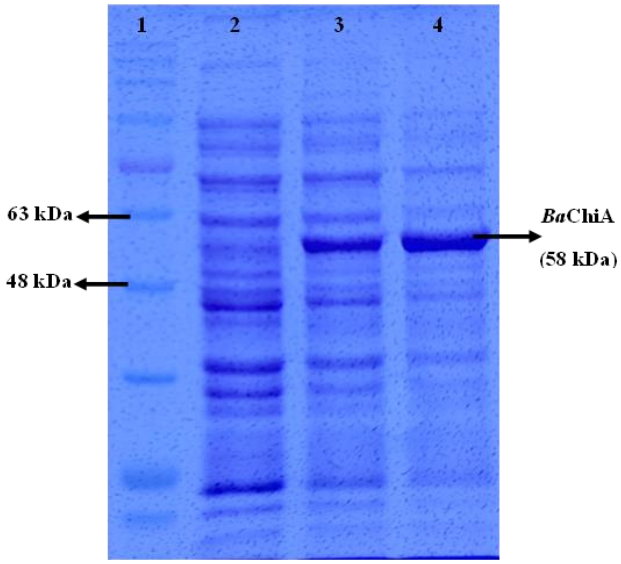

Figure 5.34 SDS PAGE of *Ba*ChiA expression

(1 – Protein Ladder, 2 – Crude protein expressed by *E. coli* with uncloned plasmid, 3 and 4 – Crude protein expressed by *E. coli* with cloned plasmid)

In lanes 3 and 4, an intracellular crude protein sample expressed by *E. coli* with cloned plasmid was added, and a thick band at 58 kDa molecular size confirmed the presence of *Ba*ChiA in the sample. In lane 2, the intracellular crude protein expressed by *E. coli* with uncloned plasmid was added. There was no chitinase band present in it. This result confirmed that the IPTG method was suitable for the chitinase expression. The molecular weight of the chitinase was calculated theoretically with its amino acid sequence, which was 58 kDa. However, expression using the IPTG induction method resulted in more inclusion body formation. Thus, process parameters were optimised using the IPTG induction method of chitinase expression.

5.13 Optimization of process parameters for IPTG induction method

5.13.1 Effect of induction at different growth phases on Inclusion bodies formation

The effect of IPTG induction of bacteria at different growth phases on inclusion bodies and soluble forms of chitinase formation was studied. From the SDS-PAGE, as shown in **Figure 5.35**, it was confirmed that IPTG induction at the Late log phase (OD at 1.5) of bacteria produced 40% of the soluble chitinase, more than induction at other growth phases.

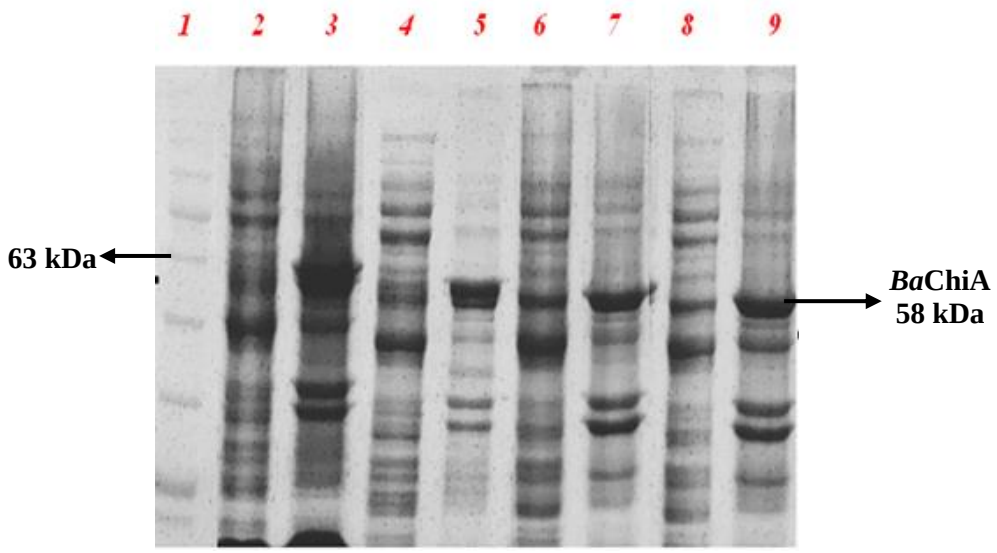

Figure 5.35 SDS PAGE of chitinase expression at different growth phases for IPTG induction (1 -Protein marker, 2- 0.6 OD (S), 3 -0.6 OD (P), 4- 1.2 OD (S), 5- 1.2 OD (P), 6- 1.5 OD (S), 7- 1.5 OD (P), 8- 1.7 OD (S), 9- 1.7 OD (P)). S- soluble protein and P – Inclusion bodies.

Induction at the early log phase (OD at 0.6) and mid-log phase (OD at 1.2) produced 5% and 20% of the soluble form of chitinase. The growth rate was high in the early and mid-log bacterial growth phase, which might increase the chitinase expression. Thus, bacteria converted the over-expressed chitinase into inclusion bodies as a defence mechanism. Thus, the inclusion bodies produced more than soluble chitinase by the bacteria when induced with IPTG in the early and mid-log phases. In the early stationary growth phase, the soluble form of chitinase produced was 30%. In the early stationary phase, the growth rate of the bacteria was constant, and metabolism was slow. So, the chitinase's solubilization was less than the late log phase. The rate of soluble form and activity of the chitinase in different growth phases is shown in **Figure 5.36**.

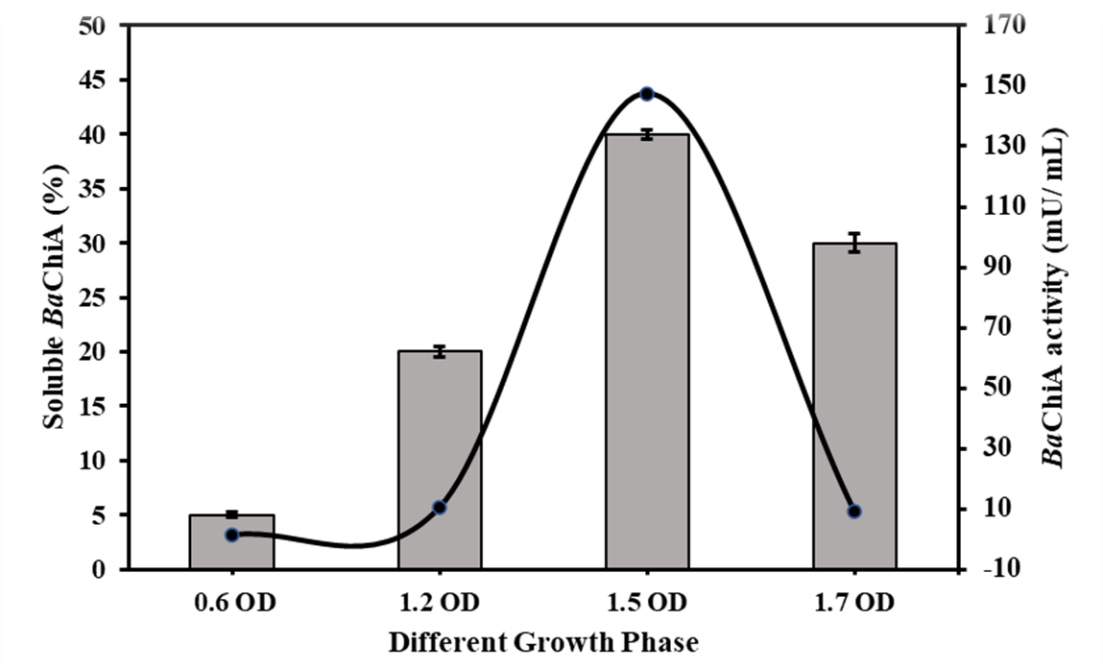

Figure 5.36 Soluble form and chitinase activity at different growth phases. (Bar graph and left scale – Soluble *Ba*ChiA concentration, Line graph and right scale – *Ba*ChiA activity)

The activity of the chitinase for all four samples was estimated. The activity for the chitinase produced after IPTG induction at early and mid-log phase were 1.23 and 10.33 mU· $mL^{-1,}$ respectively. The chitinase activity produced after induction at the late log phase was 147.5 mU· mL^{-1}. This result specified that the soluble chitinase produced in the first two cases was much less, so there was less activity. The soluble form is more in the third case, so there was high activity. In the early stationary phase sample, the activity was 10.33 mU· mL^{-1}. This decrease in activity was due to a lower growth rate of bacteria and less chitinase production.

5.13.2 Effect of IPTG concentration on Inclusion bodies formation

The effect of IPTG concentration on inclusion bodies and soluble chitinase production in recombinant *E. coli pLysS* was examined. As IPTG concentration increased to 1.5 mM, the concentration of soluble chitinase increased. The inclusion body formation increased after increasing the IPTG concentration to more than 1.5 mM. The change in the soluble form of chitinase and its activity for different IPTG concentrations is shown in **Figure 5.37**.

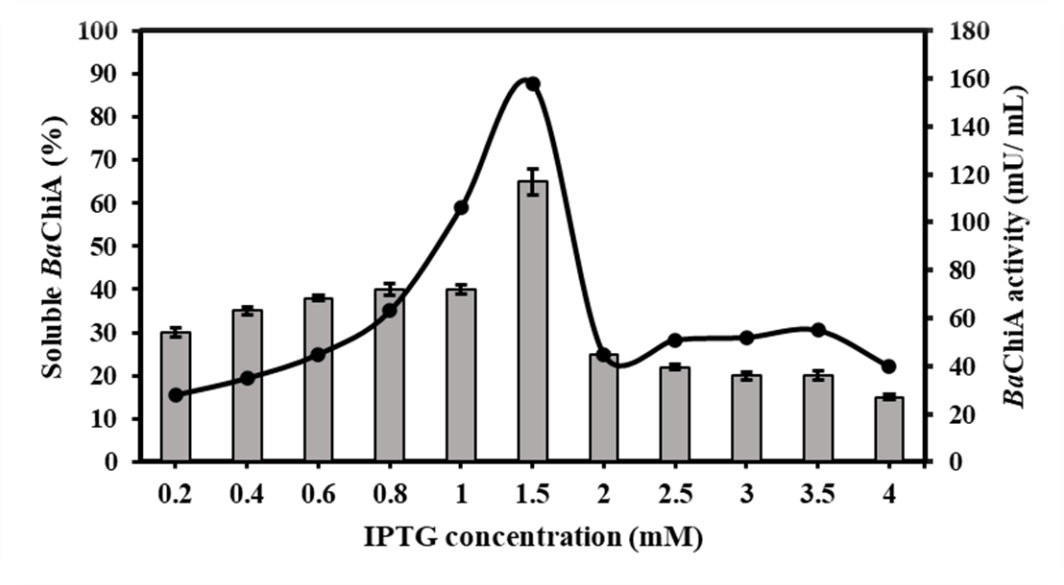

Figure 5.37 Soluble form and chitinase activity at different IPTG concentrations

(Bar graph and left scale – Soluble *Ba*ChiA concentration,

Line graph and right scale – *Ba*ChiA activity)

A maximum of 158 mU· mL^{-1} activity was achieved for the 1.5 mM IPTG concentration. 65% of soluble chitinase was obtained for this concentration. The less concertation of IPTG (0.2 to 1.5 mM) lowered the chitinase's expression rate, which increased the chitinase's solubility and activity. However, the higher concentration of IPTG (1.5 to 4 mM) increased the expression rate drastically. A higher concentration of IPTG also caused metabolic stress to bacteria. Thus, to overcome the stress, the formation of inclusion bodies was increased by bacteria, so enzyme activity decreased drastically (Shafiee et al. 2015).

5.13.3 Effect of Incubation time on Inclusion bodies formation

After IPTG induction, the bacterial culture was incubated at 12, 24, 36, and 48 hours at 16^{o}C at 120 rpm. The effect of inclusion bodies and soluble chitinase formation for different incubation times was studied. The change in soluble chitinase concentration and its activity for different incubation times is shown in **Figure 5.38**. The maximum soluble chitinase (70%) was obtained after 48 hours of incubation. Since the soluble chitinase concentration increased when the incubation time increased, the chitinase activity increased when the incubation time increased from 24 to 48 hours. The maximum chitinase activity achieved was 263 mU· mL^{-1}.

However, after increasing the incubation time to 60 hours, the chitinase activity and soluble form chitinase were decreased to 85 mU· mL^{-1} and 40%, respectively.

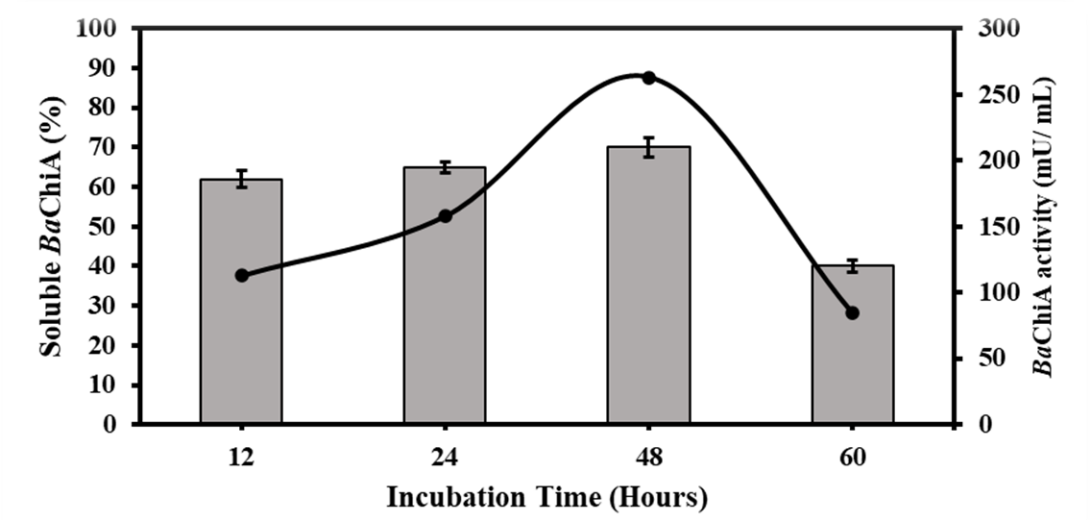

Figure 5.38 Soluble form and activity of chitinase produced at different incubation times.

(Bar graph and left scale – Soluble *Ba*ChiA concentration, Line graph and right scale – *Ba*ChiA activity)

Initially, from 12 hours to 48 hours incubation, there was no increase in soluble chitinase concentration because the increase in incubation time did not change the protein expression rate. However, the increased incubation time increased the biomass concentration, indirectly increasing the chitinase yield. Thus, there was an increase in chitinase activity. After 48 hours, the bacteria reached the death phase and decreased biomass concentration, which affected the chitinase yield. Thus, the chitinase activity and soluble chitinase concentration were decreased after 48 hours.

5.13.4 Effect of Glycerol concentration in media on inclusion bodies formation

Adding glycerol to the media may increase the carbon source availability for bacterial growth, increasing the bacterial biomass and soluble chitinase concentration. The change of soluble chitinase formation and its activity is shown in **Figure 5.39**. Different glycerol concentrations were added to the media (1 to 4%). The maximum chitinase activity of about 473 mU· mL^{-1} was achieved, and 95% of soluble chitinase was obtained from the media with 1% (v/v) glycerol concentration. Chitinase activity slightly decreased for higher concentrations (2%) of the glycerol, followed by a drastic decrease for 3 and 4% of glycerol. There is not much difference in the rate of

soluble chitinase enzyme formation.

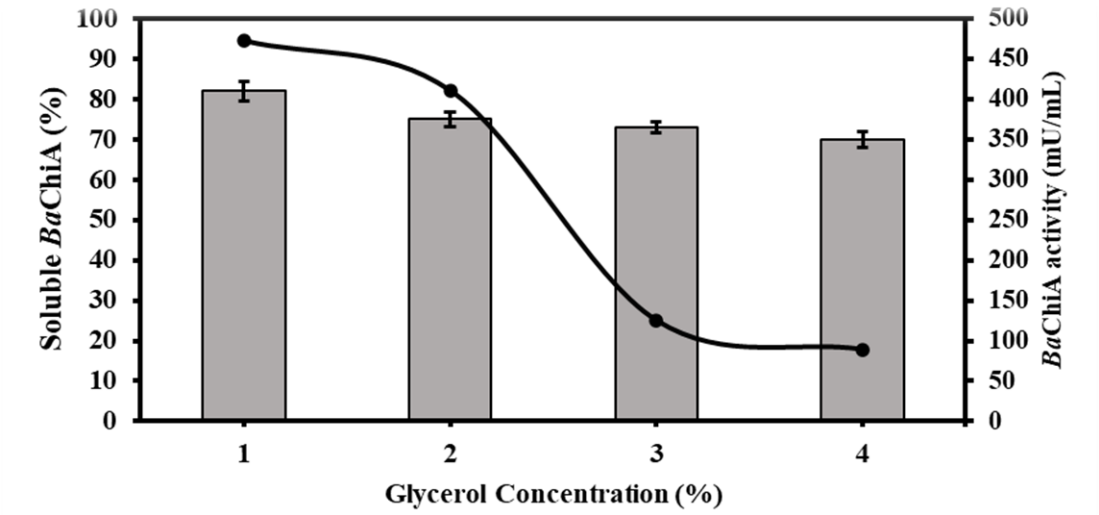

Figure 5.39 Soluble form and activity of chitinase produced at different Glycerol concentrations.

(Bar graph and left scale – Soluble *Ba*ChiA concentration,

Line graph and right scale – *Ba*ChiA activity)

The lower concentration of glycerol (0.1 to 1%) did not affect the growth of bacteria and its adhesion and cellulolytic properties. However, the increase in glycerol concentration (above 2%) affected the cell growth. Previous Research also proved that higher glycerol concentrations affected bacterial growth (Roger et al. 1992) and confirmed that incubating bacteria with glycerol for a longer time affected its growth. This was because the glycerol might have altered the cell shape and size. Thus, a decrease in bacterial growth in higher glycerol concentrations decreased the chitinase activity. SDS PAGE of Soluble protein and inclusion bodies for different glycerol concentration samples is shown in **Figure 5.40**.

Thus, by optimizing the above parameters, the formation of inclusion bodies decreased from 80% to 5%. Chitinase activity was improved from 1.23 $mU \cdot mL^{-1}$ to 473 $mU \cdot mL^{-1}$. In IPTG induction, after 48 hours of incubation, the biomass concentration obtained was 2 $mg \cdot mL^{-1,}$ which was less.

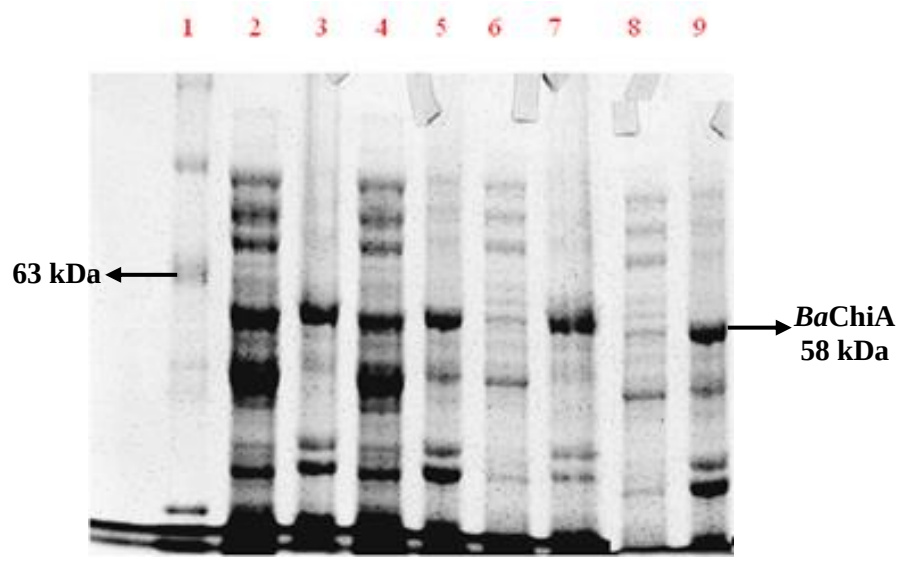

Figure 5.40 SDS PAGE of Soluble protein and inclusion bodies for different Glycerol concentrations (1 – Protein ladder, 2- 1% (S), 3- 1% (P),4- 2% (S), 5- 2% (P), 6- 3% (S), 7- 3% (P), 8- 4% (S), 9- 4% (P))

S- soluble protein and P – Inclusion bodies.

Thus, to increase the biomass and chitinase yield, the autoinduction method of terrific broth was used for chitinase expression. Also, an auto-induction medium was used to replace IPTG to reduce the cost of the medium, improve downstream processing and reduce the toxic effects of IPTG on the cells. This method's process parameters were optimised to achieve the highest chitinase activity.

5.14 Statistical optimization of chitinase expression using the Taguchi method

The Taguchi method was used to determine the optimum process parameters to improve the expression of the soluble form of recombinant chitinase in *E. coli Rosetta pLysS*. A total of 25 experiments were performed with five variables at different levels, as shown in **Table 5.5**. The “larger is better” option of the S/N ratio was considered as it represented the best levels for each parameter to achieve maximum soluble chitinase. Taguchi's response analysis is shown in **Figure 5.41**, representing the optimum values of each parameter within the levels chosen. **Figure 5.41** represents the main effect plots of the S/N ratio for maximum soluble chitinase yield against Temperature (10 to 20℃), Shaking speed (120 to 160 rpm), incubation time (12 to 60 hours), glucose concentration (0 to 0.1%) and lactose concertation (0.5 to 2.5%). Based on S/N ratio analysis, the optimum parameter levels for maximum

soluble chitinase yield were temperature at 12.5℃, shaking speed at 150 rpm, glucose concentration of 0.075%, lactose concertation of 1.5% and Incubation time of 36 hours.

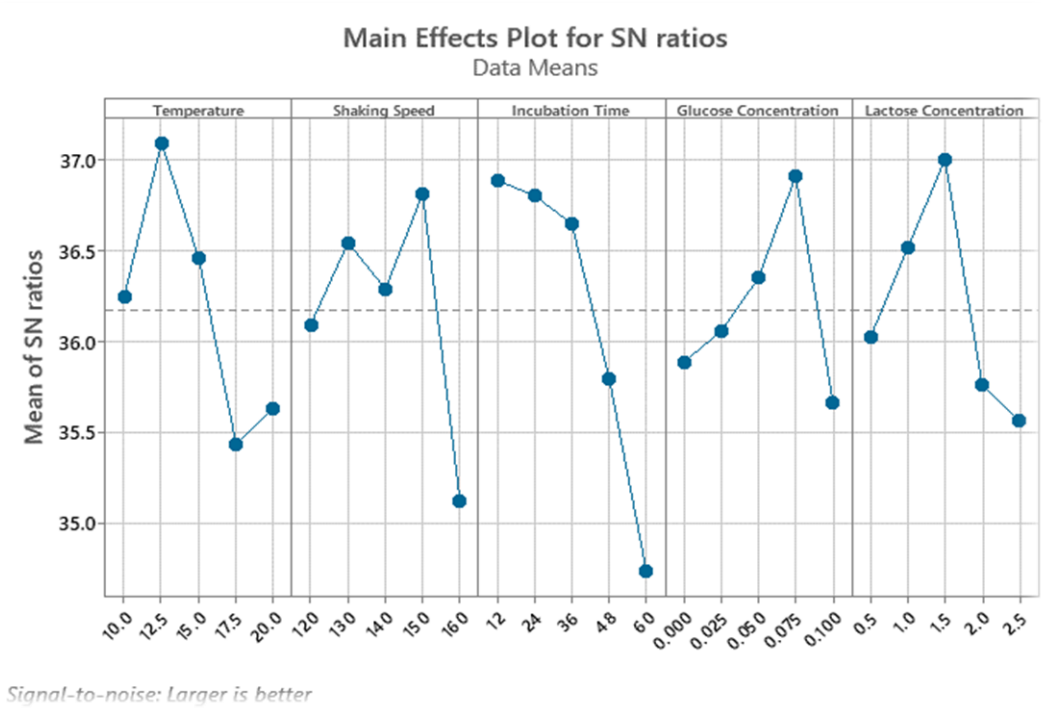

Figure 5.41 S/N ratio of different variables for different levels.

The maximum (predicted) soluble chitinase yield achieved using optimized parameters was 85.3% (S/N ratio 40.00). After this analysis, the experiments were performed in the above-optimized conditions. 80% of the soluble form of chitinase was obtained. The chitinase concentration of 10.53 µg. mL^{-1} and its yield of 133 µg. mg^{-1} of biomass was achieved, which was 3.6 folds higher than the IPTG method. The maximum chitinase activity achieved was 2.55 U. mL^{-1}, fivefold higher than the IPTG method. Higher concentration of Yeast extract and peptone in the terrific broth helps for higher bacterial growth. Addition of glucose and lactose makes the bacteria to depend on these compounds for carbon source. The concentration of glucose was very less compared to lactose. After glucose depletion, the bacteria consume lactose for carbon sources. The lactose also binds to the T7 lac promotor and initiates the expression of the chitinase gene cloned to the pET 23a vector.

Thus, the components in the autoinduction media promotes the higher enzyme expression levels. Moreover, usage of IPTG will be toxic and stress to the bacteria. This autoinduction media will overcome this challenge.

Temperature (℃)	**Shaking Speed (rpm)**	**Incubation Time (Hours)**	**Glucose Concentration (%)**	**Lactose Concentration (%)**	**Soluble enzyme yield (%)**	**S/N ratio**
10	120	12	0	0.5	65.45	36.44
10	150	48	0.075	2	69.73	36.83
10	130	24	0.025	1	75.20	37.47
10	140	36	0.05	1.5	79.47	37.83
10	160	60	0.1	2.5	42.22	32.64
12.5	130	36	0.075	2.5	78.87	38.06
12.5	140	48	0.1	0.5	64.70	36.16
12.5	120	24	0.05	2	73.02	37.40
12.5	150	60	0	1	66.92	36.34
12.5	160	12	0.025	1.5	75.21	37.46
15	130	48	0	1.5	69.64	36.98
15	140	60	0.025	2	52.96	34.60
15	150	12	0.05	2.5	74.39	37.37
15	160	24	0.075	0.5	69.09	36.62
15	120	36	0.1	1	68.50	36.67
17.5	150	24	0.1	1.5	69.94	37.01
17.5	160	36	0	2	51.36	34.15
17.5	140	12	0.075	1	72.51	37.34
17.5	120	48	0.025	2.5	52.60	34.25
17.5	130	60	0.05	0.5	52.67	34.39
20	120	60	0.075	1.5	61.20	35.68
20	150	36	0.025	0.5	65.66	36.47
20	140	24	0	2.5	59.70	35.48
20	130	12	0.1	2	62.78	35.79
20	160	48	0.05	1	53.68	34.72

Table 5.5 Different experiments for five variables using the Taguchi method with obtained response and S/N ratio.

5.15 Purification of chitinase by Ni-NTA affinity chromatography

The purification of expressed recombinant chitinase was performed using Ni-NTA affinity chromatography, which was specific to the 6X Histidine tag present in the C terminal end of the chitinase. After purification, five samples, such as crude, flow-through, wash 1, wash 2 and elution samples, were analysed using SDS PAGE, as shown in **Figure 5.42**. In lane 2, the intracellular crude sample was obtained after the expression was added. The thick band at 58 kDa was identified in that sample, confirming the presence of chitinase in the crude sample. In lane 3, the flow-through sample was added.

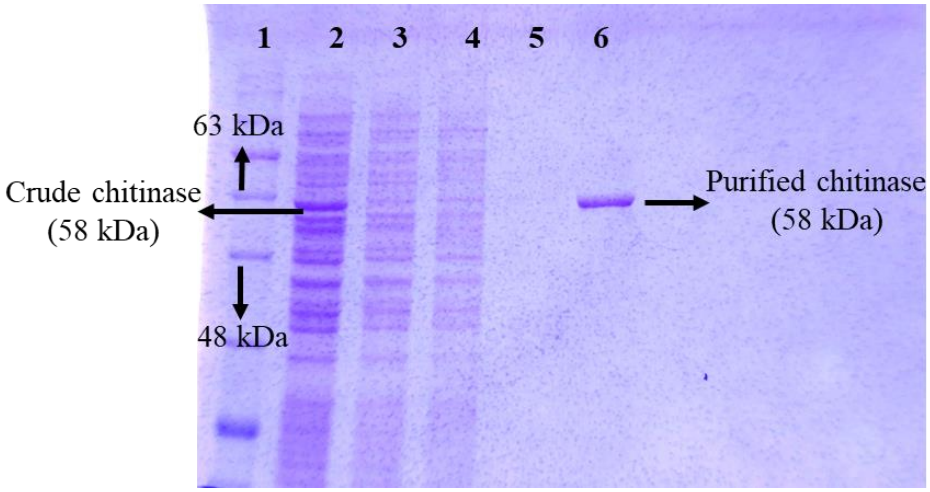

Figure 5.42 Purification of recombinant chitinase

(1 – Protein marker, 2 – Crude enzyme, 3 – Flow through, 4 and 5 – Wash sample and 6 – Elution sample)

In this sample, there was no chitinase band. This result confirmed that chitinase was firmly bound to the Ni-NTA column. Wash samples were added to lanes 4 and 5. In lane 4, the other proteins except chitinase were present, confirming that other non-specific bounded protein was removed successfully. And there was no band present in the lane 5. This result confirmed no other proteins were present in the column after the washing step. In lane 6, the eluted sample was added. In this lane, the presence of chitinase at 58 kDa was confirmed, and no other bands were present. Thus, the purified chitinase was obtained using Ni-NTA affinity chromatography. Further, chitinase characterization was performed to study the properties of chitinase. The final concentration of purified chitinase obtained was estimated as 0.13 mg· mL^{-1}. The specific chitinase yield obtained was 0.054 mg· g^{-1} of biomass. The activity and

specific activity of purified chitinase against colloidal chitin corresponded to 8.23 U· mL^{-1} and 63.3 U· $mg^{-1,}$ respectively.

5.16 *Ba*ChiA Characterization Study

5.16.1 Effect of pH, Buffer, and Temperature on chitinase Activity

The effect of chitinase activity at different pH and buffer compositions such as 50 mM citrate buffer (pH 5, 6), sodium phosphate buffer (pH 6, 7), Tris base buffer (pH 7, 8), Borate buffer (pH 8, 9) is shown in **Figure 5.43**. The figure confirms that the specific chitinase activity was high at pH 6 to 8, with the maximum at pH 8, which was 64 U· mg^{-1}. The specific activity at pH 7 was 87% of maximum activity.

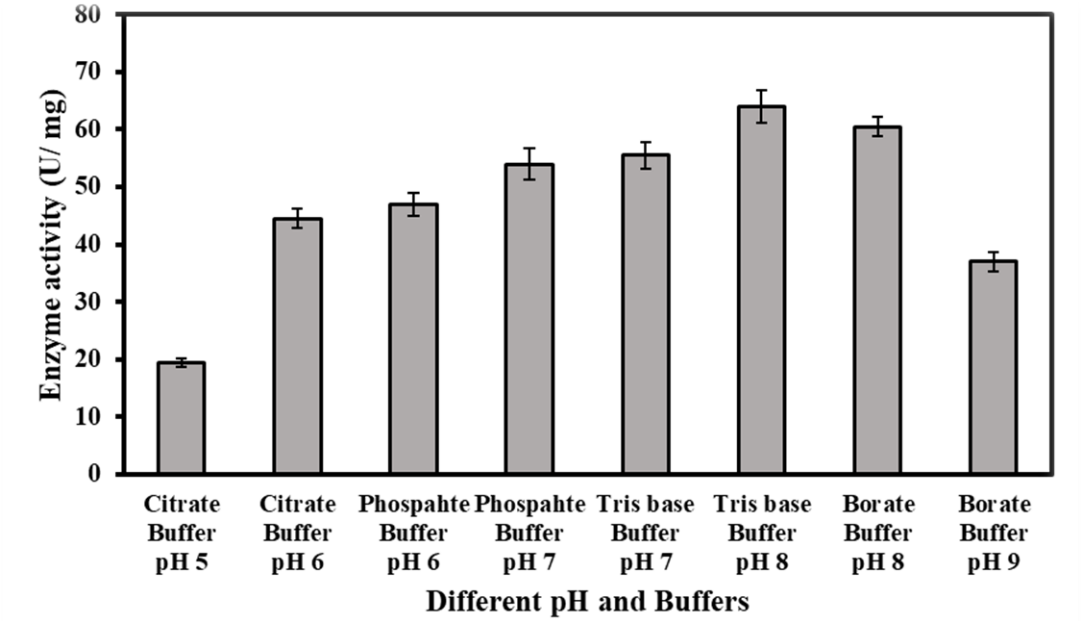

Figure 5.43 Chitinase specific activity at different pH and Buffers

The specific activity at pH 6 was 73.5% of maximum specific activity. However, the specific activity at pH 5 and 9 decreased by less than 50% of the maximum specific activity. These results proved that chitinase was unstable at pH 5 and 9. At pH 8, the specific chitinase activity was higher in the Tris base buffer than in the borate buffer. The average pH of the marine environment was 8, and chitinase was obtained from the same environment. Thus, the chitinase was stable and achieved maximum activity at pH 8. The chitinase stability was affected in extreme acidic and alkaline pH by excess H^+ and OH^- ions. Various research showed that the bacterial chitinase from different sources, such as marine and soil, possessed the highest activity at a pH range

of 6 to 8 (Farag et al. 2016; Ray et al. 2019a; Subramanian et al. 2020b). The effect of temperature on chitinase activity was determined. The chitinase activity at different temperatures is shown in **Figure 5.44**. The highest specific chitinase activity achieved at 55℃ was 138 U· mg^{-1}. The chitinase was also stable at 60℃ and possessed a specific activity of 76.5% of maximum specific activity. The specific chitinase activity at 65℃ decreased by less than 60% of the maximum specific activity.

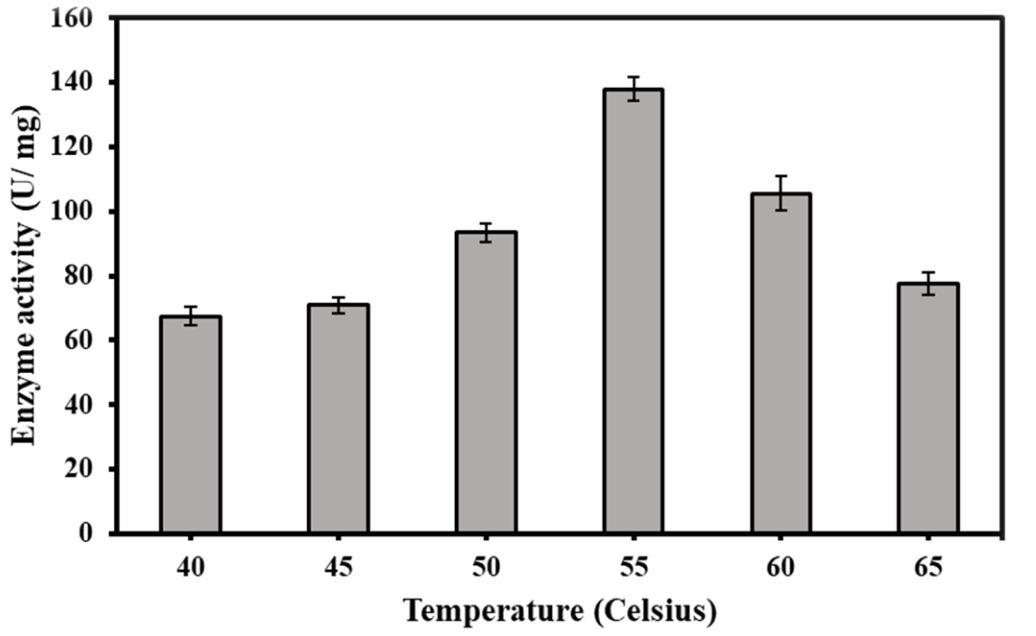

Figure 5.44 Chitinase specific activity at different temperatures

The specific activity at 40℃ and 45℃ was less than 50% of maximum specific activity. The above explanation confirmed that the chitinase enzyme was stable till 60℃ and had the highest specific activity achieved at 55℃. The specific activity increased from 40 to 55℃ when the temperature increased. This was because the increase in temperature increased the ionization of water molecules, which might improve the efficiency of the hydrolytic activity of chitinase. The chitinase was also stable at higher temperatures, so the specific activity increased. When the temperature increased to 60 and 65℃, the specific chitinase activity was decreased because chitinase's stability might be affected by high temperature. The justification was proved by various research. Most of the chitinase from different sources, such as marine, soil, etc., also possessed the highest activity at the temperature range from 50 ℃ to 60 ℃ (Farag et al. 2016; Ray et al. 2019b; a; Subramanian et al. 2020b).

5.16.2 Effect of Metal ions and NaCl on Enzyme Activity

The effect of different metal ions (Mn^{2+}, Mg^{2+}, Ni^{2+}, Co^{2+}, Ca^{2+}, and Na^{+}) on chitinase activity is shown in **Figure 5.45**. The highest specific chitinase activity of 452 U· mg^{-1} was achieved in the presence of sodium ions in the reaction mixture, with 327% activity without metal ions. This result proved that chitinase activity was enhanced in the presence of sodium chloride. Since the chitinase was from a marine source, the sodium ions play a significant role in chitinase activity enhancement. Moreover, many researchers confirmed the above results. The activity of marine chitinase from bacteria and fungus was improved by adding NaCl to the reaction mixture of the concentration range from 200 to 500 mM (He et al. 2022; Liu et al. 2020; Loni et al. 2014).

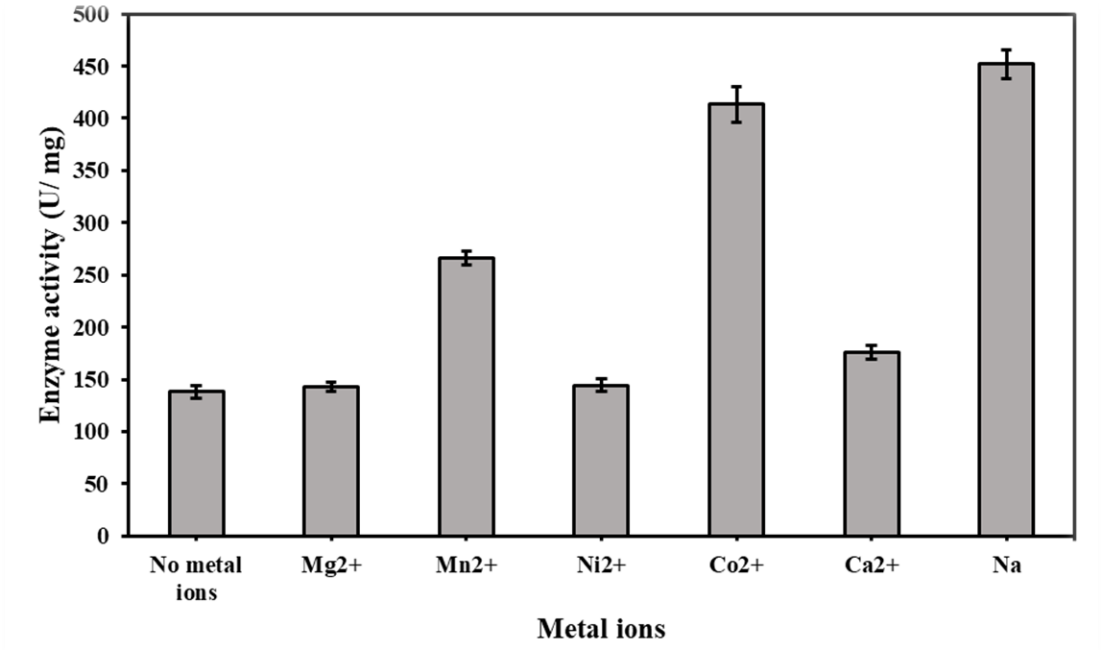

Figure 5.45 Chitinase specific activity at different Metal ions

Similarly, specific chitinase activity of 413.5 U· mg^{-1} was obtained with the presence of Cobalt metal ions, which is 300%. The specific chitinase activity achieved was 266 U. mg^{-1} and 175 U. mg^{-1}, 193% and 127% of specific activity without metal ions for Manganese and calcium metal ions, respectively. However, the magnesium, nickel and calcium ions had no changes in enzyme activity, the same as without metal ions. Several research studies also proved that both wildtype and recombinant chitinase enzyme activity was enhanced by cobalt and manganese metal ions (Lee et al. 2007;

Saima et al. 2013; Shivalee et al. 2018). Hydrolases of carbohydrates with metal were achieved when both amino acid side chains and transition metal ions combine and enhance the transfer of protons between the substrates and metal ions. This property is the main reason for stabilising intermediates, which is essential to perform hydrolytic reactions efficiently. The metal also enhances the reactivity of the water nucleophile and intermediates stabilization (Hernick and Fierke 2010). Thus, the addition of metal ions enhanced the chitinase activity.

5.16.3 Michaelis Menten kinetic study of *Ba*ChiA

The Michaelis Menten kinetics parameters such as *Km*, *Vmax*, *turnover number* (*Kcat*) and *catalytic efficiency* (*Kcat/Km*) for the *Ba*ChiA were determined. The enzyme velocity was determined for the different colloidal chitin concentrations (0.1 mg. mL^{-1} to 50 mg. mL^{-1}).

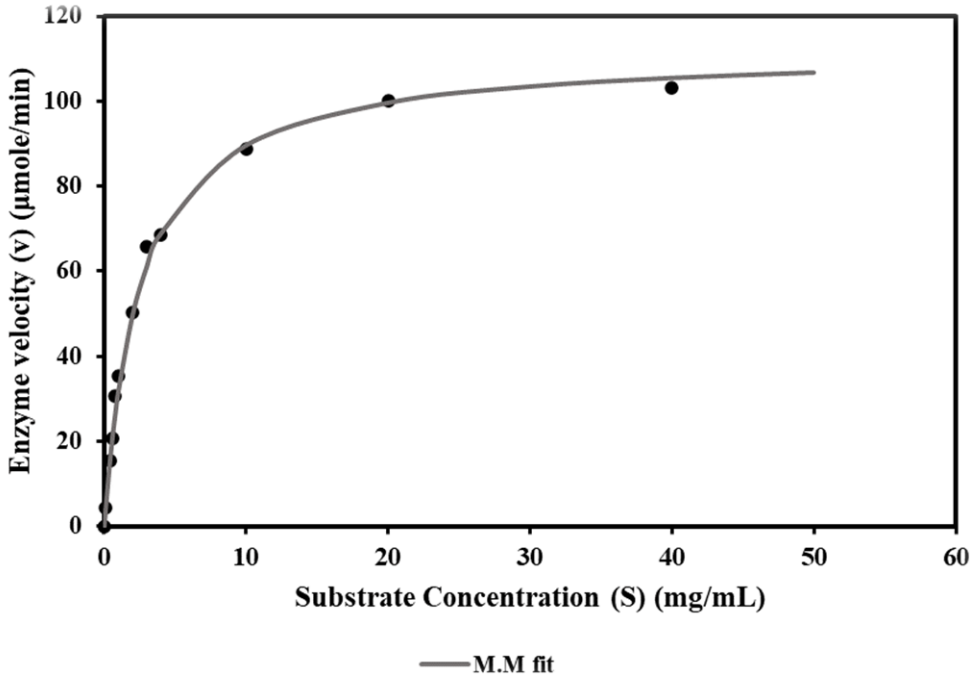

Figure 5.46 Michaelis Menten fit for chitinase at different substrate concentrations

The graph was plotted between enzyme velocity as the Y axis and substrate concentration as the X axis to verify the Michaelis Menten fitting. The graph is shown in **Figure 5.46**. The chitinase velocity fitted the Michaelis Menten curve for the above substrate concentration. Moreover, the kinetics parameters were determined by plotting the Lineweaver Burk plot between *1/ S* as the X-axis and *1/ V* as the Y-axis,

in which the slope of the graph was *Km/ Vmax* and the intercept was *1/ Vmax*. The plot is shown in **Figure 5.47.** The *Vmax* and *Km* of the chitinase determined were 112.3 µmole· min^{-1} and 2.5 mg· mL^{-1}. The *Kcat* and *catalytic efficiency* of the *Ba*ChiA determined was 192 min^{-1} and 1.28 mL· mg^{-1}. $second^{-1}$ respectively.

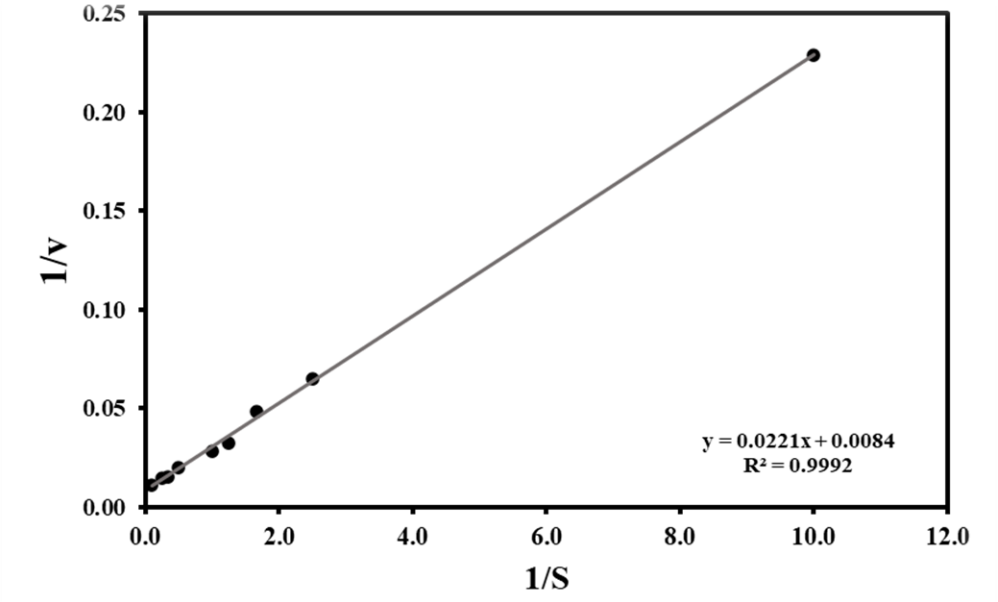

Figure 5.47 Lineweaver Burk plot to determine kinetics parameter

Moreover, chitinase against insoluble chitin substrates such as chitin powder and flakes was determined.

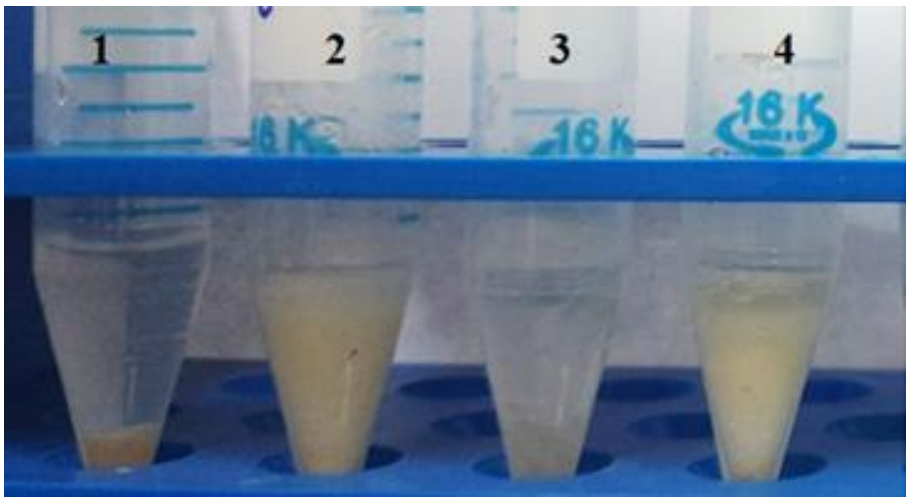

Figure 5.48a Chitin substrates before and after treatment with purified chitinase (1 and 3 – Chitin powder and flakes before treatment, 2 and 4 Chitin powder and flakes after treatment)

The chitinase activity against chitin powder and flakes was 875 U· mg^{-1} and 625 U· $mg^{-1,}$ respectively. The visual appearance of insoluble chitin substrates before and after treatment with recombinant chitinase is shown in **Figure 5.48**. The insoluble powder and flakes were degraded and converted to colloidal form within 1 hour of reaction with recombinant chitinase. In **Figure 5.48a**, both untreated substrates were settled in the bottom of the tubes without dissolving. However, the treated substrates were converted into colloidal form. Thus, it had a turbid appearance. Further incubation of these till 24 hours resulted in the formation of clear solution in the top, as shown in **Figure 5.48b**.

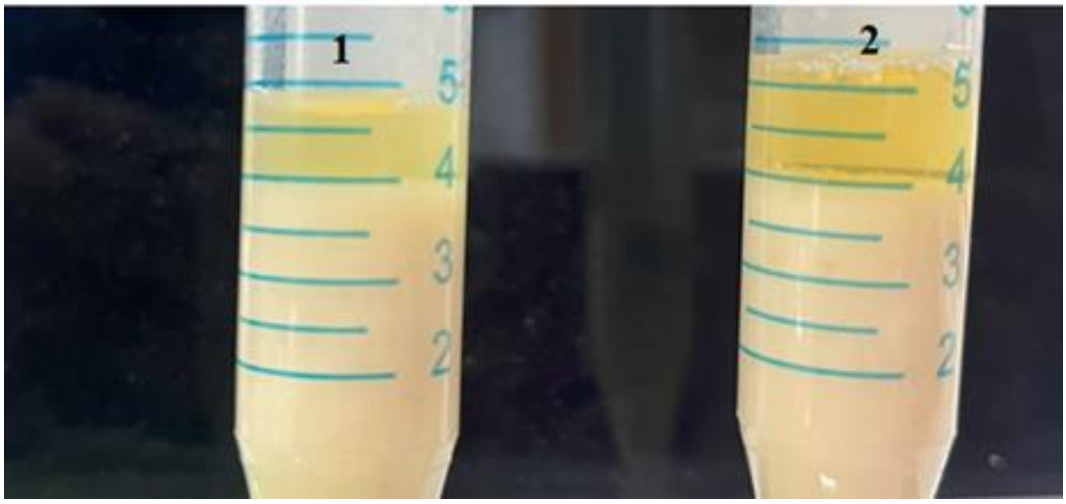

Figure 5.48b Chitin substrates after treatment with purified chitinase for 24 hours (1 and 2 – chitin powder and flakes, respectively)

The level of this clear solution increased with the increase in incubation time. This confirmed that recombinant chitinase completely solubilized the insoluble chitin substrates into soluble chitin oligomers. The above results proved that *Bacillus aryabhattai*'s chitinase efficiently helped convert the insoluble chitin wastes into valuable products such as chitin oligomers. Thus, this study solved a significant research gap in producing chitin oligomers from insoluble chitin. Using strong acids to convert the insoluble chitin into colloidal chitin can be avoided while producing chitin oligomers from insoluble chitin wastes.

The types of chitin oligomer products developed from insoluble chitin substrates using this recombinant chitinase were also studied using TLC and LC-MS techniques.

5.17 TLC analysis of chitin oligomers produced by recombinant chitinase

TLC analysis of reaction samples of recombinant chitinase with different chitin substrates is shown in **Figure 5.49**. The separation of 3 different samples was achieved using a TLC plate. The chitin oligomers standard was added to lane 1, consisting of chitin monomer to hexamer. The separation of six compounds was achieved using TLC, which was used to confirm the presence of oligomers in the reaction samples.

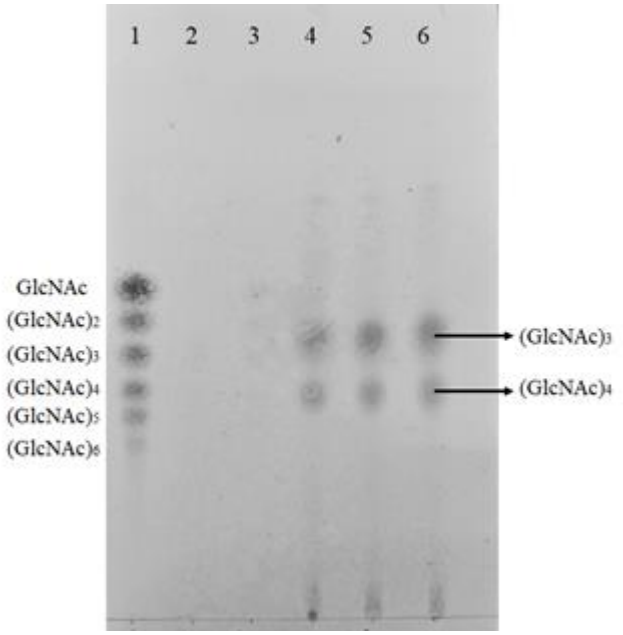

Figure 5.49 TLC study for chitinase enzymatic reaction sample against different chitin substrates (GlcNAc – N-acetyl glucosamine) (1 - Chitin oligomer standard, 2,3 – Substrate and enzyme blank, 4,5 and 6 – reaction samples of colloidal chitin, chitin powder and flakes, respectively)

In lanes 2 and 3, the substrate and enzyme blank samples were added. No spots were identified in these samples, which confirmed that no chitin oligomer products were formed from the enzyme and substrates individually. In lanes 4, 5 and 6, the reaction samples of colloidal chitin, chitin flakes and powder were added. There were two spots in all three samples, the same as the spot of chitin trimer and tetramer in the standard sample.

This result confirmed that chitin oligomers such as trimer and tetramer were produced by recombinant chitinase from chitin powder, flakes and colloidal chitin. The recombinant chitinase developed by this study might belong to the endochitinases family. Endo chitinase acts in the middle of the chitin polymer chains and produces chitin oligomers. However, exo chitinase acts on the end of the chitin chain and produces only N-acetyl glucosamine (chitin monomer). Previous research also ensured that endochitinase produced chitin oligomers such as dimer till hexamers from colloidal chitin substrates (Dravid et al. 2015; Li et al. 2019; Menghiu et al. 2019). Chitinase belongs to the endochitinases family will produce different oligomers with DP from 2 to 20. Thus, there was a possibility of production of oligomers other than trimer and tetramer. The significant drawbacks of TLC were the low resolution and sensitivity, which makes it challenging to identify the compounds with less concentration (below 500 ppm). It was essential to find the oligomers other than trimer and tetramer in the reaction samples using LC-MS. Thus, the above samples used for TLC were subjected to LC-MS analysis.

5.18 Liquid chromatography - Mass spectrometry (LC-MS) analysis of Chitin oligomer

LC-MS analysis of the chitin oligomers standard was performed. The LC chromatogram of different chitin oligomers is shown in **Figure 5.50a.** From **Figure 5.50a**, the retention time for the monomer to hexamer was obtained. Two different peaks were obtained for each compound because two different isomers have existed for these compounds (Lopes and Gaspar 2008).

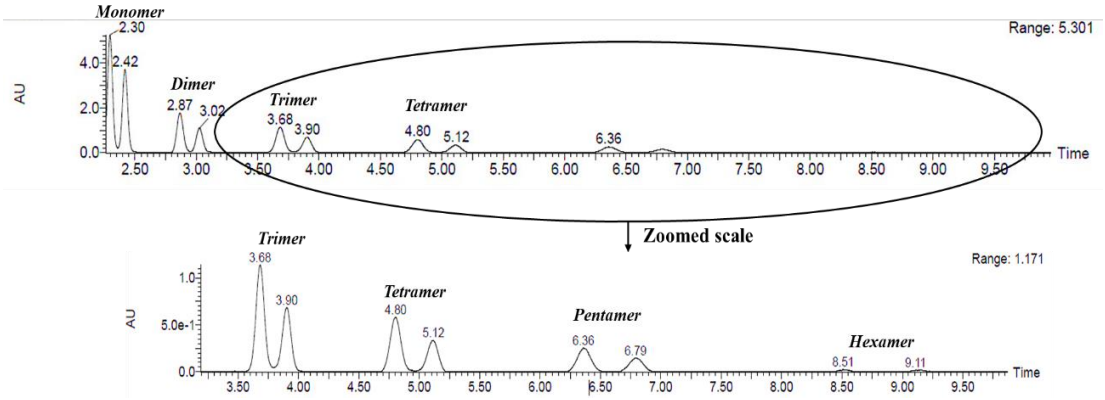

Figure 5.50a LC chromatogram for standard chitin oligomers

The retention time for monomer was 2.30 and 2.42 min, for dimer was 2.87 and 3.02 min, for trimer was 3.68 and 3.90 min, for tetramer was 4.80 and 5.12 min, for pentamer was 6.36 and 6.79 min and for hexamer was 8.51 and 9.11 min. Moreover, the MS analysis was performed for the LC peak of each oligomer, and a unique m/z peak was determined for each oligomer.

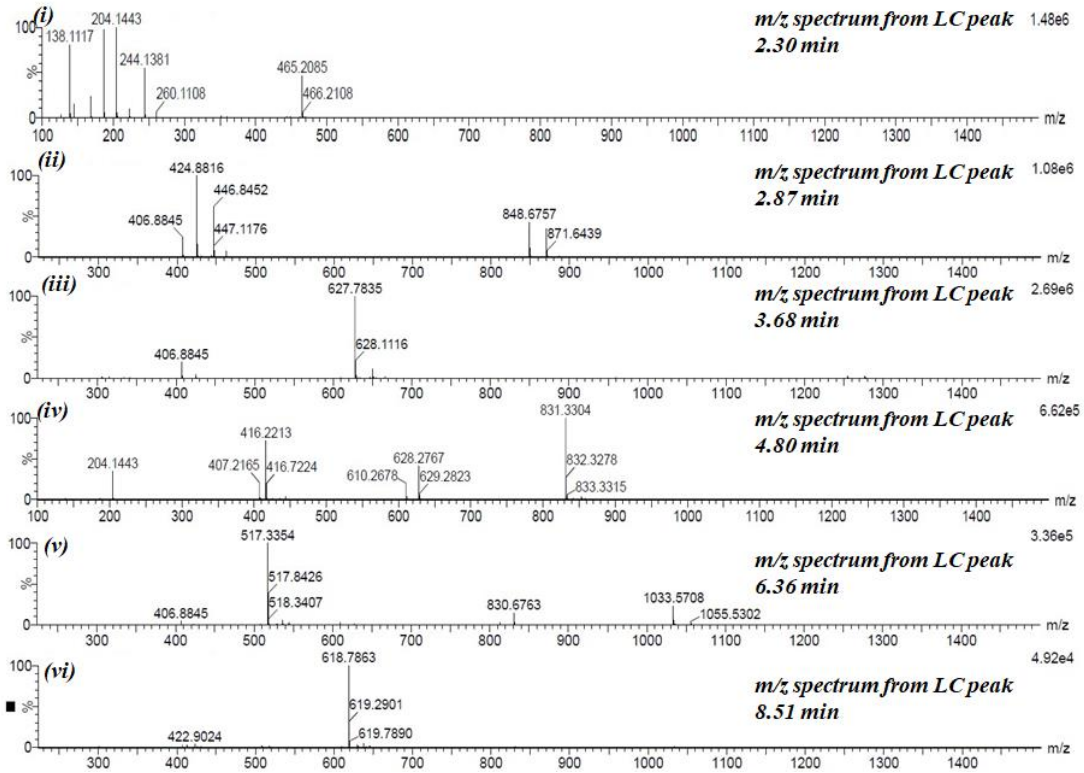

Figure 5.50b MS Spectrum for standard chitin oligomers (i – Monomer, ii – Dimer, iii – Trimer, iv – Tetramer, v – Pentamer and vi – Hexamer)

The m/z peaks obtained for monomer was 243.9, for dimer was 424.8 and 446.8, for

trimer was 627.7, for tetramer was 830.6, for pentamer was 517.3 and 1033.5 and for hexamer was 618.7. The m/z spectrum for each compound is shown in **Figure 5.50b**. The LC chromatogram and MS spectrum were used to identify the chitin oligomers in reaction samples of colloidal chitin, chitin powder and flakes. Further, the LC chromatogram of all three reaction and substrate blank samples is shown in **Figure 5.51**. Peaks obtained at 3.90 min and 4.04 min for colloidal chitin and chitin powder samples and at 3.68 min and 4.02 min for chitin flakes were close to the retention time of trimer peaks of the standard sample. Peaks obtained at 4.84 and 5.32 min for colloidal chitin, 5.11 min for chitin flakes and 4.94 and 5.36 min for chitin powder were also close to the retention time of tetramer peaks of the standard sample. Peaks obtained at 6.20 and 6.52 min for colloidal chitin, chitin powder and flakes were close to the retention time of pentamer of the standard sample.

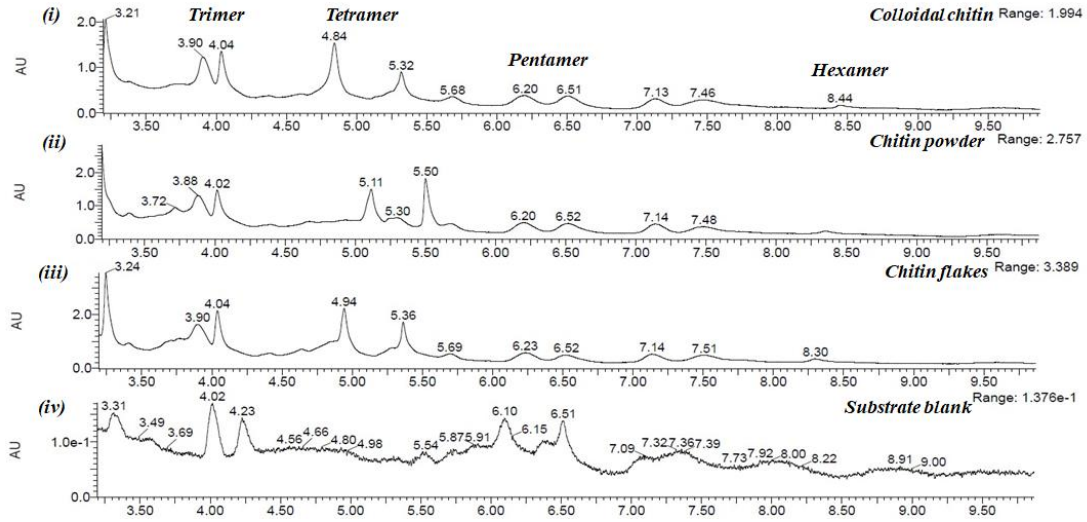

Figure 5.51 LC chromatogram of different reaction samples

(i – colloidal chitin, ii – chitin powder, iii – chitin flakes and iv – substrate blank)

Peaks obtained at 8.44 min for colloidal chitin and 8.30 min for chitin powder and flakes were close to the retention time of the hexamer peak of the standard sample. The peaks obtained at 4.02 and 6.51 min for the substrate blank sample were close to the retention time of the trimer and pentamer of reaction samples.

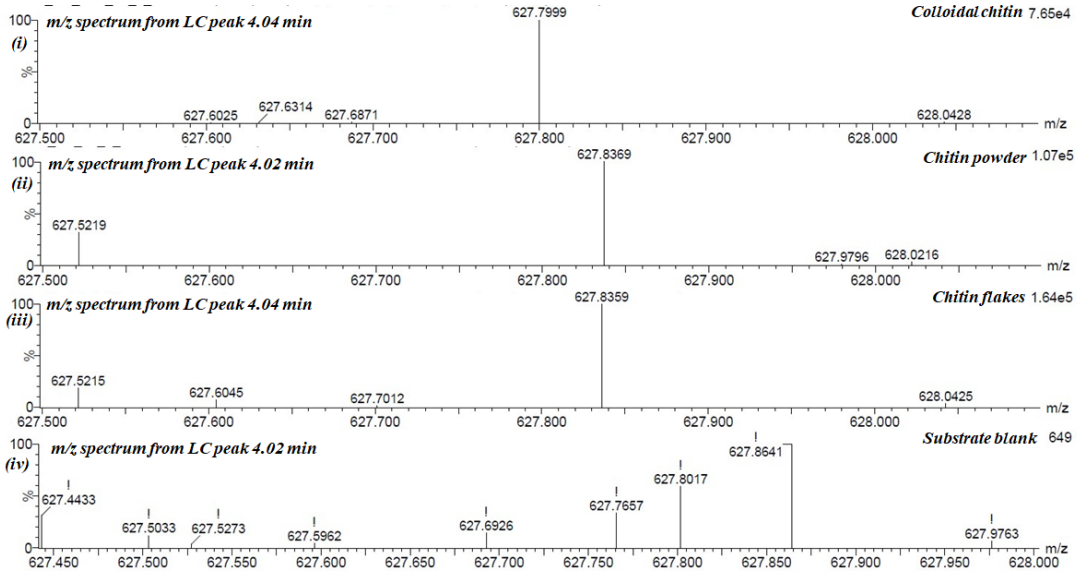

Figure 5.52a MS Spectrum of chitin trimer peak for reaction sample against different chitin substrates

However, the concentration of those peaks was 10-fold less than the sample peaks, which confirmed that the peaks obtained were not due to chitin oligomers. Each of the peaks mentioned above was subjected to MS analysis. The m/z spectrum for trimer, tetramer, pentamer, and hexamer in the reaction sample and two substrate blank peaks are shown in **Figure 5.52 a, b, c, and d,** respectively. In **Figure 5.52a**, the m/z peaks of chitin trimer obtained from different reaction samples are shown. The m/z peak obtained for reaction samples was 627.79, 627.83 and 627.83 for colloidal chitin, chitin powder and flakes, respectively. These m/z peaks were the same as the m/z peaks of the chitin trimer of the standard sample, which was at 627.78. The m/z peaks obtained from the substrate blank sample were also 627.80 and 627.86. However, the concentration of those peaks was 10^5 folds less than the peaks obtained from the reaction sample. So, this confirmed that chitin trimer was not produced in substrate blank. The above results confirmed the presence of chitin trimer in all reaction samples. In **Figure 5.52b,** the m/z peaks for chitin tetramer are shown. The m/z peaks obtained for colloidal chitin, chitin powder and flakes were 416.99 m/z, the same as the m/z peak of chitin tetramer from the standard sample. This result confirmed the presence of chitin tetramer in all three reaction samples. In **Figure 5.52c**, the m/z peaks for chitin pentamer are shown. The m/z peaks obtained were at 517.87, 517.88 and 517.88 for colloidal chitin, chitin powder and flakes, respectively.

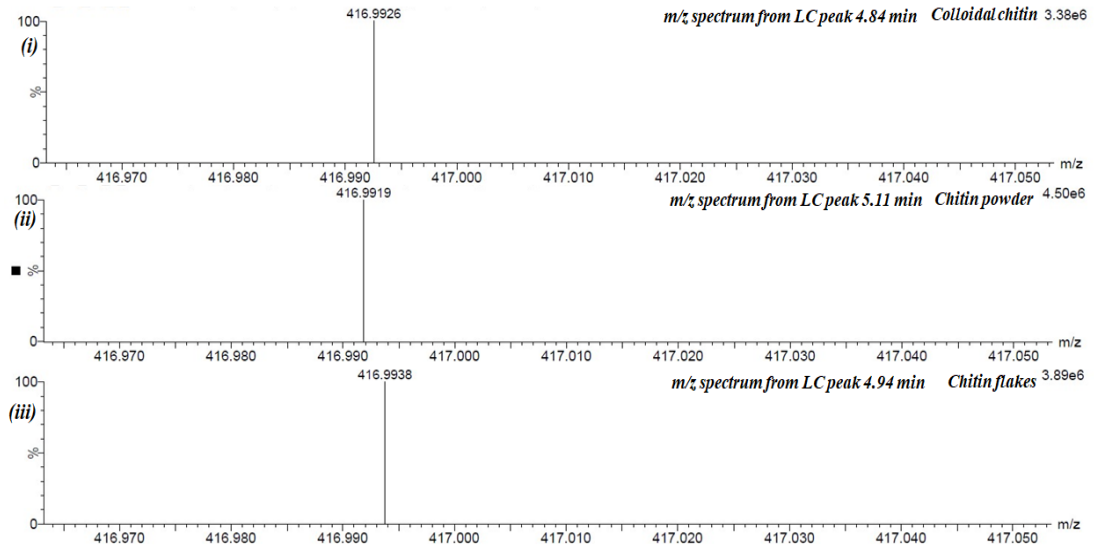

Figure 5.52b MS Spectrum of chitin tetramer peak for reaction sample against different chitin substrates

These m/z peaks were the same m/z peak of chitin pentamer from the standard sample, which was 517.33. The m/z peak obtained for substrate blank was at 517.48. However, the concentration was 10^4 folds less than the peaks of reaction samples, which confirms that no chitin pentamer was formed in the substrate blank sample.

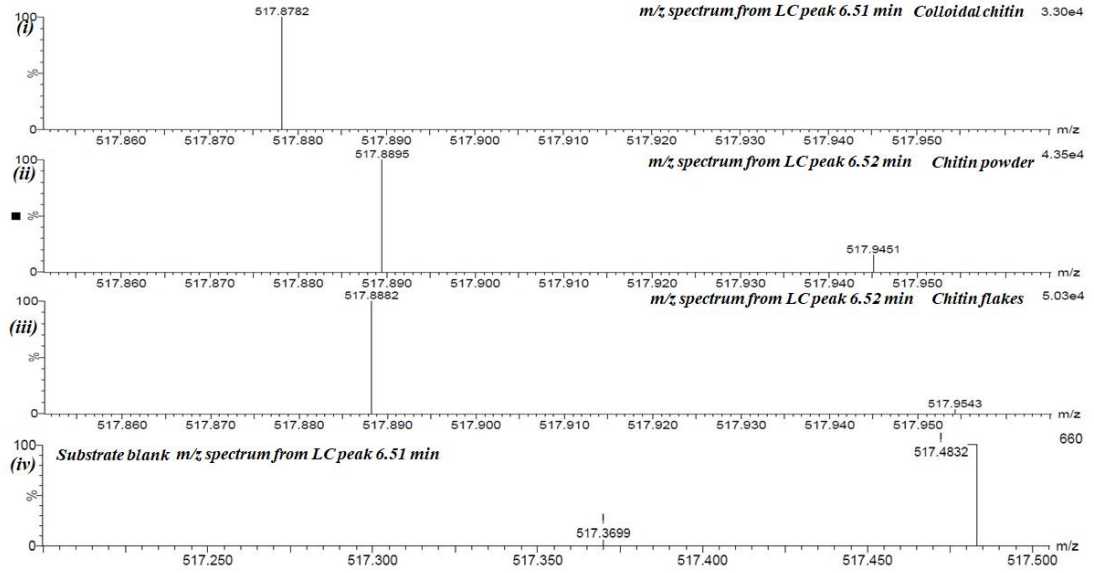

Figure 5.52c MS Spectrum of chitin pentamer peak for reaction sample against different chitin substrates

This result confirmed that the chitin pentamer was present in the reaction samples. In **Figure 5.52d**, the m/z peaks for chitin hexamer are shown. The m/z peaks were obtained at 618.5 for colloidal chitin and chitin powder and 618.52 for chitin flakes.

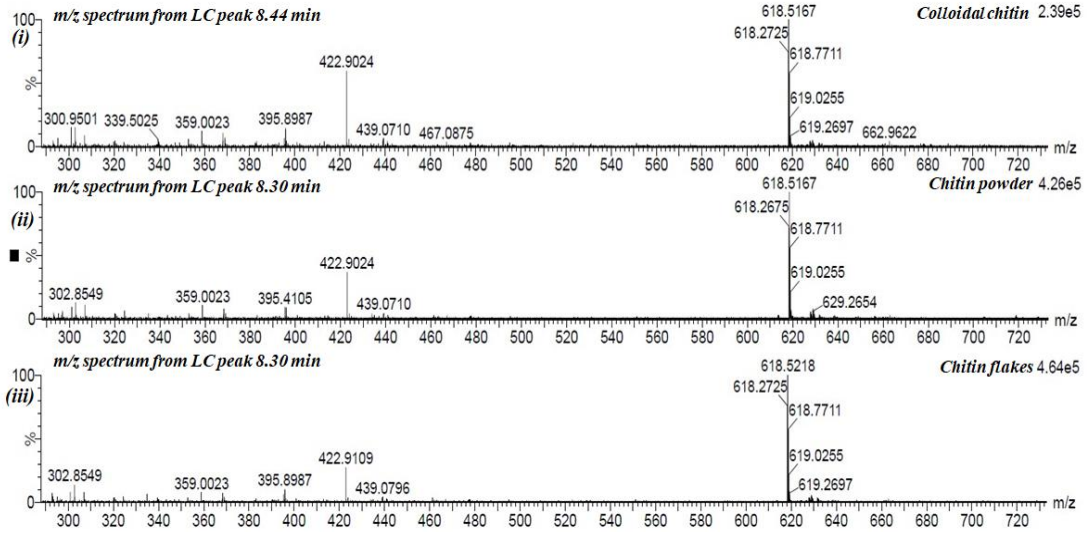

Figure 5.52d MS Spectrum of chitin hexamer peak for reaction sample against different chitin substrates

These m/z peaks obtained for all three reaction samples were the same as the m/z peak of chitin hexamer from the standard sample, which was 618.78. This result confirmed the presence of chitin hexamer in the all-reaction samples. The LC-MS results finally proved that recombinant chitinase developed from *Bacillus aryabhattai*, a marine bacteria, possessed high enzyme activity and catalytic efficiency to produce chitin oligomers (trimer, tetramer, pentamer and hexamer) from insoluble chitin substrates such as chitin powder and flakes. Several recent studies were developed recombinant chitinase from different bacteria such as *Streptomyces sampsonii*, *Chitinibacter tainanensis*, *Serratia marcescens*, *Bacillus thuringiensis*, *Paenibacillus xylanexedens*, *Aeromonas sp* etc. (Okay and Alshehri 2020b; Wang et al. 2023b; a; Wang and Wu 2020b; Zhang et al. 2021b) and from some fungal species such as *Rasamsonia emersonii* (Dwyer et al. 2023) However, recombinant chitinase developed from the above organisms performed activity against soluble chitin oligomers and colloidal chitin. There was no proof of the action of these recombinant chitinases on insoluble chitin substrates.

Moreover, very few studies on recombinant chitinase developed from *Bacillus velezensis*, *Streptomyces alfalfae* (Lv et al. 2021; Tran et al. 2022) showed the activity against insoluble chitin substrate. In a study performed by Patel Nilpa et al. (Nilpa et al. 2022), the fused chitinase gene of *Serratia marcescens* with the alkaline protease gene of *Bacillus circulans* was developed for better performance of enzyme against

insoluble chitin substrates. In the study performed by Aron Paek et al. (Paek et al. 2020), a hybrid recombinant enzyme was developed by fusing the chitinase catalytic domain from *Bacillus thuringiensis* bacteria with the chitin-binding domain from *Mamestra brassicae* insect, which improved the binding efficiency of chitinase enzyme towards insoluble chitin. However, the activity of the above-developed recombinant chitinase against insoluble chitin was less than that of recombinant chitinase from *Bacillus aryabhattai*, developed in the present study. The highest specificity of this recombinant chitinase from *Bacillus aryabhattai* was achieved because of the presence of two LysM domains. This LysM domain was the carbohydrate-binding domain, which makes the enzyme anchor to the crystalline chitin. *Bacillus aryabhattai* chitinase was the first marine bacterial chitinase to have two LysM domains in the N terminal region of the enzyme (Subramani et al. 2022).

5.19 Antifungal activity of recombinant *Ba*ChiA

Antifungal activity of recombinant chitinase was assessed against three different fungal species. Three fungal species were used for this study: *Candida albicans,* a common fungus in humans *with* less concentration. The increased growth of this fungus can cause several diseases in humans (Ho et al. 2021; Nikou et al. 2019), *Fusarium solani* is highly pathogenic to several plants such as Tomato, soya beans, strawberries etc., which causes several diseases in roots and leaves (Kurt et al. 2020; Roy 2007) and *Penicillium chrysogenum* is commonly available *Penicillium* species. The antifungal activity results against *Candida albicans Fusarium solani* and *Penicillium chrysogenum* are shown in **Figure 5.53 a, b, and c,** respectively**.**

Figure 5.53 Antifungal assessment of recombinant chitinase against (a) *Candida albicans*, (b) *Fusarium solani*, and (c) *Penicillium chrysogenum*.
(1 - 100 µL of purified chitinase, 2 - uninduced crude lysate sample, and 3 - autoclaved LB broth)

In each plate, three wells were prepared. Well 1 consists of recombinant chitinase around which a clear zone was developed. This result confirmed that chitinase inhibited fungus growth by degrading chitin in its cell wall. In ***wells 2 and 3,*** there was no clear zone, which also confirmed that growth inhibition was only by chitinase and not by any other enzymes. The above results confirmed that developed recombinant chitinase possesses antifungal activity.

CHAPTER 6
SUMMARY AND CONCLUSION

The study reports the isolation and screening of a novel chitinase- producing marine bacterium, *Bacillus aryabhattai,* which can grow on crystalline chitin. The chitinase upon sequence domain analysis revealed a characteristic LysM domain that helps act upon crystalline chitin. The effect of the domain was interrogated with substrates of different crystallinity, which displayed activity against crystalline chitin powder, chitin flakes, and colloidal chitin. Further, the enzymatic reaction resulted in the generation of chitin-oligomers, as evidenced by the TLC. Moreover, optimizing media composition and process parameters results in the highest specific chitinase activity of about ±115.2 U· mg^{-1}, ±63.02 U· mg^{-1} and ±146.1 U· mg^{-1} of protein in supernatant against chitin powder, chitin flakes and colloidal chitin respectively. The antifungal assay proved that the produced chitinase can act as a plant protectant against fungal pathogens. The TLC and LC-MS analysis confirmed that chitin oligomers, such as chitin monomer till hexamer, were produced from insoluble chitin substrates using spent media of *Bacillus aryabhattai*. The recombinant chitinase from *Bacillus aryabhattai* was expressed in the *E. coli Rosetta PLysS* and purified successfully using Ni-NTA affinity chromatography. The highest yield of chitinase was achieved by optimizing the process parameters involved in chitinase expression. The best conditions were IPTG induction in the late log phase (1.5 OD), IPTG concentration of 1.5 mM, 1% glycerol, and 48 hours incubation time. After optimization, the soluble form improved from 5% to 80%. Taguchi's optimization of process parameters used in the autoinduction method using TB media helped to achieve 80% soluble chitinase and an activity of 2 U· mL^{-1}. These findings suggest that the best conditions were TB media (containing 1% glycerol), 12.5℃ temperature, 150 rpm shaking speed, 48 hours of incubation time, 0.075% glucose, and 1.5% lactose. Enzyme characterization revealed the highest specific activity of 450 U. mg^{-1} in Tris buffer at pH 8, Temperature 55℃, in the presence of 400 mM Sodium metal ions. Kinetic parameters such as *Km, Vmax, Kcat and catalytic efficiency (Kcat/Km*) for purified chitinase were 2.5 mg· mL^{-1}, 112.3 μmole· min^{-1}, 192 min^{-1} and 1.28 mg^{-1}· mL· $second^{-1}$ respectively. Also, it was proven that recombinant chitinase efficiently acted on insoluble chitin substrates such as chitin flakes and powder prepared from shrimp shells with activity of 875 and 625 U· mg^{-1}, respectively. The TLC and LC-MS results proved that different chitin oligomers from trimer to hexamer were

produced from insoluble chitin substrates using recombinant chitinase developed in this study. Thus, an efficient process was developed to degrade the insoluble chitin wastes from marine using the eco-friendly enzymatic method in this study. This identified novel *Ba*ChiA can skip the acid treatment step of converting the insoluble and crystalline chitin into a soluble form, making the process more sustainable and eco-friendly.

CHAPTER 7
RESEARCH OUTCOME

Patents

- A patent was granted on the topic “Method for direct generation of bioethanol from chitin substrates using *Candida sp*” in March 2023. (Application Number: 202341011489)

- A patent was granted on the topic “Methods for producing Chitin degrading enzymes and chitin oligomers by way of *Bacillus aryabhattai*” in October 2023. (Application Number: 202341068137)

Publications

- Subramani Arun Kumar, Raval Ritu, Sundareshan Subramaniam, Sivasengh Rashmi, and Raval Keyur. (2022). “A marine chitinase from *Bacillus aryabhattai* with antifungal activity and broad specificity toward crystalline chitin degradation.” *Prep Biochem Biotechnol*, 52(10), 1160–1172.

- Subramani Arun kumar, Ramachandra Reshma, Thote Sachin, Govindaraj Vishnupriya, Vanzara Piyush, Raval Ritu, and Raval Keyur. (2024). “Engineering a recombinant chitinase from the marine bacterium *Bacillus aryabhattai* with targeted activity on insoluble crystalline chitin for chitin oligomer production.” *Journal of Biological Macromolecules*, 264, Part 2,130499.

- Govindaraj Vishnupriya, Subramani Arun Kumar, Gopalakrishnan Ramya, Kim Se Kwon, Raval Ritu, and Raval Keyur. (2023). “Bioethanol: A New Synergy between Marine Chitinases from *Bacillus haynesii* and Ethanol Production by *Mucor circinelloides*.” *Fermentation*, 9(1).

Book Chapter

- Subramani Arun Kumar, Raval Keyur, and Raval Ritu. (2024). “Evaluation of Chitosan and Its Derivatives in Immunomodulating Blood Sentinel Cells.” *Hematopoiesis*, Gutti Ravi Kumar, ed., *Apple Academic Press*, 51–71.

CHAPTER 8

REFERENCES

A. H. Fahmy, R. A. Hassanein, H. A. Hashem, A. S. Ibrahim, O. M. El Shihy, and E. A. Qaid. (2018). “Developing of transgenic wheat cultivars for improved disease resistance.” *J Appl Biol Biotechnol*, 20(13), 3350–3368.

A. T. Nasseri, S. Rasoul-Amini, M.H. Morowvat, and Y. Ghasemi. (2011). “Single cell protein: Production and Process.” *Am J Food Technol*, 6(2), 103–116.

Abu-Tahon, M. A., and Isaac, G. S. (2020). “Anticancer and antifungal efficiencies of purified chitinase produced from Trichoderma viride under submerged fermentation.” *Journal of General and Applied Microbiology*, 66(1), 32–40.

Adrangi, S., and Faramarzi, M. A. (2013). “From bacteria to human: A journey into the world of chitinases.” *Biotechnol Adv*, 31(8), 1786–1795.

Allonsius, C. N., Vandenheuvel, D., Oerlemans, E. F. M., Petrova, M. I., Donders, G. G. G., Cos, P., Delputte, P., and Lebeer, S. (2019). *Inhibition of Candida albicans morphogenesis by chitinase from Lactobacillus rhamnosus GG*. *Sci Rep*, Nature Publishing Group.

Annamalai, N., Rajeswari, M. V., Vijayalakshmi, S., and Balasubramanian, T. (2011a). “Purification and characterization of chitinase from Alcaligenes faecalis AU02 by utilizing marine wastes and its antioxidant activity.” *Ann Microbiol*, 61(4), 801–807.

Annamalai, N., Rajeswari, M. V., Vijayalakshmi, S., and Balasubramanian, T. (2011b). “Purification and characterization of chitinase from Alcaligenes faecalis AU02 by utilizing marine wastes and its antioxidant activity.” *Ann Microbiol*, 61(4), 801–807.

Bateman, A. (2019). “UniProt: A worldwide hub of protein knowledge.” *Nucleic Acids Res*, 47(D1), D506–D515.

Bateman, A., and Bycroft, M. (2000). “The structure of a LysM domain from E. coli membrane-bound lytic murein transglycosylase D (MltD).” *J Mol Biol*, 299(4), 1113–1119.

Bonnet, M., Lagier, J. C., Raoult, D., and Khelaifia, S. (2020). “Bacterial culture through selective and non-selective conditions: the evolution of culture media in clinical microbiology.” *New Microbes New Infect*, Elsevier Ltd.

Castillo, B. M., Dunn, M. F., Navarro, K. G., Meléndez, F. H., Ortiz, M. H., Guevara, S. E., and Palacios, G. H. (2016). “Antifungal performance of extracellular chitinases

and culture supernatants of Streptomyces galilaeus CFFSUR-B12 against Mycosphaerella fijiensis Morelet." *World J Microbiol Biotechnol*, 32(3), 1–12.

Chang, M.-M., Horovitz, D., Culley, D., and Hadwiger, L. A. (1995). "Molecular cloning and characterization of a pea chitinase gene expressed in response to wounding, fungal infection and the elicitor chitosan." *Plant Mol Biol*, 28, 105–111.

Cheba, B. A., Zaghloul, T. I., EL-Mahdy, A. R., and EL-Massry, M. H. (2016). "Effect of pH and Temperature on Bacillus sp. R2 Chitinase Activity and Stability." *Procedia Technology*, 22, 471–477.

Cheba, B. A., Zaghloul, T. I., El-Massry, M. H., and El-Mahdy, A. R. (2017). "Kinetics Properties of Marine Chitinase from Novel Red Sea Strain of Bacillus." *Procedia Eng*, Elsevier Ltd, 146–152.

Chen, Y. T., Hsu, L. H., Huang, I. P., Tsai, T. C., Lee, G. C., and Shaw, J. F. (2007). "Gene cloning and characterization of a novel recombinant antifungal chitinase from papaya (carica papaya)." *J Agric Food Chem*, 55(3), 714–722.

Deng, J. J., Shi, D., Mao, H. hua, Li, Z. wei, Liang, S., Ke, Y., and Luo, X. chun. (2019). "Heterologous expression and characterization of an antifungal chitinase (Chit46)from Trichoderma harzianum GIM 3.442 and its application in colloidal chitin conversion." *Int J Biol Macromol*, 134, 113–121.

Djenane, Z., Nateche, F., Amziane, M., Gomis-Cebolla, J., El-Aichar, F., Khorf, H., and Ferré, J. (2017). "Assessment of the antimicrobial activity and the entomocidal potential of Bacillus thuringiensis isolates from Algeria." *Toxins (Basel)*, 9(4), 139–155.

Doan, C. T., Tran, T. N., Nguyen, V. B., Nguyen, A. D., and Wang, S. L. (2018). "Reclamation of marine chitinous materials for chitosanase production via microbial conversion by paenibacillus macerans." *Mar Drugs*, 16(11), 429–440.

Dravid, P., Kaushal, D. C., Saxena, J. K., and Kaushal, N. A. (2015). "Isolation and characterization of endochitinase and exochitinase of Setaria cervi." *Parasitol Int*, 64(6), 579–586.

Duo-Chuan, L. (2006). "Review of fungal chitinases." *Mycopathologia*, 161(6), 345–360.

Dwyer, K., Bentley, I. S., Fitzpatrick, D. A., Saleh, A. A., Tighe, E., McGleenan, E., Gaffney, D., and Walsh, G. (2023). "Recombinant production, characterization and

industrial application testing of a novel acidic exo/endo-chitinase from Rasamsonia emersonii." *Extremophiles*, 27(2), 10–25.

Farag, A. M., Abd-Elnabey, H. M., Ibrahim, H. A. H., and El-Shenawy, M. (2016). "Purification, characterization and antimicrobial activity of chitinase from marine-derived Aspergillus terreus." *Egypt J Aquat Res*, 42(2), 185–192.

Ferreira, M. G. S., Simões, A. M. P., Compere, C., Rondot, B., and Cunha Belo, M. Da. (1998). "Semiconducting behaviour of stainless steel passive films in contact with artificial seawater." *Materials Science Forum*, 289–292(PART 2), 887–894.

Funkhouser, J. D., and Aronson, N. N. (2007). "Chitinase family GH18: Evolutionary insights from the genomic history of a diverse protein family." *BMC Evol Biol*, 7, 96–111.

Gao, L., Sun, J., Secundo, F., Gao, X., Xue, C., and Mao, X. (2018). "Cloning, characterization and substrate degradation mode of a novel chitinase from Streptomyces albolongus ATCC 27414." *Food Chem*, 261, 329–336.

Gohel, V., Chaudhary, T., Vyas, P., and Chhatpar, H. S. (2006). "Statistical screenings of medium components for the production of chitinase by the marine isolate Pantoea dispersa." *Biochem Eng J*, 28(1), 50–56.

Goldman, D. L., and Vicencio, A. G. (2012). "The chitin connection." *mBio*, 3(2), 1–4.

Gomaa, E. Z. (2021). "Microbial chitinases: properties, enhancement and potential applications." *Protoplasma*, 258, 675–710.

Gortari, M. C., and Hours, R. A. (2008). "Fungal chitinases and their biological role in the antagonism onto nematode eggs. A review." *Mycol Prog*, 7(4), 221–238.

Gutiérrez-Román, M. I., Dunn, M. F., Tinoco-Valencia, R., Holguín-Meléndez, F., Huerta-Palacios, G., and Guillén-Navarro, K. (2014). "Potentiation of the synergistic activities of chitinases ChiA, ChiB and ChiC from Serratia marcescens CFFSUR-B2 by chitobiase (Chb) and chitin binding protein (CBP)." *World J Microbiol Biotechnol*, 30(1), 33–42.

Halbedel, S., Prager, R., Banerji, S., Kleta, S., Trost, E., Nishanth, G., Alles, G., Hölzel, C., Schlesiger, F., Pietzka, A., Schlüter, D., and Flieger, A. (2019). "A Listeria monocytogenes ST2 clone lacking chitinase ChiB from an outbreak of non-invasive gastroenteritis." *Emerg Microbes Infect*, 8(1), 17–28.

Hamid, R., Khan, M. A., Ahmad, M., Ahmad, M. M., Abdin, M. Z., Musarrat, J., and Javed, S. (2013). “Chitinases: An update.” *J Pharm Bioallied Sci*, 5(1), 21–29.

Han, B., Zhou, K., Li, Z., Sun, B., Ni, Q., Meng, X., Pan, G., Li, C., Long, M., Li, T., Zhou, C., Li, W., and Zhou, Z. (2016). “Characterization of the First Fungal Glycosyl Hydrolase Family 19 Chitinase (NbchiA) from Nosema bombycis (Nb).” *Journal of Eukaryotic Microbiology*, 63(1), 37–45.

Han, Y., Yang, B., Zhang, F., Miao, X., and Li, Z. (2009). “Characterization of antifungal chitinase from marine Streptomyces sp. DA11 associated with South China sea sponge Craniella australiensis.” *Marine Biotechnology*, 11(1), 132–140.

He, B., Yang, L., Yang, D., Jiang, M., Ling, C., Chen, H., Ji, F., and Pan, L. (2022). “Biochemical purification and characterization of a truncated acidic, thermostable chitinase from marine fungus for N-acetylglucosamine production.” *Front Bioeng Biotechnol*, 10, 1–17.

Hee Kuk, J., Jin Jung, W., Hyun Jo, G., Seob Ahn, J., Yong Kim, K., and Dong Park, R. (2005). “Selective preparation of N-acetyl-D D-glucosamine and N,N¢-diacetylchitobiose from chitin using a crude enzyme preparation from Aeromonas sp.” *Biotechnol Lett*, 27, 7–11.

Hernick, M., and Fierke, C. (2010). “Mechanisms of Metal-Dependent Hydrolases in Metabolism.” *Comprehensive Natural Products II*, 8, 547–576.

Ho, J., Camilli, G., Griffiths, J. S., Richardson, J. P., Kichik, N., and Naglik, J. R. (2021). “Candida albicans and candidalysin in inflammatory disorders and cancer.” *Immunology*, 162(1), 11–16.

Huang, Q. S., Xie, X. L., Liang, G., Gong, F., Wang, Y., Wei, X. Q., Wang, Q., Ji, Z. L., and Chen, Q. X. (2012). “The GH18 family of chitinases: Their domain architectures, functions and evolutions.” *Glycobiology*, 22(1), 23–34.

Hurtado-Guerrero, R., and Aalten, D. M. F. van. (2007). “Structure of Saccharomyces cerevisiae Chitinase 1 and Screening-Based Discovery of Potent Inhibitors.” *Chem Biol*, 14(5), 589–599.

Inamine, S., Onaga, S., Ohnuma, T., Fukamizo, T., and Taira, T. (2015a). “Purification, cDNA cloning, and characterization of LysM-containing plant chitinase from horsetail (Equisetum arvense).” *Biosci Biotechnol Biochem*, 79(8), 1296–1304.

Inamine, S., Onaga, S., Ohnuma, T., Fukamizo, T., and Taira, T. (2015b).

"Purification, cDNA cloning, and characterization of LysM-containing plant chitinase from horsetail (Equisetum arvense)." *Biosci Biotechnol Biochem*, 79(8), 1296–1304.

Inamine, S., Onaga, S., Ohnuma, T., Fukamizo, T., and Taira, T. (2015c). "Purification, cDNA cloning, and characterization of LysM-containing plant chitinase from horsetail (Equisetum arvense)." *Biosci Biotechnol Biochem*, 79(8), 1296–1304.

Itoh, T., and Kimoto, H. (2019). "Bacterial chitinase system as a model of chitin biodegradation." *Adv Exp Med Biol*, Springer New York LLC, 131–151.

Jolles, P., Muzzarelli, R. A. A., Robertus, J. D., and Monzingo, A. F. (1999). "The structure and action of chitinases." *BioMed central*, 1–9.

Juarez-Hernandez, E. O., Casados-Vázquez, L. E., Brieba, L. G., Torres-Larios, A., Jimenez-Sandoval, P., and Barboza-Corona, J. E. (2019). "The crystal structure of the chitinase ChiA74 of Bacillus thuringiensis has a multidomain assembly." *Sci Rep*, 9(1), 2591–2610.

Junges, Â., Boldo, J. T., Souza, B. K., Guedes, R. L. M., Sbaraini, N., Kmetzsch, L., Thompson, C. E., Staats, C. C., Almeida, L. G. P. De, Vasconcelos, A. T. R. De, Vainstein, M. H., and Schrank, A. (2014). "Genomic analyses and transcriptional profiles of the glycoside hydrolase family 18 genes of the entomopathogenic fungus Metarhizium anisopliae." *PLoS One*, 9(9), 1–16.

Kästner, B., Tenhaken, R., and Kauss, H. (1998). "Chitinase in cucumber hypocotyls is induced by germinating fungal spores and by fungal elicitor in synergism with inducers of acquired resistance." *Plant Journal*, 13(4), 447–454.

Keyhani, N. O., and Roseman, S. (1999). "Physiological aspects of chitin catabolism in marine bacteria." *Biochimica et Biophysica Acta (BBA) - General Subjects*, 1473(1), 108–122.

Kim, S. K., and Rajapakse, N. (2005). "Enzymatic production and biological activities of chitosan oligosaccharides (COS): A review." *Carbohydr Polym*, 62(4), 357–368.

Kitaoku, Y., Fukamizo, T., Numata, T., and Ohnuma, T. (2017). "Chitin oligosaccharide binding to the lysin motif of a novel type of chitinase from the multicellular green alga, Volvox carteri." *Plant Mol Biol*, 93(1–2), 97–108.

Kobayashi, D. Y., Reedy, R. M., Bick, J. A., and Oudemans, P. V. (2002). "Characterization of a chitinase gene from Stenotrophomonas maltophilia strain 34S1 and its involvement in biological control." *Appl Environ Microbiol*, 68(3), 1047–

1054.

Krithika, S., and Chellaram, C. (2016). “Isolation, Screening, and Characterization of Chitinase producing Bacteria from marine wastes.” *Int J Pharm Pharm Sci*.

Kulichevskaya, I. S., Naumoff, D. G., Ivanova, A. A., Rakitin, A. L., and Dedysh, S. N. (2019). “Detection of Chitinolytic Capabilities in the Freshwater Planctomycete Planctomicrobium piriforme.” *Microbiology (Russian Federation)*, 88(4), 423–432.

Kumar, S., Stecher, G., Li, M., Knyaz, C., and Tamura, K. (2018). “MEGA X: Molecular evolutionary genetics analysis across computing platforms.” *Mol Biol Evol*, 35(6), 1547–1549.

Kurandas, M. J., and Robbins, P. W. (1975). “Chitinase Is Required for Cell Separation during Growth of Saccharomyces cerevisiae".” *J Biol Chem*, 266(29).

Kurandas, M. J., and Robbins, P. W. (1991). “Chitinase Is Required for Cell Separation during Growth of Saccharomyces cerevisiae".” *J Biol Chem*, 266(29), 19758–19767.

Kurt, Ş., Uysal, A., Soylu, E. M., Kara, M., and Soylu, S. (2020). “Characterization and pathogenicity of Fusarium solani associated with dry root rot of citrus in the eastern Mediterranean region of Turkey.” *Journal of General Plant Pathology*, 86(4), 326–332.

Kusaoke, H., Shinya, S., Fukamizo, T., and Kimoto, H. (2017). “Biochemical and biotechnological trends in chitin, chitosan, and related enzymes produced by Paenibacillus IK-5 Strain.” *Int J Biol Macromol*, 104, 1633–1640.

Langner, T., Öztürk, M., Hartmann, S., Cord-Landwehr, S., Moerschbacher, B., Walton, J. D., and Göhrea, V. (2015). “Chitinases are essential for cell separation in Ustilago maydis.” *Eukaryot Cell*, 14(9), 846–857.

Las Mercedes Dana, M. De, Pintor-Toro, J. A., and Cubero, B. (2006). “Transgenic tobacco plants overexpressing chitinases of fungal origin show enhanced resistance to biotic and abiotic stress agents.” *Plant Physiol*, 142(2), 722–730.

Le, B., and Yang, S. H. (2018). “Characterization of a chitinase from Salinivibrio sp. BAO-1801 as an antifungal activity and a biocatalyst for producing chitobiose.” *J Basic Microbiol*, 58(10), 848–856.

Le, B., and Yang, S. H. (2019). “Microbial chitinases: properties, current state and biotechnological applications.” *World J Microbiol Biotechnol*, 35(9), 1–12.

Lee, Y. S., Park, I. H., Yoo, J. S., Chung, S. Y., Lee, Y. C., Cho, Y. S., Ahn, S. C., Kim, C. M., and Choi, Y. L. (2007). "Cloning, purification, and characterization of chitinase from Bacillus sp. DAU101." *Bioresour Technol*, 98(14), 2734–2741.

Li, Z., Xia, C., Wang, Y., Li, X., Qiao, Y., Li, C., Zhou, J., Zhang, L., Ye, X., Huang, Y., and Cui, Z. (2019). "Identification of an endo-chitinase from Corallococcus sp. EGB and evaluation of its antifungal properties." *Int J Biol Macromol*, 132, 1235–1243.

Liang, T. W., Chen, W. T., Lin, Z. H., Kuo, Y. H., Nguyen, A. D., Pan, P. S., and Wang, S. L. (2016). "An amphiprotic novel chitosanase from Bacillus mycoides and its application in the production of chitooligomers with their antioxidant and anti-inflammatory evaluation." *Int J Mol Sci*, 17(8), 1302–1318.

Liu, C., Shen, N., Wu, J., Jiang, M., Shi, S., Wang, J., Wei, Y., and Yang, L. (2020). "Cloning, expression and characterization of a chitinase from Paenibacillus chitinolyticus strain UMBR 0002." *PeerJ*, 2020(3).

Liu, J., NanGong, Z., Zhang, J., Song, P., Tang, Y., Gao, Y., and Wang, Q. (2019). "Expression and characterization of two chitinases with synergistic effect and antifungal activity from Xenorhabdus nematophila." *World J Microbiol Biotechnol*, 35(7), 106–120.

Lodhi, G., Kim, Y. S., Hwang, J. W., Kim, S. K., Jeon, Y. J., Je, J. Y., Ahn, C. B., Moon, S. H., Jeon, B. T., and Park, P. J. (2014). "Chitooligosaccharide and its derivatives: Preparation and biological applications." *Biomed Res Int*, 2014, 1–14.

Loni, P. P., Patil, J. U., Phugare, S. S., and Bajekal, S. S. (2014). "Purification and characterization of alkaline chitinase from Paenibacillus pasadenensis NCIM 5434." *J Basic Microbiol*, 54(10), 1080–1089.

Lopes, J. F., and Gaspar, E. M. S. M. (2008). "Simultaneous chromatographic separation of enantiomers, anomers and structural isomers of some biologically relevant monosaccharides." *J Chromatogr A*, 1188(1), 34–42.

Lv, C., Gu, T., Ma, R., Yao, W., Huang, Y., Gu, J., and Zhao, G. (2021). "Biochemical characterization of a GH19 chitinase from Streptomyces alfalfae and its applications in crystalline chitin conversion and biocontrol." *Int J Biol Macromol*, 167, 193–201.

Madhuprakash, J., Dalhus, B., Vaaje-Kolstad, G., Sakuda, S., Podile, A. R., Eijsink,

V. G. H., and Sørlie, M. (2019). “Structural and Thermodynamic Signatures of Ligand Binding to the Enigmatic Chitinase D of Serratia proteamaculans.” *Journal of Physical Chemistry B*, 123(10), 2270–2279.

Madhuprakash, J., Gueddari, N. E. El, Moerschbacher, B. M., and Podile, A. R. (2015). “Catalytic efficiency of chitinase-D on insoluble chitinous substrates was improved by fusing auxiliary domains.” *PLoS One*, 10(1), 1–19.

Martínez-Absalón, S., Rojas-Solís, D., Hernández-León, R., Prieto-Barajas, C., Orozco-Mosqueda, M. del C., Peña-Cabriales, J. J., Sakuda, S., Valencia-Cantero, E., and Santoyo, G. (2014). “Potential use and mode of action of the new strain Bacillus thuringiensis UM96 for the biological control of the grey mould phytopathogen Botrytis cinerea.” *Biocontrol Sci Technol*, 24(12), 1349–1362.

Mekasha, S., Byman, I. R., Lynch, C., Toupalová, H., Anděra, L., Næs, T., Vaaje-Kolstad, G., and Eijsink, V. G. H. (2017). “Development of enzyme cocktails for complete saccharification of chitin using mono-component enzymes from Serratia marcescens.” *Process Biochemistry*, 56, 132–138.

Menghiu, G., Ostafe, V., Prodanovic, R., Fischer, R., and Ostafe, R. (2019). “Biochemical characterization of chitinase A from Bacillus licheniformis DSM8785 expressed in Pichia pastoris KM71H.” *Protein Expr Purif*, 154, 25–32.

Meriem, G., and Mahmoud, K. (2017). “Optimization of chitinase production by a new Streptomyces griseorubens C9 isolate using response surface methodology.” *Ann Microbiol*, 67(2), 175–183.

Monreal, J., and Reese, E. T. (1968). “The chitinase of Serratia marcescens.” *Can J Microbiol*, 15, 689–696.

Murthy, N., and Bleakley, B. (2012). “Simplified Method of Preparing Colloidal Chitin Used For Screening of Chitinase-Producing Microorganisms.” *Internet J Microbiol*, 10(2), 1–5.

Nikou, S. A., Kichik, N., Brown, R., Ponde, N. O., Ho, J., Naglik, J. R., and Richardson, J. P. (2019). “Candida albicans interactions with mucosal surfaces during health and disease.” *Pathogens*, 8(2), 53–80.

Nilpa, P., Chintan, K., Sayyed, R. Z., Enshasy, H. El, Adawi, H. El, Alhazmi, A., Almalki, A. H., and Haque, S. (2022). “Formation of recombinant bifunctional fusion protein: A newer approach to combine the activities of two enzymes in a single

protein.” *PLoS One*, Public Library of Science.

Ohishi,', K., Murase, K., Ohta, T., and Etoh2, A. H. (2000). “Cloning and Sequencing of a Chitinase Vibrio alginolyticus H-8 Gene from.” *J Biosci Bioeng*, 89(5), 501–505.

Ohnuma, T., Taira, T., Umemoto, N., Kitaoku, Y., Sørlie, M., Numata, T., and Fukamizo, T. (2017). “Crystal structure and thermodynamic dissection of chitin oligosaccharide binding to the LysM module of chitinase-A from Pteris ryukyuensis.” *Biochem Biophys Res Commun*, 494(3–4), 736–741.

Okay, S., and Alshehri, W. A. (2020a). “Overexpression of Chitinase A Gene from Serratia marcescens in Bacillus subtilis and Characterization of Enhanced Chitinolytic Activity.” *Brazilian Archives of Biology and Technology*, 63, 1–8.

Okay, S., and Alshehri, W. A. (2020b). “Overexpression of Chitinase A Gene from Serratia marcescens in Bacillus subtilis and Characterization of Enhanced Chitinolytic Activity.” *Brazilian Archives of Biology and Technology*, 63, 1–8.

Paek, A., Kim, M. J., Park, H. Y., Yoo, J. G., and Jeong, S. E. (2020). “Functional expression of recombinant hybrid enzymes composed of bacterial and insect’s chitinase domains in E. coli.” *Enzyme Microb Technol*, 136, 109492–109511.

Pan, M., Li, J., Lv, X., Du, G., and Liu, L. (2019). “Molecular engineering of chitinase from Bacillus sp. DAU101 for enzymatic production of chitooligosaccharides.” *Enzyme Microb Technol*, 124, 54–62.

Pan Xing Q., Shih Chu C., and Harday John. (2005). “Chitinase Induces Lysis of MCF-7 Cells in Culture and of Human Breast Cancer Xenograft B11-2 in SCID Mice.” *Anticancer Res*, 25, 3167–3172.

Patidar, P., Agrawal, D., Banerjee, T., and Patil, S. (2005a). “Optimisation of process parameters for chitinase production by soil isolates of Penicillium chrysogenum under solid substrate fermentation.” *Process Biochemistry*, 40(9), 2962–2967.

Patidar, P., Agrawal, D., Banerjee, T., and Patil, S. (2005b). “Optimisation of process parameters for chitinase production by soil isolates of Penicillium chrysogenum under solid substrate fermentation.” *Process Biochemistry*, 40(9), 2962–2967.

Patil, N. S., and Jadhav, J. P. (2014). “Enzymatic production of N-acetyl-D-glucosamine by solid state fermentation of chitinase by Penicillium ochrochloron MTCC 517 using agricultural residues.” *Int Biodeterior Biodegradation*, 91, 9–17.

Paulsen, S. S., Andersen, B., Gram, L., and MacHado, H. (2016). “Biological

potential of chitinolytic marine bacteria." *Mar Drugs*, 14(12).

Pell, G., Williamson, M. P., Walters, C., Du, H., Gilbert, H. J., and Bolam, D. N. (2003). "Importance of hydrophobic and polar residues in ligand binding in the family 15 carbohydrate-binding module from Cellvibrio japonicus Xyn10C." *Biochemistry*, 42(31), 9316–9323.

Pinnamaneni, R., Kalidas, P., and Rao, K. R. S. S. (2010). *Cloning and Expression of Bbchit1 gene of Beauveria bassiana*. *Open Entomol J*.

Ralph Berger, L., and Reynolds, D. M. (1958). *The Chitinase system of a strain of Streptomyces griseus*. *Biochim Biophys Acta*.

Rathore, A. S., and Gupta, R. D. (2015). "Chitinases from Bacteria to Human: Properties, Applications, and Future Perspectives." *Enzyme Res*, Hindawi Publishing Corporation.

Ray, L., Panda, A. N., Mishra, S. R., Pattanaik, A. K., Adhya, T. K., Suar, M., and Raina, V. (2019a). "Purification and characterization of an extracellular thermo-alkali stable, metal tolerant chitinase from Streptomyces chilikensis RC1830 isolated from a brackish water lake sediment." *Biotechnology Reports*, 21.

Ray, L., Panda, A. N., Mishra, S. R., Pattanaik, A. K., Adhya, T. K., Suar, M., and Raina, V. (2019b). "Purification and characterization of an extracellular thermo-alkali stable, metal tolerant chitinase from Streptomyces chilikensis RC1830 isolated from a brackish water lake sediment." *Biotechnology Reports*, 21, 311–319.

Revathi, M., Saravanan, R., and Shanmugam, A. (2012). "Production and characterization of chitinase from Vibrio species, a head waste of shrimp Metapenaeus dobsonii (Miers, 1878) and chitin of Sepiella inermis Orbigny, 1848." *Advances in Bioscience and Biotechnology*, 03(04), 392–397.

Robbins, P. W., Albright, C., and Benfield, B. (1988). "Cloning and expression of a Streptomyces plicatus chitinase (chitinase-63) in Escherichia coli." *Journal of Biological Chemistry*, 263(1), 443–447.

Roger, V., Fonty, G., Andre, C., and Gouet, P. (1992). "Effects of Glycerol on the Growth, Adhesion, and Cellulolytic Activity of Rumen Cellulolytic Bacteria and Anaerobic Fungi." *Curr Microbiol*, 25, 197–201.

Roy, K. W. (2007). "Fusarium solani on Soybean Roots: Nomenclature of the Causal Agent of Sudden Death Syndrome and Identity and Relevance of F. solani form B."

Plant Dis, 81(3), 259–266.

Sadfi, N., Chérif, M., Fliss, I., Boudabbous, A., and Antoun, H. (2001). *Evaluation of bacterial isolates from salty soils and Bacillus thuringiensis strains for the biocontrol of Fusarium dry rot of potato tubers*. *Source: Journal of Plant Pathology*.

Saima, Kuddus, M., Roohi, and Ahmad, I. Z. (2013). "Isolation of novel chitinolytic bacteria and production optimization of extracellular chitinase." *Journal of Genetic Engineering and Biotechnology*, 11(1), 39–46.

Santhi, R. (2016). "Isolation of chitinase producing Streptomyces albus FS12, production and optimization of extracellular chitinase." *International Journal of Advanced Research in Biological Sciences* , 3(4), 229–237.

Selenius, O., Korpela, J., Salminen, S., and Gomez Gallego, C. (2018). "Effect of Chitin and Chitooligosaccharide on In vitro Growth of Lactobacillus rhamnosus GG and Escherichia coli TG." *Applied Food Biotechnology*, 5(3), 163–172.

Shafiee, F., Moazen, F., Rabbani, M., and Sadeghi, H. M. M. (2015). "Optimization of the expression of reteplase in Escherichia coli TOP10 using arabinose promoter." *Journal of Natural Pharmaceutical Products*, 10(1), 1–19.

Sharma, R. R., Singh, D., and Singh, R. (2009). "Biological control of postharvest diseases of fruits and vegetables by microbial antagonists: A review." *Biological Control*, 50(3), 205–221.

Shin, S., Mackintosh, C. A., Lewis, J., Heinen, S. J., Radmer, L., Dill-Macky, R., Baldridge, G. D., Zeyen, R. J., and Muehlbauer, G. J. (2008). "Transgenic wheat expressing a barley class II chitinase gene has enhanced resistance against Fusarium graminearum." *J Exp Bot*, 59(9), 2371–2378.

Shivalee, A., Lingappa, K., and Mahesh, D. (2018). "Influence of bioprocess variables on the production of extracellular chitinase under submerged fermentation by Streptomyces pratensis strain KLSL55." *Journal of Genetic Engineering and Biotechnology*, 16(2), 421–426.

Shrestha, A., Sultana, R., Chae, J. C., Kim, K., and Lee, K. J. (2015). "Bacillus thuringiensis C25 which is rich in cell wall degrading enzymes efficiently controls lettuce drop caused by Sclerotinia minor." *Eur J Plant Pathol*, 142(3), 577–589.

Sousa, A. J. S., Silva, C. F. B., Sousa, J. S., Monteiro, J. E., Freire, J. E. C., Sousa, B. L., Lobo, M. D. P., Monteiro-Moreira, A. C. O., and Grangeiro, T. B. (2019). "A

thermostable chitinase from the antagonistic Chromobacterium violaceum that inhibits the development of phytopathogenic fungi." *Enzyme Microb Technol*, 126, 50–61.

Stefanidi, E., and Vorgias, C. E. (2008). "Molecular analysis of the gene encoding a new chitinase from the marine psychrophilic bacterium Moritella marina and biochemical characterization of the recombinant enzyme." *Extremophiles*, 12(4), 541–552.

Stoykov, Y. M., Pavlov, A. I., and Krastanov, A. I. (2015). "Chitinase biotechnology: Production, purification, and application." *Eng Life Sci*, 15(1), 30–38.

Subramani, A. K., Raval, R., Sundareshan, S., Sivasengh, R., and Raval, K. (2022). "A marine chitinase from Bacillus aryabhattai with antifungal activity and broad specificity toward crystalline chitin degradation." *Prep Biochem Biotechnol*, 52(10), 1160–1172.

Subramanian, K., Sadaiappan, B., Aruni, W., Kumarappan, A., Thirunavukarasu, R., Srinivasan, G. P., Bharathi, S., Nainangu, P., Renuga, P. S., Elamaran, A., Balaraman, D., and Subramanian, M. (2020a). "Bioconversion of chitin and concomitant production of chitinase and N-acetylglucosamine by novel Achromobacter xylosoxidans isolated from shrimp waste disposal area." *Sci Rep*, 10(1), 11898–11912.

Subramanian, K., Sadaiappan, B., Aruni, W., Kumarappan, A., Thirunavukarasu, R., Srinivasan, G. P., Bharathi, S., Nainangu, P., Renuga, P. S., Elamaran, A., Balaraman, D., and Subramanian, M. (2020b). "Bioconversion of chitin and concomitant production of chitinase and N-acetylglucosamine by novel Achromobacter xylosoxidans isolated from shrimp waste disposal area." *Sci Rep*, 10(1).

Swiontek Brzezinska, M., Jankiewicz, U., Burkowska, A., and Walczak, M. (2014). "Chitinolytic microorganisms and their possible application in environmental protection." *Curr Microbiol*, 68(1), 71–81.

Take, K., Fujiki, H., Suyotha, W., Hayashi, J., Takagi, K., Yano, S., and Wakayama, M. (2018). "Enzymatic and molecular characterization of an acidic and thermostable chitinase 1 from Streptomyces thermodiastaticus HF3-3." *Journal of General and Applied Microbiology*, 64(4), 190–197.

Tamadoni Jahromi, S., and Barzkar, N. (2018a). "Marine bacterial chitinase as

sources of energy, eco-friendly agent, and industrial biocatalyst." *Int J Biol Macromol*, Elsevier B.V.

Tamadoni Jahromi, S., and Barzkar, N. (2018b). "Marine bacterial chitinase as sources of energy, eco-friendly agent, and industrial biocatalyst." *Int J Biol Macromol*, 120, 2147–2154.

Tanaka, T., Fujiwara, S., Nishikori, S., Fukui, T., Takagi, M., and Imanaka, T. (1999). "A Unique Chitinase with Dual Active Sites and Triple Substrate Binding Sites from the Hyperthermophilic Archaeon Pyrococcus kodakaraensis KOD1." *Appl Environ Microbiol*, 65(12), 5338–5344.

Tanakal, H., and Phaff, H. J. (1965). "Enzymatic Hydrolysis of Yeast Cell Walls I. Isolation of Wall-Decomposing Organisms and Separation and Purification of Lytic Enzymes." *J Bacteriol*, 89(6), 1570–1580.

Tao, A., Pang, F., Huang, S., Yu, G., Li, B., and Wang, T. (2014). "Characterisation of endophytic Bacillus thuringiensis strains isolated from wheat plants as biocontrol agents against wheat flag smut." *Biocontrol Sci Technol*, 24(8), 901–924.

Terrapon, N., Lombard, V., Drula, E., Coutinho, P. M., and Henrissat, B. (2017). "The CAZy Database/the Carbohydrate-Active Enzyme (CAZy) Database: Principles and Usage Guidelines." *A Practical Guide to Using Glycomics Databases*, Springer Japan, 117–131.

Tom, R. A., and Carroad Paul A. (1981). "Effect of Reaction Conditions on Hydrolysis of Chitin by Serratia marcescens QMBI 466 chitinase." *Journal of Food technology*, 46, 646–647.

Tran, D. M., Huynh, T. U., Nguyen, T. H., Do, T. O., Pentekhina, I., Nguyen, Q. V., and Nguyen, A. D. (2022). "Expression, purification, and basic properties of a novel domain structure possessing chitinase from Escherichia coli carrying the family 18 chitinase gene of Bacillus velezensis strain RB.IBE29." *Mol Biol Rep*, 49(5), 4141–4148.

Tuveng, T. R., Hagen, L. H., Mekasha, S., Frank, J., Arntzen, M. Ø., Vaaje-Kolstad, G., and Eijsink, V. G. H. (2017). "Genomic, proteomic and biochemical analysis of the chitinolytic machinery of Serratia marcescens BJL200." *Biochim Biophys Acta Proteins Proteom*, 1865(4), 414–421.

Vaaje Kolstad, G., Horn, S. J., Sørlie, M., and Eijsink, V. G. H. (2013). "The

chitinolytic machinery of Serratia marcescens - A model system for enzymatic degradation of recalcitrant polysaccharides." *FEBS Journal*, 3028–3049.

Vaikuntapu, P. R., Rambabu, S., Madhuprakash, J., and Podile, A. R. (2016). "A new chitinase-D from a plant growth promoting Serratia marcescens GPS5 for enzymatic conversion of chitin." *Bioresour Technol*, 220, 200–207.

Vincy, V., Shoba, M. V., Viveka, S., Vijaya, T. M., Jasmin, G., and Rani, B. (2014). "Isolation and characterization of chitinase from bacteria of Shrimp pond." *European Journal of Experimental Biology*, 4(3), 78–82.

Vo, T. S., Ngo, D. H., Bach, L. G., Ngo, D. N., and Kim, S. K. (2017). "The free radical scavenging and anti-inflammatory activities of gallate-chitooligosaccharides in human lung epithelial A549 cells." *Process Biochemistry*, 54, 188–194.

Vyas, P., and Deshpande, M. (1991). "Enzymatic Hydrolysis of Chitin by Myrothecium verbucaria chitinase complex and its utilization to produce SCP." *Journal of General Applied Microbiology*, 37, 267–275.

Wang, J., Zhang, J., Song, F., Gui, T., and Xiang, J. (2015). "Purification and characterization of chitinases from ridgetail white prawn Exopalaemon carinicauda." *Molecules*, 20(2), 1955–1967.

Wang, S., Fang, X., Liang, K., Li, S., Han, S., and Zhu, T. (2023a). "Cloning, expression and antifungal effect of the recombinant chitinase from Streptomyces sampsonii KJ40." *Ciência Rural*, 53(4).

Wang, S., Fang, X., Liang, K., Li, S., Han, S., and Zhu, T. (2023b). "Cloning, expression and antifungal effect of the recombinant chitinase from Streptomyces sampsonii KJ40." *Ciência Rural*, 53(4).

Wang, S.-L., Yieh, T.-C., and Shih, I.-L. (1999). "Purification and characterization of a new antifungal compound produced by Pseudomonas aeruginosa K-187 in a shrimp and crab shell powder medium." *Enzyme Microb Technol*, 25(3), 439–446.

Wang, X., Zhao, Y., Tan, H., Chi, N., Zhang, Q., Du, Y., and Yin, H. (2014). "Characterisation of a chitinase from Pseudoalteromonas sp. DL-6, a marine psychrophilic bacterium." *Int J Biol Macromol*, 70, 455–462.

Wang, Y. T., and Wu, P. L. (2020a). "Gene cloning, characterization, and molecular simulations of a novel recombinant chitinase from chitinibacter tainanensis CT01 appropriate for chitin enzymatic hydrolysis." *Polymers (Basel)*, 12(8).

Wang, Y. T., and Wu, P. L. (2020b). “Gene cloning, characterization, and molecular simulations of a novel recombinant chitinase from chitinibacter tainanensis CT01 appropriate for chitin enzymatic hydrolysis.” *Polymers (Basel)*, 12(8), 1648–1661.

Watanabe, T., Oyanagi, W., Suzuki,’, K., Ohnishi, K., and Tanaka’, H. (1992). “Structure of the Gene Encoding Chitinase D of Bacillus circulans WL-12 and Possible Homology of the Enzyme to Other Prokaryotic Chitinases and Class III Plant Chitinases.” *J Bacteriol*, 174(2), 408–414.

Yan, Q., and Fong, S. S. (2018). “Cloning and characterization of a chitinase from Thermobifida fusca reveals Tfu_0580 as a thermostable and acidic endochitinase.” *Biotechnology Reports*, 19, 274–290.

Yandigeri, M. S., Malviya, N., Solanki, M. K., Shrivastava, P., and Sivakumar, G. (2015). “Chitinolytic Streptomyces vinaceusdrappus S5MW2 isolated from Chilika lake, India enhances plant growth and biocontrol efficacy through chitin supplementation against Rhizoctonia solani.” *World J Microbiol Biotechnol*, 31(8), 1217–1225.

Yu, P., Wang, X., Ma, J., Zhang, Q., and Chen, Q. (2022). “Chaperone-assisted soluble expression and characterization of chitinase chiZJ408 in Escherichia coli BL21 and the chitin degradation by recombinant enzyme.” *Prep Biochem Biotechnol*, 52(3), 273–282.

Zhang, W., Ma, J., Yan, Q., Jiang, Z., and Yang, S. (2021a). “Biochemical characterization of a novel acidic chitinase with antifungal activity from Paenibacillus xylanexedens Z2–4.” *Int J Biol Macromol*, 182, 1528–1536.

Zhang, W., Ma, J., Yan, Q., Jiang, Z., and Yang, S. (2021b). “Biochemical characterization of a novel acidic chitinase with antifungal activity from Paenibacillus xylanexedens Z2–4.” *Int J Biol Macromol*, 182, 1528–1536.

Zhou, J., Chen, L., Kang, L., Liu, Z., Bai, Y., Yang, Y., and Yuan, S. (2018). “ChiE1 from Coprinopsis cinerea is Characterized as a Processive Exochitinase and Revealed to Have a Significant Synergistic Action with Endochitinase ChiIII on Chitin Degradation.” *J Agric Food Chem*, 66(48), 12773–12782.

APPENDICES

1 Phenol sulfuric acid method standard

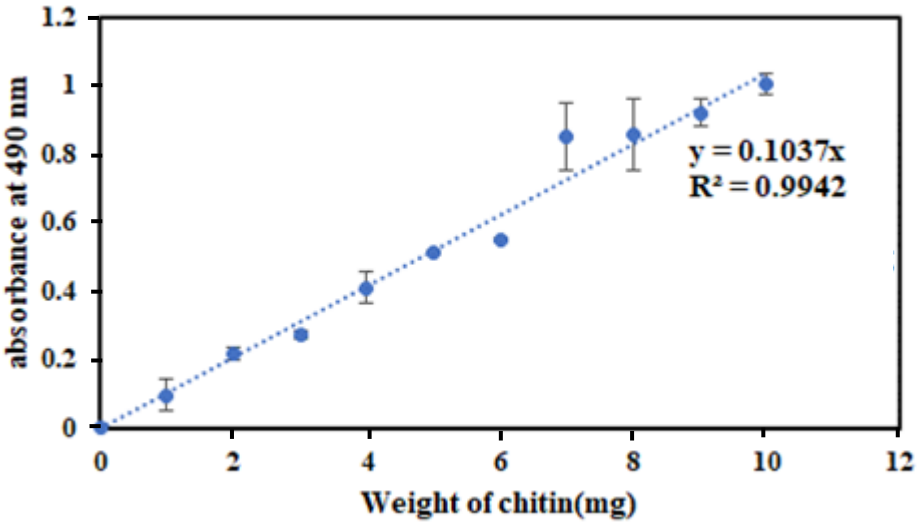

2 N-acetyl glucosamine (NAG) standard using DNSA method

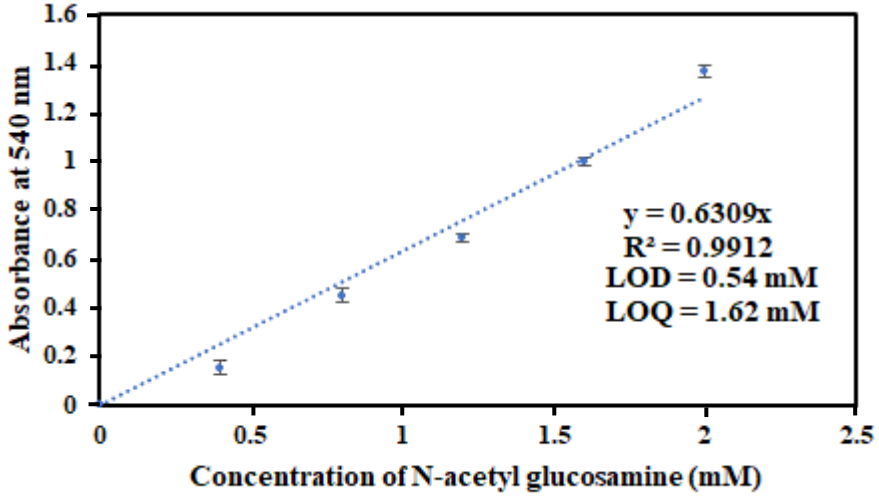

3 Bovine serum albumin (BSA) standard using Bradford method

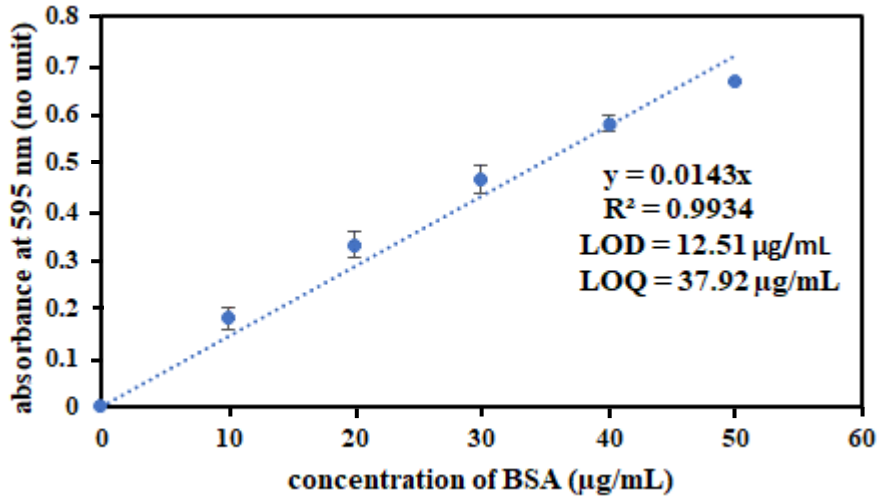

4 Biomass Vs OD (660 nm) Standard for *E. coli Rosetta PLysS*

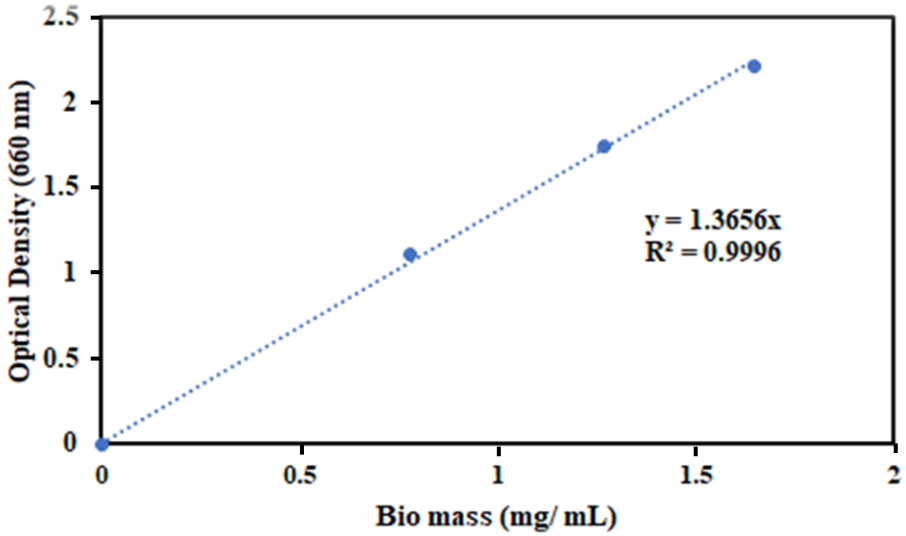

5 Percentage of soluble chitinase enzyme and its activity at different growth phases (Figure 5.36).

Growth phase (OD)	Soluble enzyme (%)	Enzyme Activity (U/L)
Early log (0.6 OD)	5	1.23
Mid log (1.2 OD)	20	10.33
Late log (1.5 OD)	40	147.5
Early Stationary (1.7 OD)	30	9.1

6 Soluble chitinase and activity of chitinase enzyme produced at different IPTG concentration (Figure 5.37).

IPTG concentration (mM)	Soluble Enzyme (%)	Enzyme activity (U/L)
0.2	30	28
0.4	35	35
0.6	38	45
0.8	40	63
1	40	106
1.5	65	158
2	25	45
2.5	22	51
3	20	52
3.5	20	55
4	15	40

7 Soluble chitinase and activity of chitinase enzyme produced at different incubation time (Figure 5.38)

Incubation Time (Hours)	Soluble enzyme (%)	Enzyme activity (U/L)
12	62	113
24	65	158
48	70	263
60	40	85

8 Soluble form and activity of chitinase enzyme produced at different Glycerol concentrations (Figure 5.39).

Glycerol (%)	Soluble enzyme (%)	Enzyme activity (U/L)
0.5	59	221
1	82	473
2	75	411
3	73	125
4	70	89

9 Different experiments for five variables using Taguchi method with obtained response and S/N ratio.

Temperature (°C)	Shaking Speed (rpm)	Incubation Time (Hours)	Glucose Concentration (%)	Lactose Concentration (%)	Soluble enzyme yield (%)	S/N ratio
10	120	12	0	0.5	65.4545	36.44
10	150	48	0.075	2	69.7368	36.83
10	130	24	0.025	1	75.2089	37.47
10	140	36	0.05	1.5	79.476	37.83
10	160	60	0.1	2.5	42.221	32.64
12.5	130	36	0.075	2.5	78.8746	38.06
12.5	140	48	0.1	0.5	64.7059	36.16
12.5	120	24	0.05	2	73.0223	37.40
12.5	150	60	0	1	66.9291	36.34
12.5	160	12	0.025	1.5	75	37.46
15	130	48	0	1.5	69.64	36.98
15	140	60	0.025	2	52.9661	34.60
15	150	12	0.05	2.5	74.392	37.37
15	160	24	0.075	0.5	69.0987	36.62
15	120	36	0.1	1	68.5039	36.67
17.5	150	24	0.1	1.5	69.9418	37.019
17.5	160	36	0	2	51.3611	34.15
17.5	140	12	0.075	1	72.5124	37.34
17.5	120	48	0.025	2.5	52.6066	34.25
17.5	130	60	0.05	0.5	52.6728	34.39
20	120	60	0.075	1.5	61.2019	35.68
20	150	36	0.025	0.5	65.66	36.47
20	140	24	0	2.5	59.7015	35.48
20	130	12	0.1	2	62.7848	35.79
20	160	48	0.05	1	53.6842	34.72

10 Sequence of Recombinant chitinase gene and protein

Gene Sequeunce

ATAAGTAAAGGAGACGCTGCTTCTTCAGTAGGCACTGTCAAAGGTGATAATGTAA
ATGTGTATCGTTCTCCATCTTTGCATTCTTCGATTGTTCAGACAGTGAAAAAAGGA
GAAGAGTTTCCTGCTATTTCATCTGAAGCGGGAGATGCAGCTCAAGTTATCACCC
ATAAAGTAGTGCCAGGAAATACACTATGGCTACTAGCTAAACAATATGGTGTAA
CAGTCAGCGAGCTAATAAAACAAAATCAGCTAAAAACGACGGAGCTAACTCCGG
GGCAAACGCTGAAAATACCACCAAAAGGCTTGTTACATAAAGTAGTATCAGGAG
ATACGCTTTGGAAAATCTCTGTAAAGTACGGTGTAAAAGCGACTGAATTAACAAA
GTTAAATCAGCTATCATCAACAAATATTAAGCCTGGACAAATGCTTATTATTCCT
GATTACTATGTACAAGTACAGCTTTTGGAAGGGAAAAAGGGCTGGATCAAAAAA
TCTGATTTAGCACAAAAGAAGCATCAGCCAGTAGTTATGGGCTGGAGCTTTAATG
AAAAAACAGCAGGCTATGCAGAATCGATGAAACAAAAGAACTTAGACGTTGTTT
CACCACGCTGGTTTACGCTAACGCGGAGTGACAAAGTTGTTTCATCTTCTATAAA
TCCATCGTATGTTCAAACGGCTCACAAAAACGGCAAAAAAGTCTGGCCGCTCATC
GGTAACAATTTCGATGATGTGCTGACAAGTGACGTCCTAGGCAATAAAGCAAAG
CGGCAAAAGCTTGTATCGTCAGTCGAAAGTTCGCTTGTGAAAACAAACAGTGAC
GGTATTAACGTTGACTTTGAAAATATTAATATCAAAAACAAACAAGATTTTGTTT
TATTTATTAAAGAATTAAAAGGAGCGTTAAAGCCTCATGGTATGACCGTTTCAGT
AGACGTAACACGAGAGAATAATGATCCGTTTTGGTCAGGAAGCTTTGATCGAAA
ACAGATTGGTCAAGTGGCAGATTACGTCATTATGATGGGTTATGAAGAACACTGG
GGAGGAAGTCAGGTTCCAGGGTCTGTGGCTTCGCTGCCTTGGGTGAAAGAAGGA
ACAGAACTTCTTATGAAAGATGTACCTGCACACAAAATCCTGCTGGGAGTTCCTT
TTTATACGCGAGAATGGAAAACGGATCTATCTACCAAAAAAGTTGTCACAAAAG
ACTTAACGATGAAAGAAGCCGAAGCAATTATCTCTTCTAAAAAGTTAACTAAAA
AATGGGACAGCCAAGCCTCTCAGTACTATGTAGAATACACCGAAAATGGTACGA
AGCATCAAATATGGCTCGAAGACAAAGCATCTATGCAGCGCCGGGTTAAATTAA
TTAATGACTATCATTTAGGCGGGGCGGCAGCTTGGTATATTGGTTCAGAAACATC
AGATATATGGGAGTTATATAACTT

Protein Sequeunce

MSKGDAASSVGTVKGDNVNVYRSPSLHSSIVQTVKKGEEFPAISSEAGDAAQVITHK
VVPGNTLWLLAKQYGVTVSELIKQNQLKTTELTPGQTLKIPPKGLLHKVVSGDTLWK
ISVKYGVKATELTKLNQLSSTNIKPGQMLIIPDYYVQVQLLEGKKGWIKKSDLAQKK
HQPVVMGWSFNEKTAGYAESMKQKNLDVVSPRWFTLTRSDKVVSSSINPSYVQTAH
KNGKKVWPLIGNNFDDVLTSDVLGNKAKRQKLVSSVESSLVKTNSDGINVDFENINI
KNKQDFVLFIKELKGALKPHGMTVSVDVTRENNDPFWSGSFDRKQIGQVADYVIMM
GYEEHWGGSQVPGSVASLPWVKEGTELLMKDVPAHKILLGVPFYTREWKTDLSTKK
VVTKDLTMKEAEAIISSKKLTKKWDSQASQYYVEYTENGTKHQIWLEDKASMQRRV
KLINDYHLGGAAAWYIGSETSDIWELYN

11 Cloned Plasmid Sequencing results

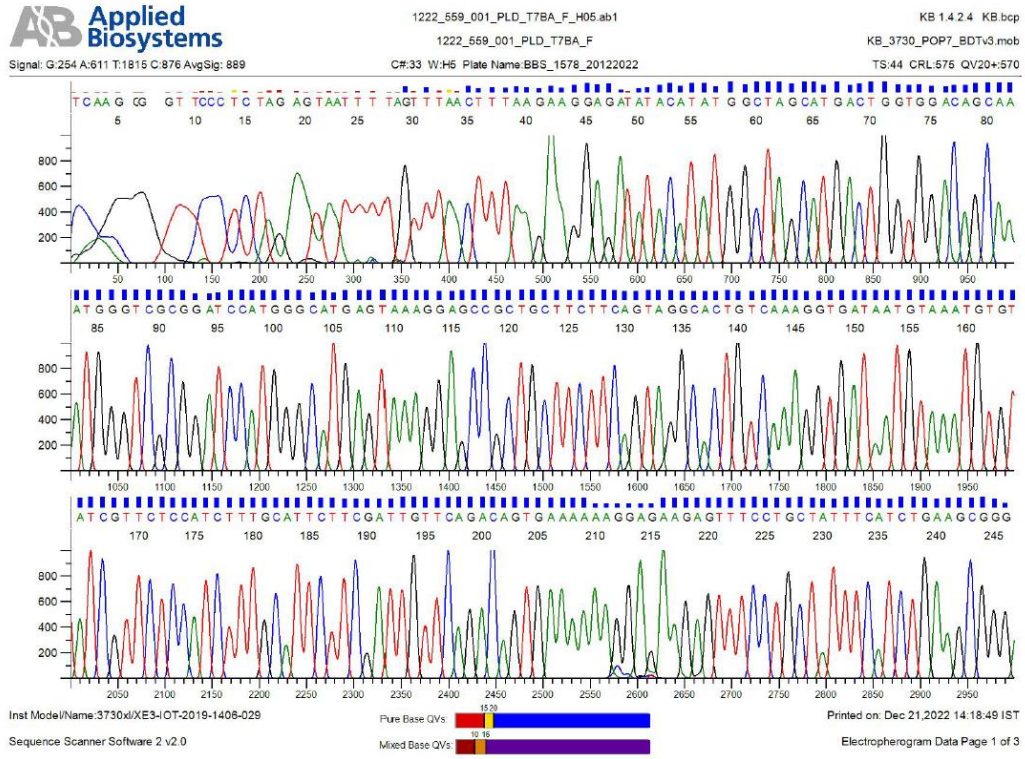

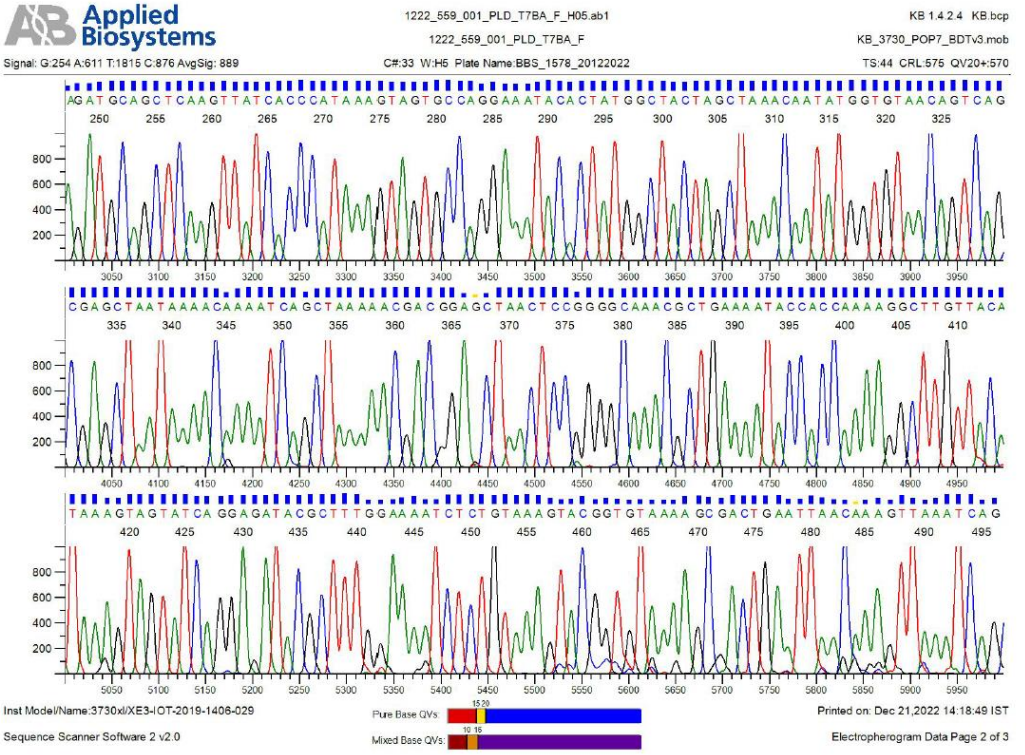

12 Enzyme activity at different pH and buffer (Figure 5.43).

Buffer	pH	Chitinase specefic activity (U/mg)
Citrate	5	19.5
	6	44.5
Phosphate	6	47
	7	54
Tris base	7	55.5
	8	64
Borate	8	60.5
	9	37

13 Enzyme activity at different temperatures (Figure 5.44)

Temperature	Chitinase specefic activity (U/mg)
40	67.5
45	71
50	93.5
55	138
60	105.5
65	77.5

14 Enzyme activity in the presence of different metal ions (Figure 5.45)

Metal ions	Chitinase specefic activity (U/mg)
Mg^{2+}	142.5
Mn^{2+}	266
Ni^{2+}	144.5
Co^{2+}	413.5
Ca^{2+}	175.5
Na	452

15 Enzyme Kinetics

For Michaelis Menten curve **(Figure 5.46)**:

Substrate concentration, S (mg/mL)	**Enzyme velocity, V (µmole/min)**
0	0
0.1	4.37
0.4	15.38
0.6	20.69
0.8	30.7
1	35.35
2	50.21
3	65.81
4	68.48
10	88.65
20	100.01
40	103.25

For Lineweaver Burk plot **(Figure 5.47)**

1/S	**1/V**
10.0	0.23
2.5	0.07
1.7	0.05
1.3	0.03
1.0	0.03
0.5	0.02
0.3	0.02
0.3	0.01
0.1	0.01
0.1	0.01

19 High Resolution Liquid chromatography mass spectrometry (HRLCMS)

20 Sample ID details (LC_MS for wildtype chitinase reaction sample)

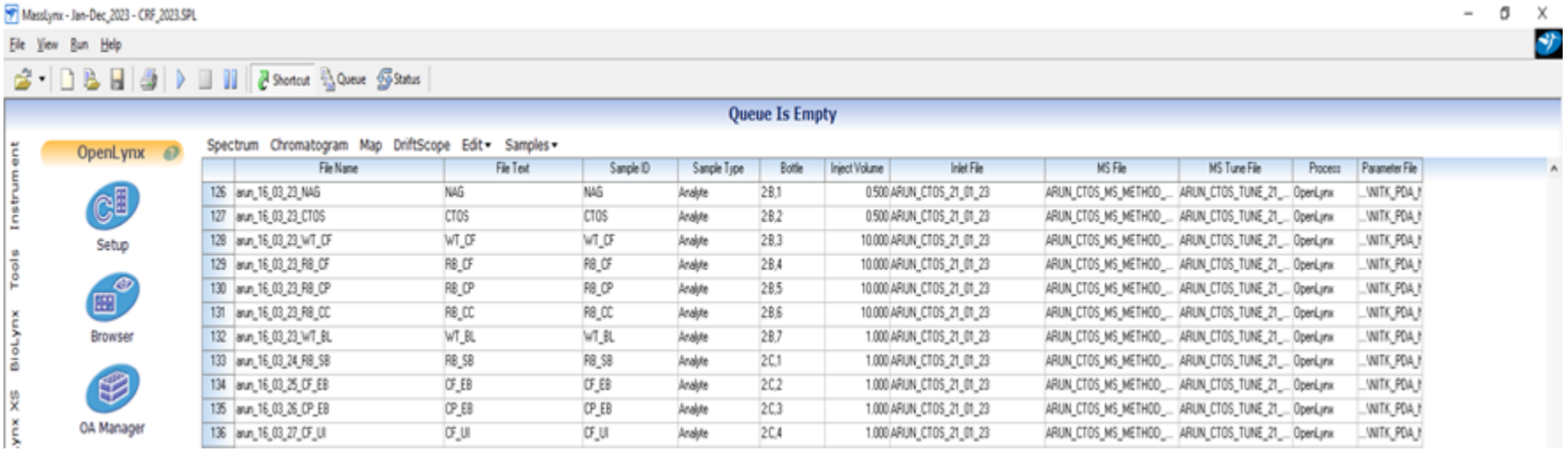

	File Name	File Text	Sample ID	Sample Type	Bottle	Inject Volume	Inlet File	MS File	MS Tune File	Process	Parameter File
126	arun_16_03_23_NAG	NAG	NAG	Analyte	2:B,1	0.500	ARUN_CTOS_21_01_23	ARUN_CTOS_MS_METHOD_...	ARUN_CTOS_TUNE_21_...	OpenLynx	...\WITK_PDA_I
127	arun_16_03_23_CTOS	CTOS	CTOS	Analyte	2:B,2	0.500	ARUN_CTOS_21_01_23	ARUN_CTOS_MS_METHOD_...	ARUN_CTOS_TUNE_21_...	OpenLynx	...\WITK_PDA_I
128	arun_16_03_23_WT_CF	WT_CF	WT_CF	Analyte	2:B,3	10.000	ARUN_CTOS_21_01_23	ARUN_CTOS_MS_METHOD_...	ARUN_CTOS_TUNE_21_...	OpenLynx	...\WITK_PDA_I
129	arun_16_03_23_RB_CF	RB_CF	RB_CF	Analyte	2:B,4	10.000	ARUN_CTOS_21_01_23	ARUN_CTOS_MS_METHOD_...	ARUN_CTOS_TUNE_21_...	OpenLynx	...\WITK_PDA_I
130	arun_16_03_23_RB_CP	RB_CP	RB_CP	Analyte	2:B,5	10.000	ARUN_CTOS_21_01_23	ARUN_CTOS_MS_METHOD_...	ARUN_CTOS_TUNE_21_...	OpenLynx	...\WITK_PDA_I
131	arun_16_03_23_RB_CC	RB_CC	RB_CC	Analyte	2:B,6	10.000	ARUN_CTOS_21_01_23	ARUN_CTOS_MS_METHOD_...	ARUN_CTOS_TUNE_21_...	OpenLynx	...\WITK_PDA_I
132	arun_16_03_23_WT_BL	WT_BL	WT_BL	Analyte	2:B,7	1.000	ARUN_CTOS_21_01_23	ARUN_CTOS_MS_METHOD_...	ARUN_CTOS_TUNE_21_...	OpenLynx	...\WITK_PDA_I
133	arun_16_03_24_RB_SB	RB_SB	RB_SB	Analyte	2:C,1	1.000	ARUN_CTOS_21_01_23	ARUN_CTOS_MS_METHOD_...	ARUN_CTOS_TUNE_21_...	OpenLynx	...\WITK_PDA_I
134	arun_16_03_25_CF_EB	CF_EB	CF_EB	Analyte	2:C,2	1.000	ARUN_CTOS_21_01_23	ARUN_CTOS_MS_METHOD_...	ARUN_CTOS_TUNE_21_...	OpenLynx	...\WITK_PDA_I
135	arun_16_03_26_CP_EB	CP_EB	CP_EB	Analyte	2:C,3	1.000	ARUN_CTOS_21_01_23	ARUN_CTOS_MS_METHOD_...	ARUN_CTOS_TUNE_21_...	OpenLynx	...\WITK_PDA_I
136	arun_16_03_27_CF_UI	CF_UI	CF_UI	Analyte	2:C,4	1.000	ARUN_CTOS_21_01_23	ARUN_CTOS_MS_METHOD_...	ARUN_CTOS_TUNE_21_...	OpenLynx	...\WITK_PDA_I

Sample ID	Sample name
WT_BL	Substrate Blank sample (Figure 5.13a and 5.13b)
CTOS	Standard sample (Figure 5.10a and 5.10b)

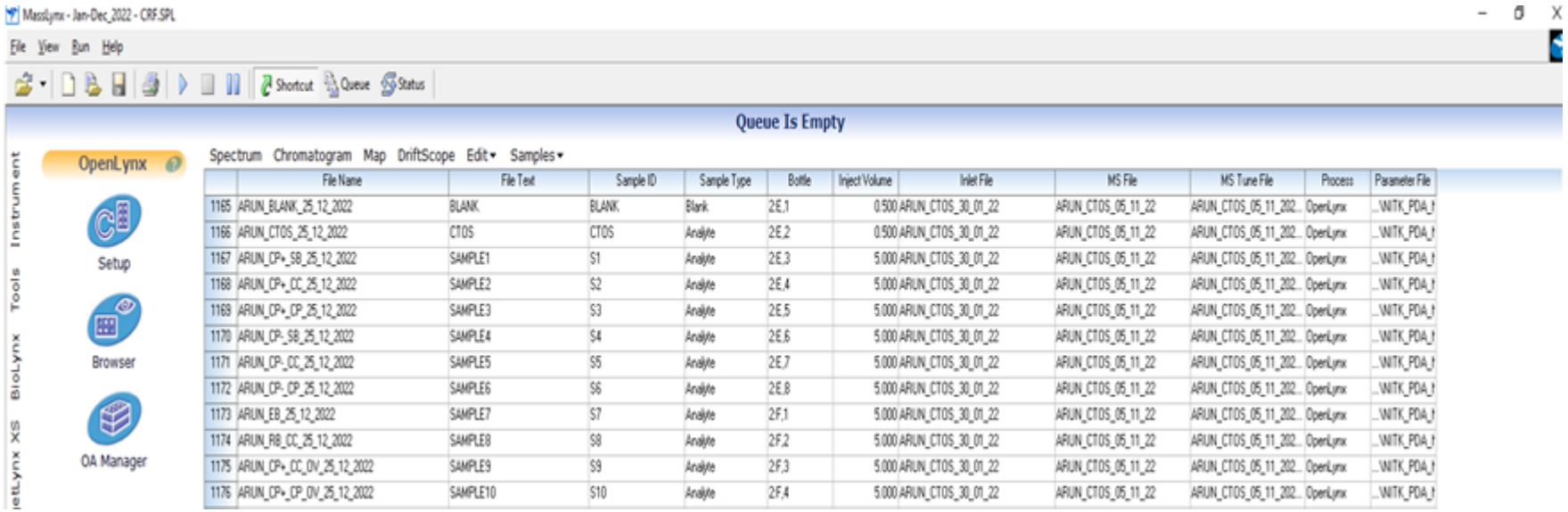

Sample ID	Sample name
S2	Chitin powder reaction sample (Figure 5.11a and 5.12a)
S8	Chitin flakes reaction sample (Figure 5.11b and 5.12b)

21 Sample ID details (LC_MS for Recombinant chitinase reaction sample)

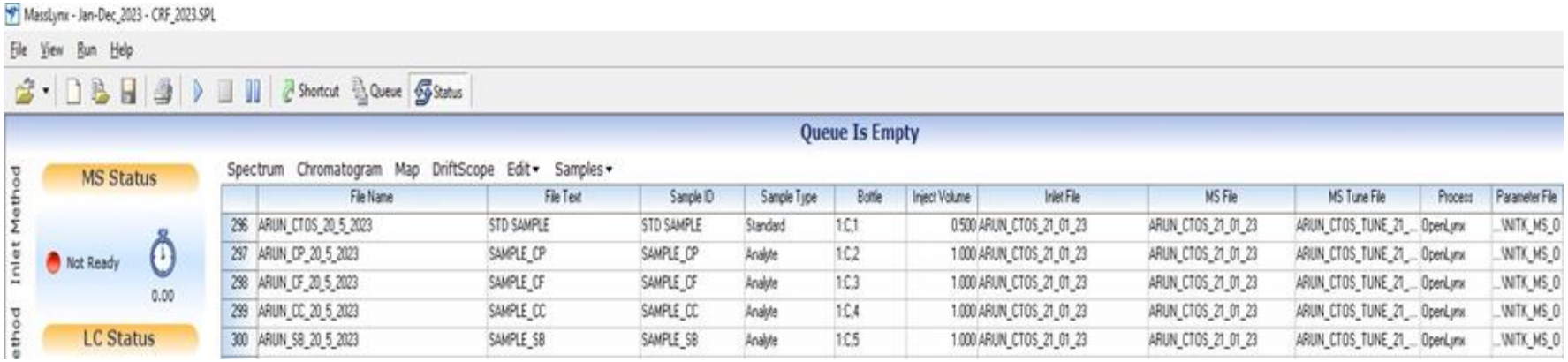

Sample ID	Sample name
STD SAMPLE	Standard sample (Figure 5.50a and 5.50b)
SAMPLE_CP	Reaction sample for Chitin powder (Figure 5.51, 5.52a, 5.52b, 5.52c and 5.52d)
SAMPLE_CF	Reaction sample for Chitin flakes (Figure 5.51, 5.52a, 5.52b, 5.52c and 5.52d)
SAMPLE_CF	Reaction sample for Colloidal Chitin (Figure 5.51, 5.52a, 5.52b, 5.52c and 5.52d)
SAMPLE_SB	Substrate Blank Sample (Figure 5.51, 5.52a, and 5.52c)